

Figure 3.1: Digital control system

F_k represents the optimal feedback, u_k^f the feedforward determined by the digital tracker, while the complete state is measured.

For reasons to be explained later we will chose the control weighting of the digital tracker everywhere equal to zero. In this case, dependent on the magnitude of the sampling time, large feedback gains occur. In practice they may cause instability. Therefore we also consider an alternative where the digital optimal control $u_d(t)$, computed from the digital tracker with the control weighting everywhere equal to zero, is presented to the system in an open loop fashion. In this case a digital optimal perturbation controller is used to control small deviations from the trajectory $u_d(t)$, $x_d(t)$ to zero. $x_d(t)$ represents the state response of the system (4) to the the digital optimal control $u_d(t)$. This optimal perturbation controller is computed using the digital optimal regulator result. In this case the choice of the weighting matrices of the digital regulator determines the feedback. These weighting matrices may ofcourse be chosen independently from the ones in the tracking problem which determined the trajectory $u_d(t)$, $x_d(t)$. So this approach seperates the choice of the optimal control from the choice of the optimal feedback. The digital control system that results in this case is represented by figure 3.2.

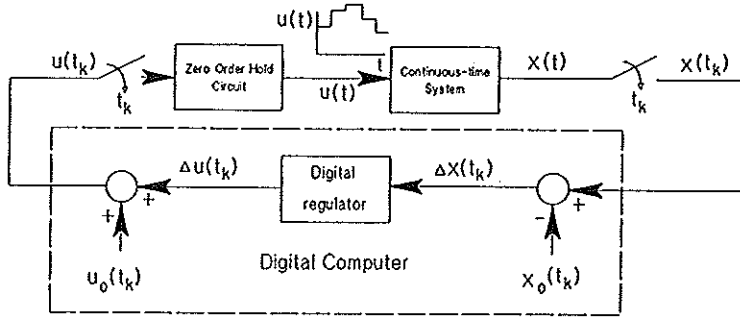


Figure 3.2: Digital perturbation control system

3.2 The digital optimal regulator and tracker for linear time varying systems

Consider the deterministic continuous-time linear time-varying system

$$\dot{x}(t) = A(t)x(t) + B(t)u(t), \quad (19a)$$

with known initial state

$$x(t_0) = x_0, \quad (19b)$$

where $A(t)$ and $B(t)$ are the system matrices. The control is piecewise constant, i.e.

$$u(t) = u(t_k), \quad t \in [t_k, t_{k+1}), \quad k=0,1,2,3,\dots, \quad (19c)$$

where t_k are the, not necessarily equidistant, sampling instants. We assume complete state information at the sampling instants, so $x(t_k)$, $k=0,1,2,3,\dots$ are available. The latter assumption is valid for the X-Y robot since both link positions and speeds, i.e. the state variables of (4), are measured. However we may replace the state $x(t_k)$ by its estimate generated by the Kalman one step ahead predictor (Van Willigenburg and De Koning, 1990b) in which case

COMPUTATION OF DIGITAL OPTIMAL CONTROLLERS FOR CARTESIAN ROBOTS

the continuous-time system and the measurements may be corrupted by additive white noise.

The *digital optimal regulator problem* for the system (19) is to minimize

$$J = \int_{t_0}^{t_f} [x^T(t) Q(t) x(t) + u^T(t) R(t) u(t)] dt + x^T(t_f) H x(t_f) \Big], \quad (20)$$

where $Q(t) \geq 0$, $H \geq 0$ and $R(t) \geq 0$. Furthermore

$$t_f = t_N, \quad (21)$$

where N is a positive integer.

The *digital optimal tracking problem* takes the following form. Given the system (19) and a reference state trajectory

$$x_r(t), \quad t_0 \leq t \leq t_f, \quad (22)$$

minimize

$$J = \int_{t_0}^{t_f} [(x(t) - x_r(t))^T Q(t) (x(t) - x_r(t)) + u^T(t) R(t) u(t)] dt + (x(t_f) - x_r(t_f))^T H (x(t_f) - x_r(t_f)) \quad (23)$$

where again (21) holds and we assume $Q(t) \geq 0$, $H \geq 0$ and $R(t) \geq 0$.

The solution of the digital optimal regulator problem called the *digital optimal regulator* is computed and given by (Van Willigenburg, 1990b)

$$u_k = -(K'_k + R_k^{-1} M_k^T) x_k, \quad k=0, 1, 2, \dots, N-1, \quad (24a)$$

$$K'_k = (\Gamma_k^T S_{k+1} \Gamma_k + R_k)^{-1} \Gamma_k^T S_{k+1} \Phi'_k, \quad (24b)$$

$$S_k = (\Phi'_k - \Gamma_k K'_k)^T S_{k+1} (\Phi'_k - \Gamma_k K'_k) + K_k'^T R_k K'_k + Q'_k, \quad S_N = H, \quad (24c)$$

$$\Phi'_k = \Phi_k - \Gamma_k R_k^{-1} M_k^T, \quad (24d)$$

$$Q'_k = Q_k - M_k R_k^{-1} M_k^T. \quad (24e)$$

where,

$$Q_k = \int_{t_k}^{t_{k+1}} \Phi^T(t, t_k) Q(t) \Phi(t, t_k) dt, \quad (25a)$$

$$M_k = \int_{t_k}^{t_{k+1}} \Phi^T(t, t_k) Q(t) \Gamma(t, t_k) dt, \quad (25b)$$

$$R_k = \int_{t_k}^{t_{k+1}} [R(t) + \Gamma^T(t, t_k) Q(t) \Gamma(t, t_k)] dt. \quad (25c)$$

and where

$$\Gamma(t, t_k) = \int_{t_k}^t \Phi(t, s) B(s) ds \quad (25d)$$

and finally

$$\Phi_k = \Phi(t_{k+1}, t_k) \quad (25e)$$

$$\Gamma_k = \Gamma(t_{k+1}, t_k) \quad (25f)$$

where Φ is the state transition matrix of system (19a). Equation (25e) and (25f) determine the so called equivalent discrete system

$$\dot{x}_{k+1} = \Phi_k x_k + \Gamma_k u_k \quad (26)$$

which describes the system behavior of (19a) at the sampling

instants.

From (24a) it is obvious that the solution is given in feedback form, since besides x_k all matrices appearing in the solution can be computed off-line (Van Willigenburg, 1990b).

The solution to the digital optimal tracking problem called the *digital optimal tracker* is given and computed by (Van Willigenburg 1990b)

$$u_k = -(K'_k + R_k^{-1} M_k^T) x_k + K_k^1 v_{k+1} + K_k^2 T_k^T, \quad k=0, 1, 2, \dots, N-1, \quad (27a)$$

$$K'_k = (\Gamma_k^T S_{k+1} \Gamma_k + R_k)^{-1} \Gamma_k^T S_{k+1} \Phi'_k, \quad (27b)$$

$$K_k^1 = (R_k + \Gamma_k^T S_{k+1} \Gamma_k)^{-1} \Gamma_k^T, \quad (27c)$$

$$K_k^2 = (R_k + \Gamma_k^T S_{k+1} \Gamma_k)^{-1}, \quad (27d)$$

$$S_k = (\Phi'_k - \Gamma_k K'_k)^T S_{k+1} (\Phi'_k - \Gamma_k K'_k) + K'_k{}^T R_k K'_k + Q'_k, \quad S_N = H, \quad (27e)$$

$$v_k = (\Phi'_k - \Gamma_k K'_k)^T v_{k+1} - K'_k{}^T T_k^T + L'_k{}^T, \quad v_N = H x_r(t_f), \quad (27f)$$

$$\Phi'_k = \Phi_k - \Gamma_k R_k^{-1} M_k^T, \quad (27g)$$

$$Q'_k = Q_k - M_k R_k^{-1} M_k^T, \quad (27h)$$

$$L'_k = L_k - T_k R_k^{-1} M_k^T. \quad (27i)$$

where (25) holds and

$$L_k = \int_{t_k}^{t_{k+1}} x_r^T(t) Q(t) \Phi(t, t_k) dt, \quad (28a)$$

$$T_k = \int_{t_k}^{t_{k+1}} x_r^T(t) Q(t) \Gamma(t, t_k) dt, \quad (28b)$$

$$x_k = \int_{t_k}^{t_{k+1}} x_r^T(t) Q(t) x_r(t) dt. \quad (28c)$$

The solution is in feedback form, which can be observed from the first term in (27a), since all matrices except x_k can be computed off-line (Van Willigenburg, 1990b). Note that the second and third term of (27a) constitute feed forward components.

3.3 Optimal digital tracking controller computation for the X-Y robot

In paragraph 3.2 we presented the digital optimal regulator and tracker for linear systems. The robot dynamics (4) may be written as

$$\begin{bmatrix} \dot{x}_p \\ \dot{y}_p \\ \ddot{x}_p \\ \ddot{y}_p \end{bmatrix} = \begin{bmatrix} 0 & 0 & 1 & 0 \\ 0 & 0 & 0 & 1 \\ 0 & 0 & -v_x & 0 \\ 0 & 0 & -v_y & 0 \end{bmatrix} \begin{bmatrix} x_p \\ y_p \\ \dot{x}_p \\ \dot{y}_p \end{bmatrix} + \begin{bmatrix} 0 & 0 \\ 0 & 0 \\ b_x & 0 \\ 0 & b_y \end{bmatrix} \begin{bmatrix} u'_x \\ u'_y \end{bmatrix}, \quad (29a)$$

where

$$\begin{bmatrix} u'_x \\ u'_y \end{bmatrix} = \begin{bmatrix} u_x \\ u_y \end{bmatrix} - \begin{bmatrix} \text{sign}(\dot{x}_p) c_x / b_x \\ \text{sign}(\dot{y}_p) c_y / b_y \end{bmatrix}. \quad (29b)$$

From (29b) we see that if both links continue to move in the same direction, the non-linear terms in (4), involving the Coulomb friction, can be compensated for by *constant values* of the control. Therefore this compensation can be realized with a piecewise constant control. Only if the direction of the motion of a link changes during a sample interval the compensation cannot be realized by a piecewise constant control. Introducing

$$x_r(t) = \begin{bmatrix} x_{pr}(t) \\ y_{pr}(t) \\ \dot{x}_{pr}(t) \\ \dot{y}_{pr}(t) \end{bmatrix}, \quad (30)$$

from (29b) we have

$$\begin{bmatrix} u_x(t) \\ u_y(t) \end{bmatrix} = \begin{bmatrix} u'_x(t) \\ u'_y(t) \end{bmatrix} + \begin{bmatrix} \text{sign}(\dot{x}_{pr}(t))c_x/b_x \\ \text{sign}(\dot{y}_{pr}(t))c_y/b_y \end{bmatrix}. \quad (31)$$

If the motion of a link during a sample interval does not continue in the same direction we will not compensate the coulomb friction. Therefore we have

$$\begin{bmatrix} u_x(t_k) \\ u_y(t_k) \end{bmatrix} = \begin{bmatrix} u'_x(t_k) \\ u'_y(t_k) \end{bmatrix} + \begin{bmatrix} m_x \text{sign}(\dot{x}_{pr}(t_k))c_x/b_x \\ m_y \text{sign}(\dot{y}_{pr}(t_k))c_y/b_y \end{bmatrix}. \quad (32a)$$

where

$$m_x = 1 \quad (32b)$$

if $\text{sign}(\dot{x}_{pr}(t_k))$ equals $\text{sign}(\dot{x}_{pr}(t_{k+1}))$ otherwise

$$m_x = 0 \quad (32c)$$

and

$$m_y = 1 \quad (32d)$$

if $\text{sign}(\dot{y}_{pr}(t_k))$ equals $\text{sign}(\dot{y}_{pr}(t_{k+1}))$, otherwise

$$m_y = 0 \quad (32e)$$

The second term in (32a) also constitutes a feed forward component, which can be computed off-line.

Given the compensation of the coulomb friction in the sequel we may consider the linear system (29a) with u'_x and u'_y being the control variables. Given any reference state trajectory (22) we can compute the digital optimal tracker (27) once $Q(t)$, $R(t)$ and

H, the design parameters, are chosen. A natural choice is to punish all deviations from the trajectory equally, i.e. to let $Q(t)$ be time-invariant. Since we want the digital control to be such that deviations from the reference state trajectory are minimized another natural choice is

$$R(t) = 0. \quad (33)$$

Any other choice of $R(t)$ would result in a *compromise* between the magnitude of the control and deviations from the reference state trajectory. The philosophy behind the choice of (33) is that if the control obtained with (33) exceeds the bound (9b) the reference state trajectory is not suited to be realized with the X-Y robot and another reference state trajectory should be obtained. Of course if one persists in using this reference state trajectory $R(t)$ can be chosen such that the bound (9b) is not violated. Note that although the continuous-time and the discrete-time tracker (Lewis 1986) do not allow (33), since this results in singular problems, the digital-tracking problem, given (33), is non-singular (Van Willigenburg and De Koning 1990a).

Since in the case of robot motion control we are generally only interested in deviations of the prescribed link positions a natural choice for $Q(t)$ is

$$Q(t) = \begin{bmatrix} q_1 & 0 & 0 & 0 \\ 0 & q_1 & 0 & 0 \\ 0 & 0 & 0 & 0 \\ 0 & 0 & 0 & 0 \end{bmatrix} \quad (34)$$

where q_1 is a constant. At the final time however we generally want the robot to stand still as well so a natural choice of H is

$$H = \begin{bmatrix} h_1 & 0 & 0 & 0 \\ 0 & h_1 & 0 & 0 \\ 0 & 0 & h_2 & 0 \\ 0 & 0 & 0 & h_2 \end{bmatrix} \quad (35)$$

where again h_1 and h_2 are constants. Given (33), (34), (35) the optimal digital control and corresponding state trajectory will depend on the ratios h_1/q_1 and h_1/h_2 . Only the minimum cost will depend on the absolute values of q_1 , h_1 and h_2 . In the sequel the following choice is made based on experiments and a compromise between the reaching of the final state and the tracking error which occurs.

$$q_1 = 1.0, \quad (36)$$

$$h_1 = 0.3, \quad (37a)$$

$$h_2 = 0.1. \quad (37b)$$

Furthermore in the sequel we will assume equal sampling intervals. i.e.

$$t_{k+1} - t_k = T, \quad (38)$$

where T is the sampling time which varies from 60 to 200ms. Finally all figures in the sequel are based on measurements or computations performed every 10ms, to insure proper monitoring of the inter-sample behavior. So given a reference state trajectory the tracking problem (19), (22), (23) is completely determined by (29a), (5), (6), (13), (14), (17), (18), (33), ..., (38). The reference state trajectory, according to (21) must be time scaled such that the final time is a multiple of the sampling time (38). The time-scaling is chosen such that the final time of the time-scaled trajectory equals the nearest multiple higher than the original final time. From the solution (27) of the tracking problem and the equivalent discrete time system dynamics (26) we may compute the digital optimal control and the corresponding state trajectory given the initial state of (26). At this stage we assume the initial state to match the reference state trajectory i.e.

$$x(t_0) = x_r(t_0) \quad (39)$$

This is a reasonable assumption since before executing the motion we control the system to the desired initial state $x_r(t_0)$. Equation (32a) should be applied to obtain the control after coulomb friction compensation. Figure 3.3a displays one component of a time-optimal reference state trajectory obtained from Van Willigenburg (1990a) after time scaling, i.e. the desired translation of the X-link. Furthermore the corresponding component of the solution computed assuming (39), i.e. the X-translation realized with the digital optimal control, obtained after coulomb friction compensation, is displayed. If the control would have been a continuous-time control from (3) and (30) we can easily see that if

$$u_x(t) = (\ddot{x}_{pr}(t) + v_x \dot{x}_{pr}(t) + c_x \text{sign}(\dot{x}_{pr}(t))) / b_x, \quad (40a)$$

$$u_y(t) = (\ddot{y}_{pr}(t) + v_y \dot{y}_{pr}(t) + c_y \text{sign}(\dot{y}_{pr}(t))) / b_y, \quad (40b)$$

we would have a situation of perfect tracking i.e.

$$x(t) = x_r(t). \quad (41)$$

Since (39) holds the differences in figure 3.3a are completely caused by the fact that the control is constrained to be piecewise constant. In fact the time-optimal reference state trajectory of figure 3.3a was obtained assuming a continuous-time control with the following conservative bounds on the control variables (Van Willigenburg, 1990a),

$$|u_x| \leq 5.00, \quad (42a)$$

$$|u_y| \leq 5.00. \quad (42b)$$

The actual bounds of the control variables are

$$|u_x| \leq 10.00, \quad (43a)$$

$$|u_y| \leq 10.00. \quad (43b)$$

Figure 3.3b shows the results for the Y-link. Figure 3.4 and 3.5 are based on the same time-optimal reference state trajectory. Only the sampling time was chosen differently. Clearly, as expected, smaller sampling times allow better tracking of the reference state trajectory. Note however that the tracking error in practical situations is not just caused by the piecewise constant nature of the control but also by modeling and measurement errors and uncertainties. In the next section we will demonstrate that modeling and measurement errors and uncertainties, dominate the tracking error in our application. Figures 3.3c,d, 3.4c,d and 3.5c,d display the values of the feedback coefficients which reach a steady state value since the linear dynamics are time-invariant. Obviously if the sampling time increases the feedback decreases. This can be explained as follows. In digital control systems the sampling time may be viewed as a dead time. It is well known that systems with a dead time are destabilized by large feedback gains, which gets worse if the dead time increases. On the other hand feedback helps to speed up or realize convergence of the tracking error. Obviously a compromise is required, where the feedback decreases if the dead time increases. Finally figure 3.6 shows results based on a time-optimal reference state trajectory, again obtained from Van Willigenburg (1990a), computed using less conservative bounds on the control variables,

$$|u_x| \leq 8.00, \quad (44a)$$

$$|u_y| \leq 8.00. \quad (44b)$$

3.4 Digital controller implementation and experimental results

Figure 3.7 displays the results obtained with the

COMPUTATION OF DIGITAL OPTIMAL CONTROLLERS FOR CARTESIAN ROBOTS

implemented digital controller considered in figure 3.3. The prescribed translations of the axes equal the realizable translations in figure 3.3. Figure 3.8 shows the results obtained with the implemented digital controller considered in figure 3.4. If we implement the digital controller considered in figure 3.5 large feedback gains, shown in figure 3.5c,d result and large tracking errors occur. We believe that this is mainly caused by backlash which from figure 2.1 is obviously present in the X-link but is not considered in the dynamic model (4). Other unmodeled dynamics such as flexibility in the transmission may also cause unsatisfactory behavior when the feedback gains become too large. One way to prevent the feedback gains from becoming too large is to chose $R(t)$ unequal to zero. Then however a compromise between the magnitude of the tracking error and the control is found, while our aim was not to compromise. We therefore want to separate the choice of the feedback from the choice of the digital optimal control. Using the solutions shown in figure 3.3 and 3.4 based on (39) we may apply the optimal digital control to the system in an open loop fashion and use a so called perturbation controller to control deviations from the state trajectory to zero. The design of this perturbation controller, as will be shown, constitutes a digital regulator problem. The feedback which determines the solution of this regulator problem is influenced by the choice of the cost matrices $R(t)$, $Q(t)$ and H in (20). These matrices can be chosen independently from the matrices $Q(t)$, $R(t)$ and H of the tracking problem (23) which resulted in the open loop control. Consider the following perturbation variables

$$\Delta x(t) = x(t) - x_d(t) \quad 0 \leq t \leq t_f, \quad (45a)$$

$$\Delta u(t) = u(t) - u_d(t) \quad 0 \leq t \leq t_f, \quad (45b)$$

where u_d and x_d constitute the solution of the tracking problem given (41) and Δu is again constrained to be piecewise constant. The linear dynamics of the perturbation variables are given by (30a), while the objective is to control Δx to zero using Δu , so we have a digital regulator problem. The solution of this digital

COMPUTATION OF DIGITAL OPTIMAL CONTROLLERS FOR CARTESIAN ROBOTS

regulator problem is given by (24) and characterized by the feedback,

$$F_k = K'_k + R_k^{-1} M_k^T, \quad k=0,1,2,\dots,N-1 \quad (46)$$

Given (44) the controller takes on the following form

$$u(t) = u_d(t_k) + F_k \Delta x(t_k), \quad t_k < t \leq t_{k+1}, \quad k=0,1,2,\dots,N-1 \quad (47)$$

Based on experiments we have chosen the following values of $Q(t)$, $R(t)$ and H for the digital regulator problem, determining the perturbation controller, i.e. the feedback (46),

$$Q(t) = \begin{bmatrix} 1 & 0 & 0 & 0 \\ 0 & 1 & 0 & 0 \\ 0 & 0 & 0 & 0 \\ 0 & 0 & 0 & 0 \end{bmatrix}, \quad 0 \leq t \leq t_f, \quad (48a)$$

$$R(t) = \begin{bmatrix} 6 & 0 \\ 0 & 0.5 \end{bmatrix} \quad 0 \leq t \leq t_f, \quad (48b)$$

$$H = \begin{bmatrix} 0.3 & 0 & 0 & 0 \\ 0 & 0.3 & 0 & 0 \\ 0 & 0 & 0.1 & 0 \\ 0 & 0 & 0 & 0.1 \end{bmatrix} \quad (48c)$$

The feedback gains F_k obtained with these values are shown in figure 3.9a,b and again reach a steady state value. Figure 3.9 furthermore shows the results obtained with the implemented controller (47). Finally figure 3.10 shows the results obtained with the implemented controller based on figure 3.6. As in the case of figures 3.7 and 3.8 we again directly implemented the digital optimal tracker result.

From the figure 3.7,...,3.10 we observe that using sampling times up to 100mS results in tracking errors smaller than 1 cm, which seems a good result observing that the link velocities reach

values of about 1 m/s. Finally observe that the tracking errors which are caused by model and measurement inaccuracies dominate the errors due to the piecewise constant constraint on the control shown in figures 3.3,...,3.6.

4 Conclusions

We have treated a procedure to design and compute digital optimal tracking controllers for cartesian robots where both viscous and coulomb friction are considered to be part of the robot dynamics and where the influence of gravity is included. The design is based on the recently developed digital optimal regulator and tracker and assumes the robot motion as a function of time, to be known in advance. While usual design procedures only consider the behavior at the sampling instants, and therefore demand "small" sampling times, both the digital optimal regulator and tracker explicitly consider the inter-sample behavior, allowing for "large" sampling times. In the case of robot control this is important since the computational burden on the computer is generally high.

Based on our procedure we designed and computed digital controllers for an industrial cartesian X-Y robot. Experimental results obtained with the implemented digital controllers demonstrated that sampling times which are generally considered too large for robot control lead to good results. A robot motion control problem is a tracking problem. The digital optimal tracker may be implemented directly since the solution is in feedback form. Large feedback gains however, may result in unsatisfactory behavior due to for instance unmodeled dynamics. Large feedback gains occur when the sampling time is "small". Therefore we also presented a method by which it is possible to design the feedback separately. The method is based on the idea of perturbation control, and the perturbation controller is designed using the digital optimal regulator result.

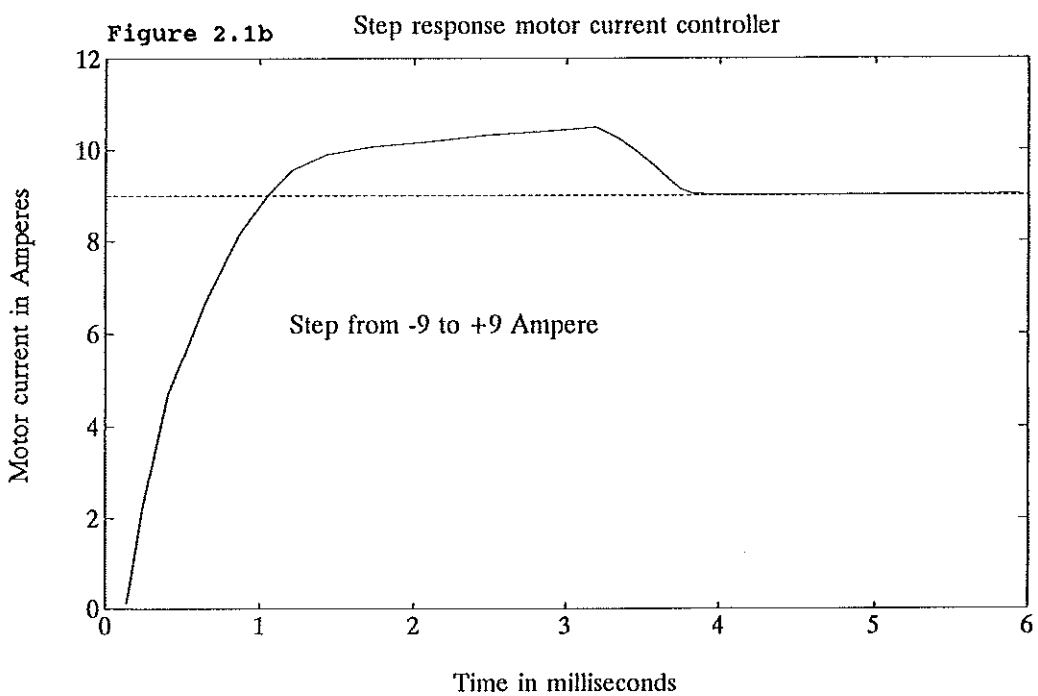
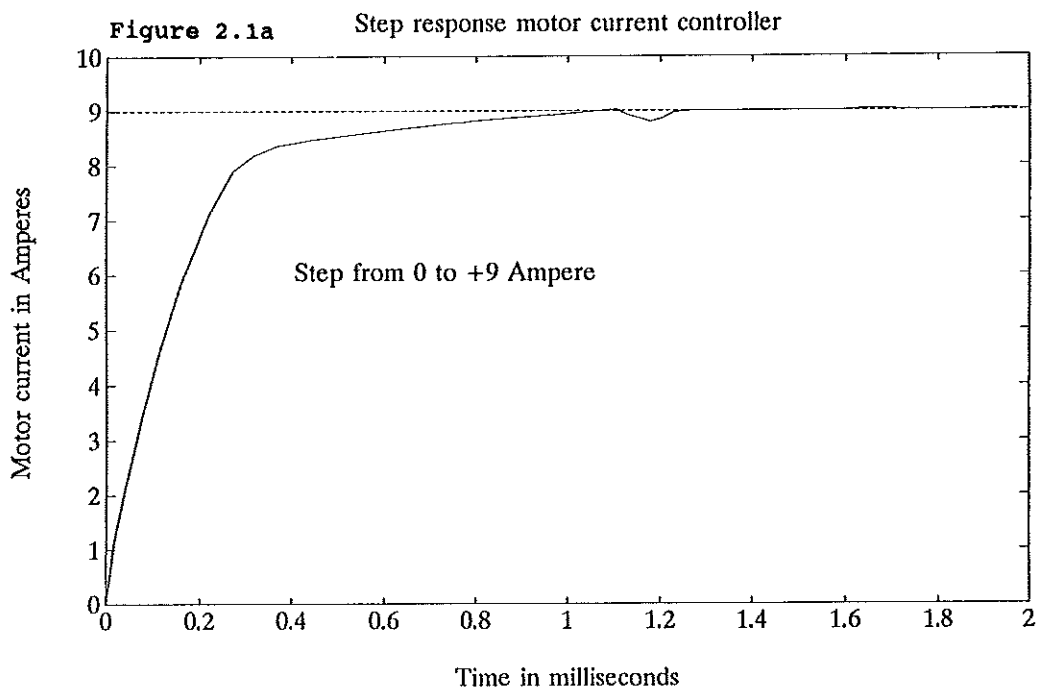
Finally if we combine our design procedure with a method to

COMPUTATION OF DIGITAL OPTIMAL CONTROLLERS FOR CARTESIAN ROBOTS

compute time-optimal motions for cartesian robots, based on continuous-time controls (Van Willigenburg, 1990a), we obtain a two step procedure to design digital time-optimal controllers for cartesian robots.

References

- ACKERMANN J., 1985, 'Sampled data control-systems', Springer Verlag.
- ASADA H., SLOTINE J.J.E., Robot Analyses and Control, Wiley: New York
- ASTROM K.J., WITTENMARK B., 1984, Computer controlled systems, Englewood Cliffs, NJ: Prentice Hall
- FRANKLIN, G.F., POWELL D., 1980, Digital control of dynamic systems, Addison and Wesley.
- LEWIS F.L., 1986, Optimal Control, Wiley
- VUKOBRATOVIC M., STOKIC D., 1982, Control of manipulation Robots: Theory and Application, Springer Verlag, Berlin
- VAN WILLIGENBURG L.G., 1989, 'True digital tracking for an orthogonal robot manipulator', Proc. ICCON '89, TP 3-5.
- VAN WILLIGENBURG L.G., 1990a, 'Computation of time-optimal motions for an industrial X-Y robot subjected to actuator and path constraints', submitted for publication
- VAN WILLIGENBURG L.G., DE KONING W.L., 1990a, 'The digital optimal regulator and tracker for deterministic time-varying systems', submitted for publication
- VAN WILLIGENBURG L.G., DE KONING W.L., 1990b, 'The digital optimal regulator and tracker for stochastic time-varying systems', submitted for publication
- VAN WILLIGENBURG L.G., 1990b, 'Numerical procedures to compute the digital optimal regulator and tracker for time-varying systems', submitted for publication



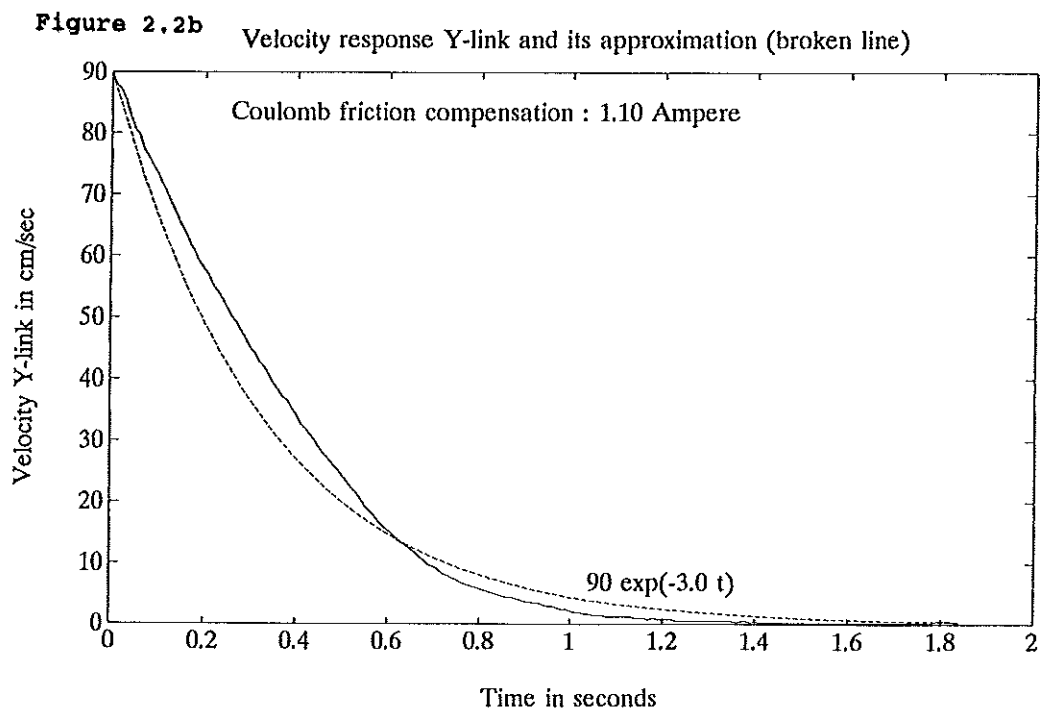
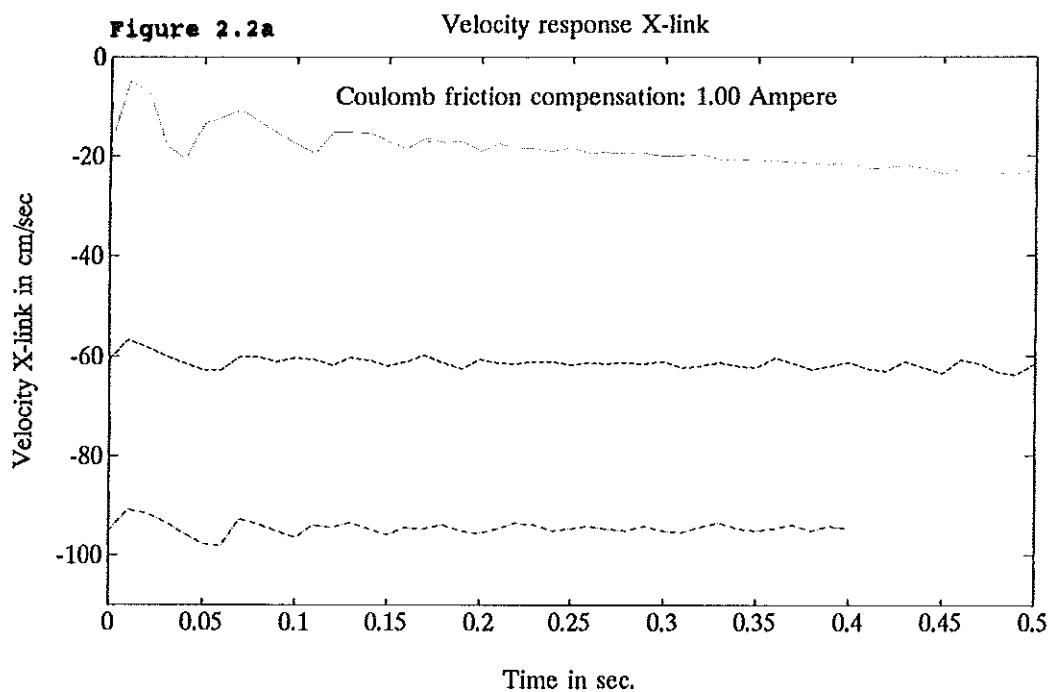


Figure 3.1a

Prescribed and realizable translation ax1

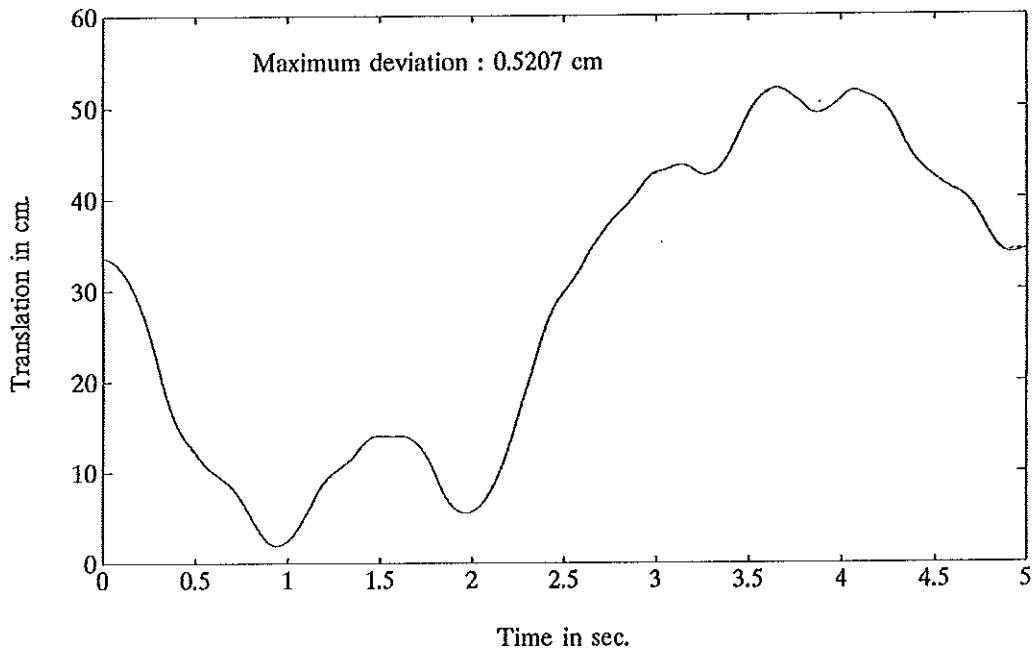


Figure 3.1b

Prescribed and realizable translation ax2

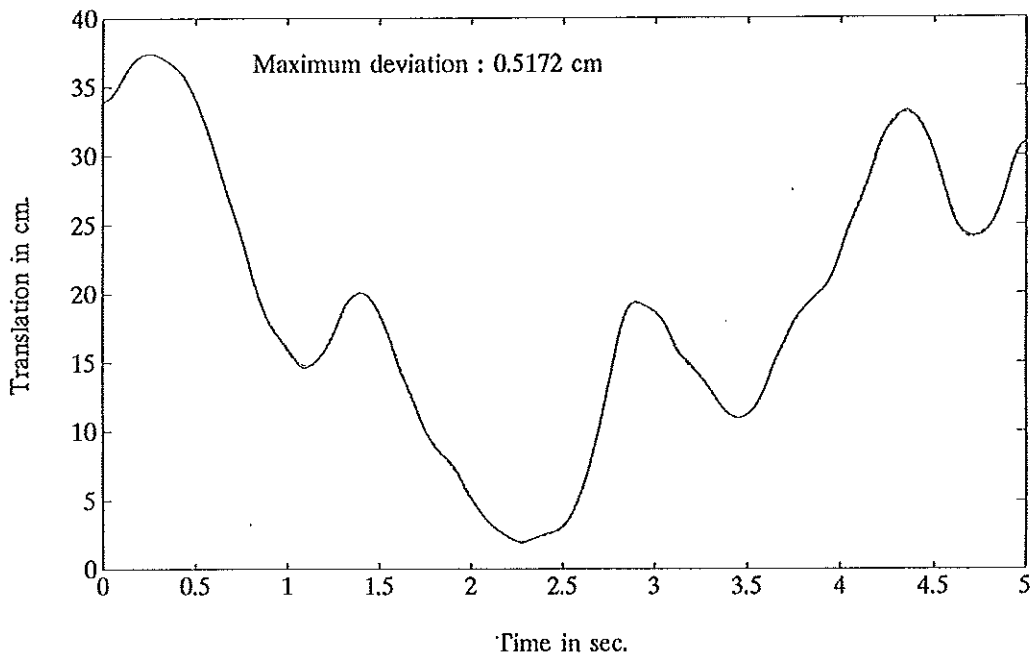


Figure 3.1c

Feedback ax1 for final 0.89 seconds

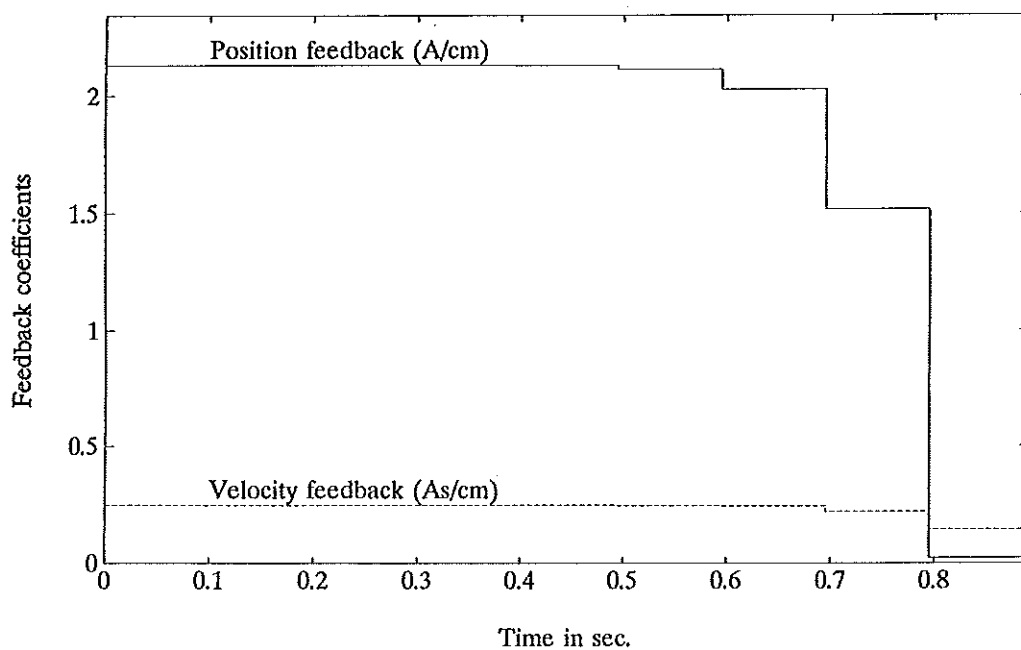


Figure 3.1d

Feedback ax2 for final 0.89 seconds

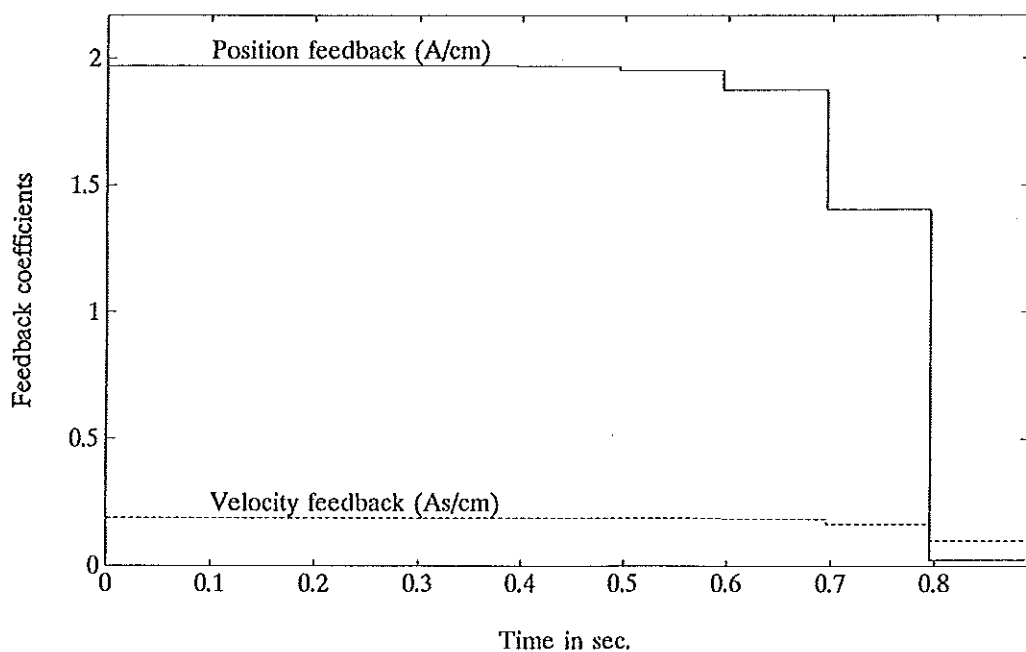


Figure 3.2a Prescribed and realizable translation ax1

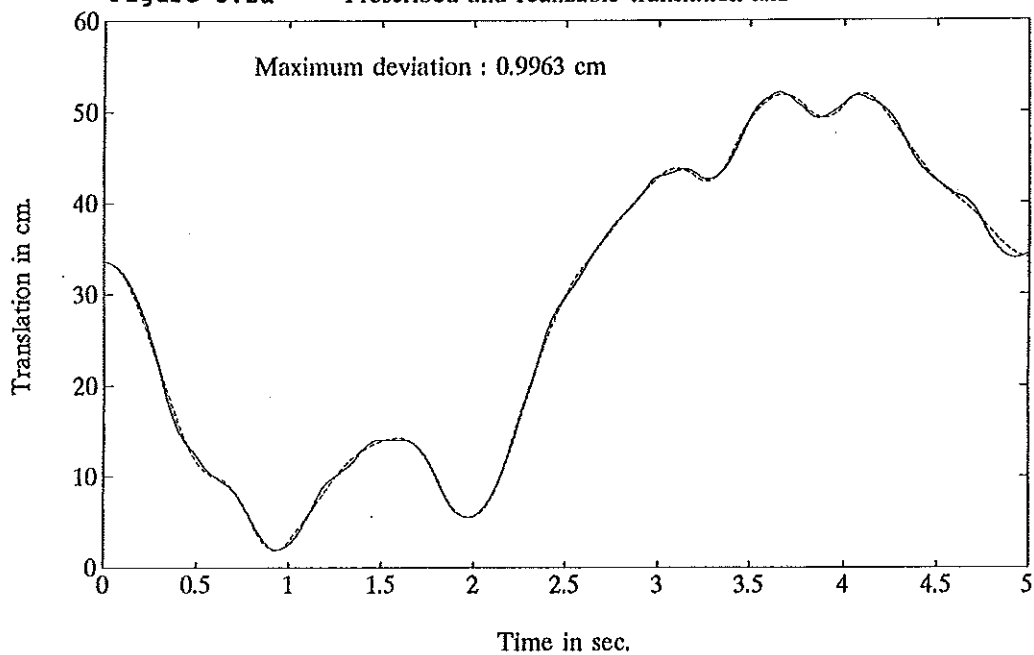


Figure 3.2b Prescribed and realizable translation ax2

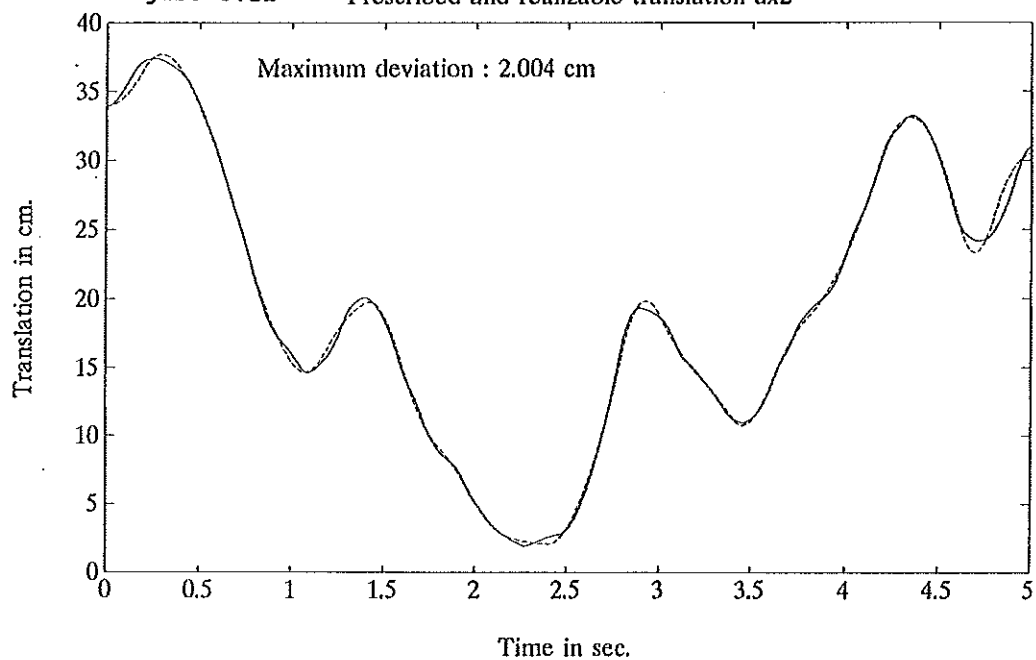


Figure 3.2c Feedback ax1 for final 0.79 seconds

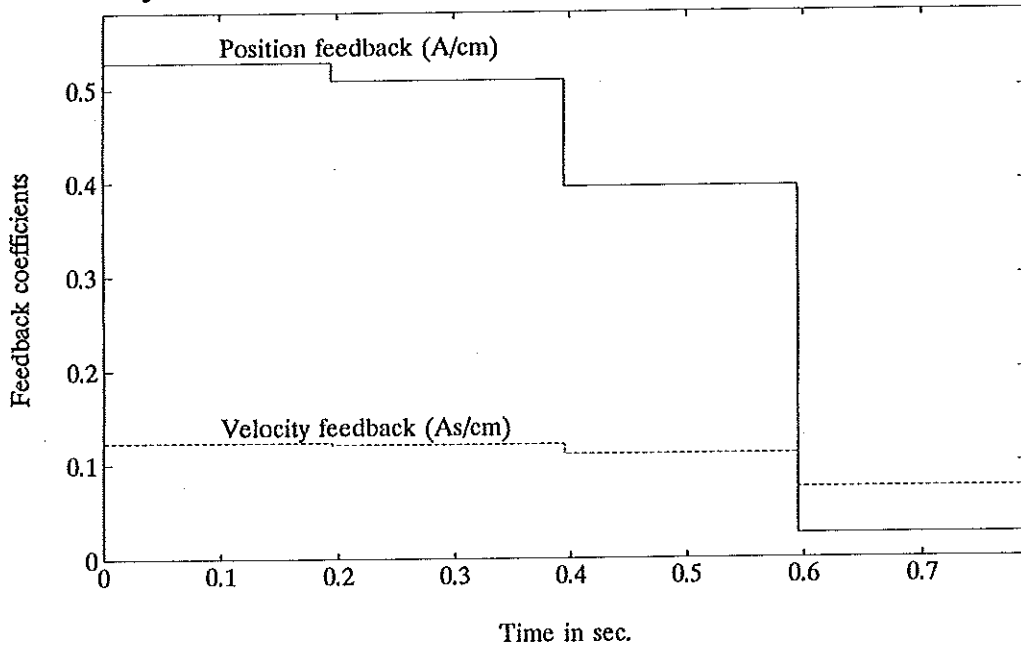
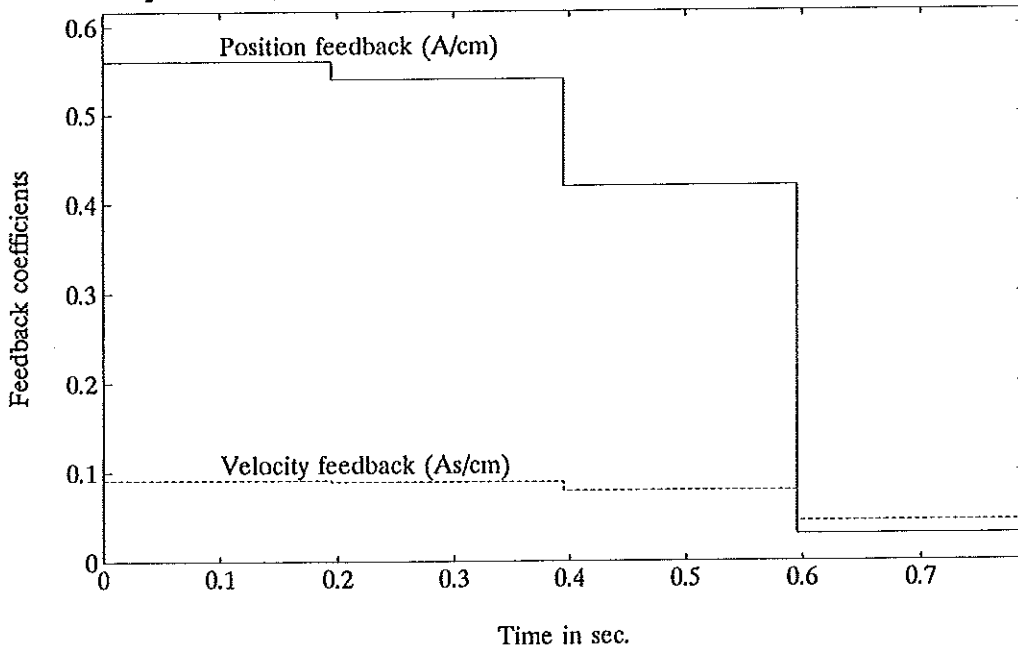


Figure 3.2d Feedback ax2 for final 0.79 seconds



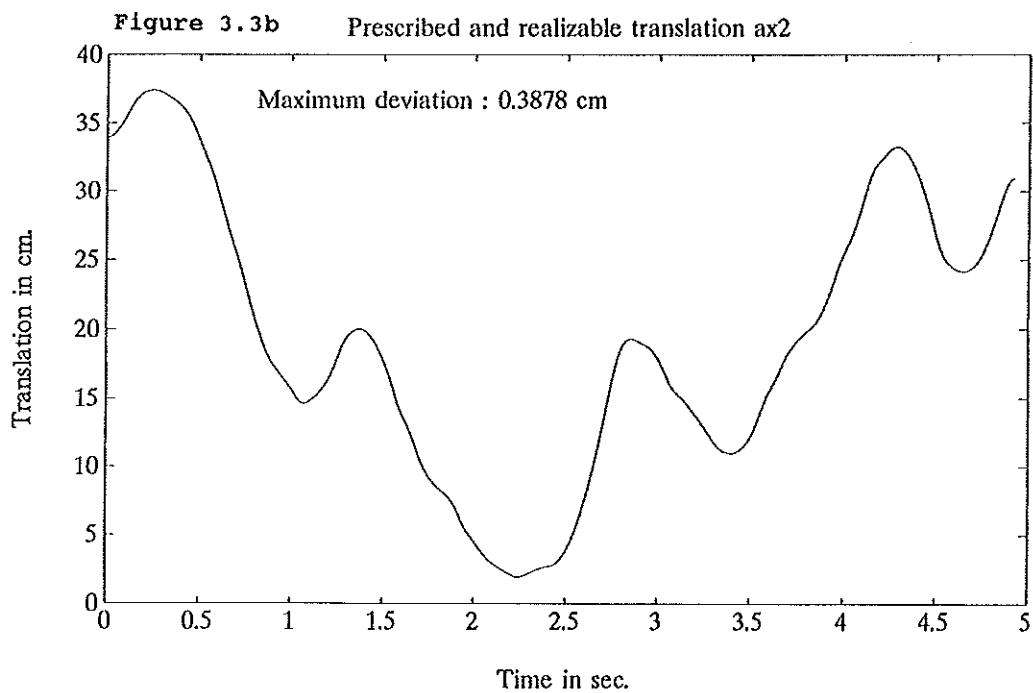
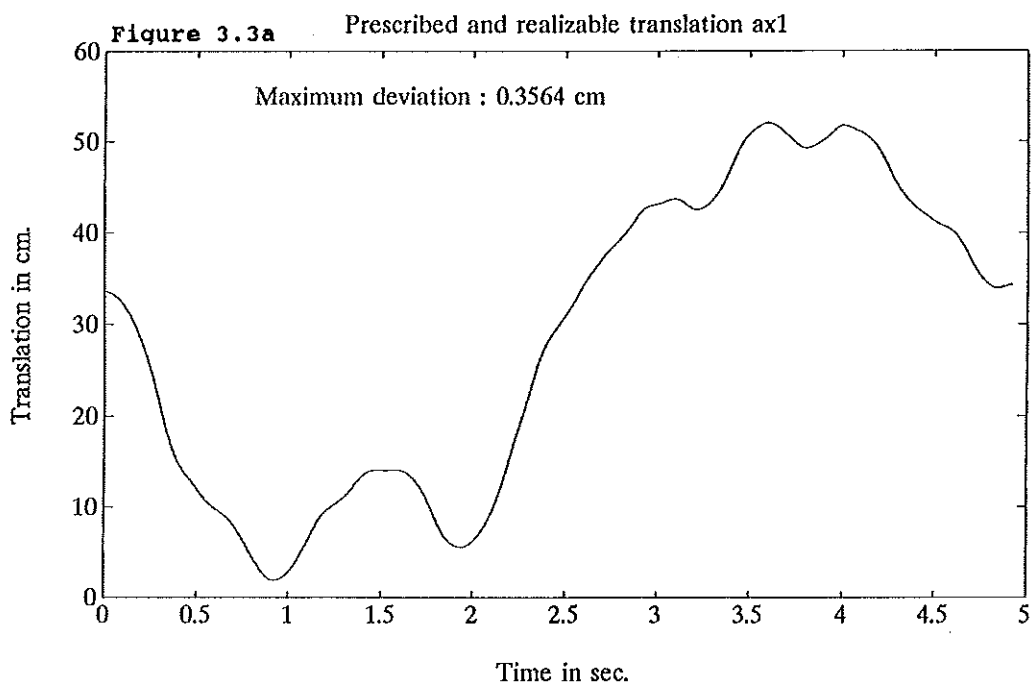


Figure 3.3c Feedback ax1 for final 0.95 seconds

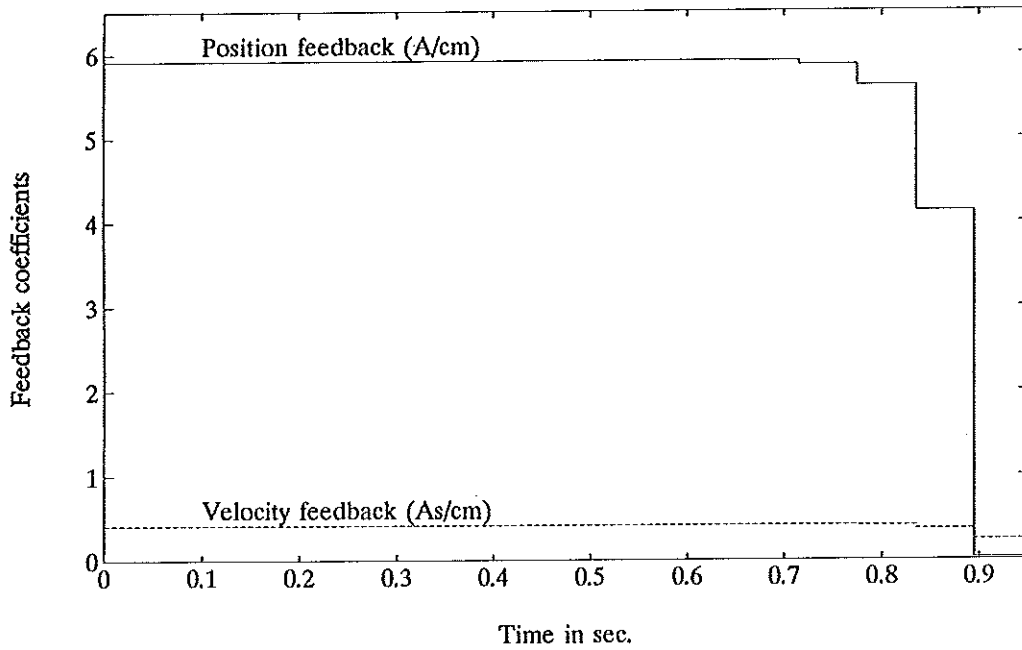


Figure 3.3d Feedback ax2 for final 0.95 seconds

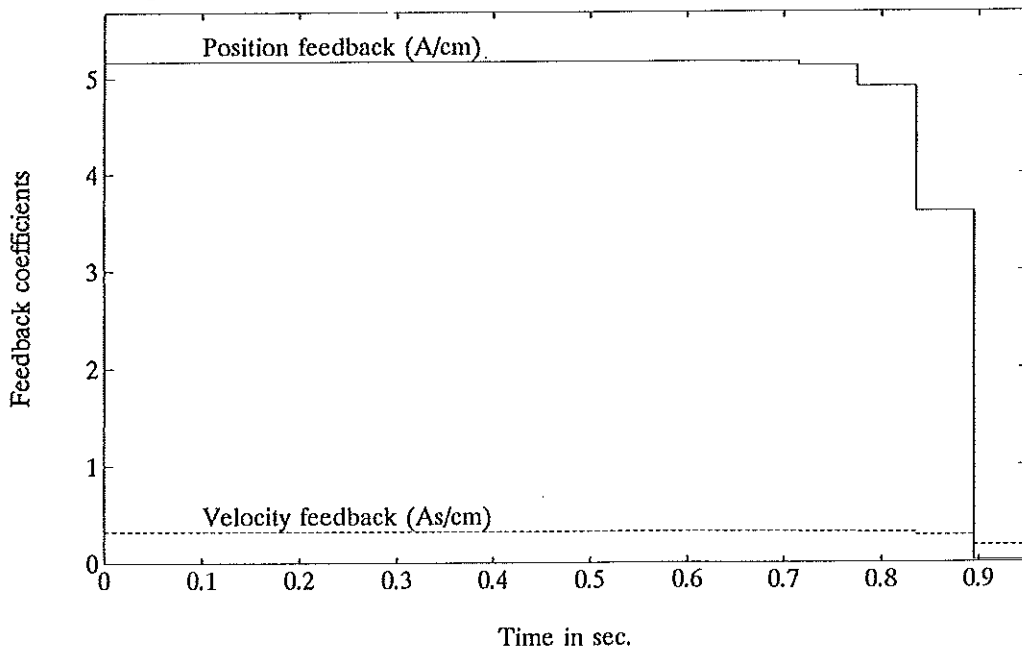


Figure 3.4a Prescribed and realizable translation ax1

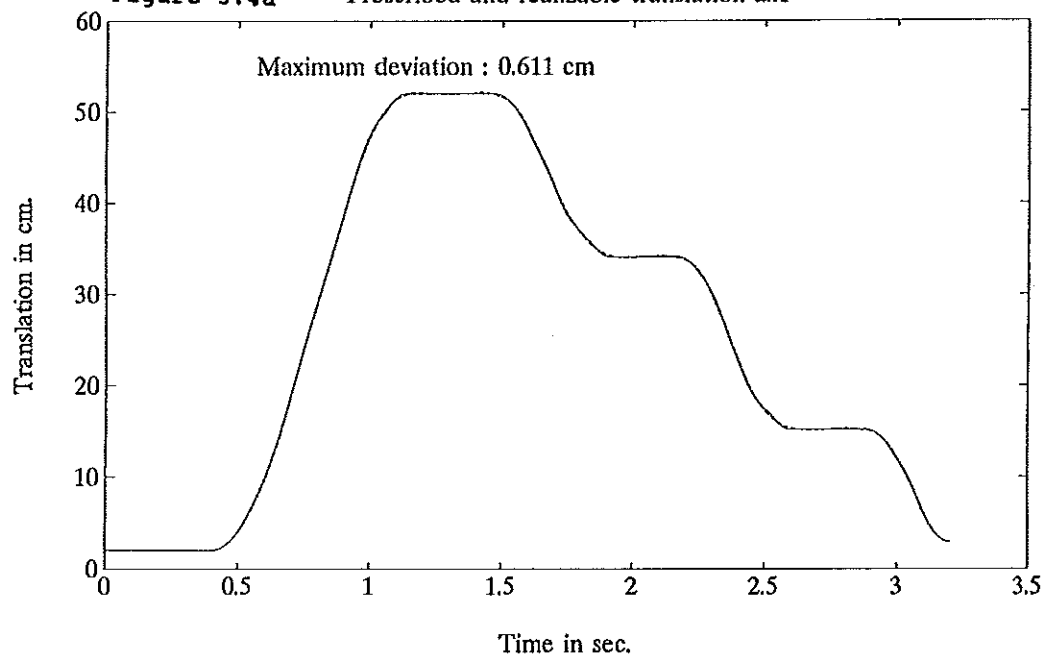


Figure 3.4b Prescribed and realizable translation ax2

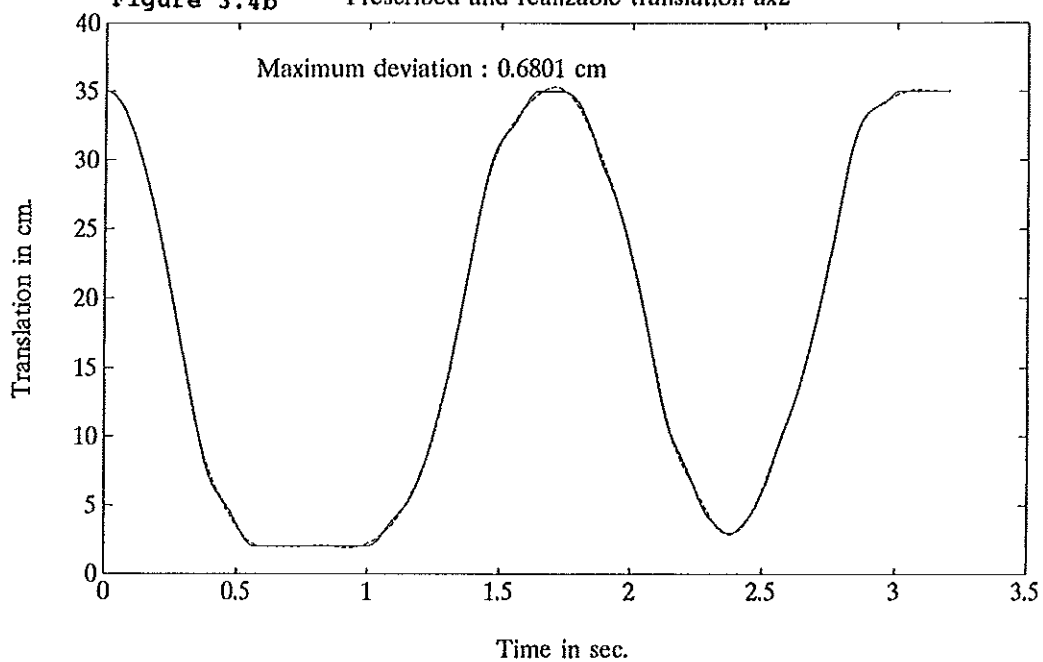


Figure 3.4c Feedback ax1 for final 0.89 seconds

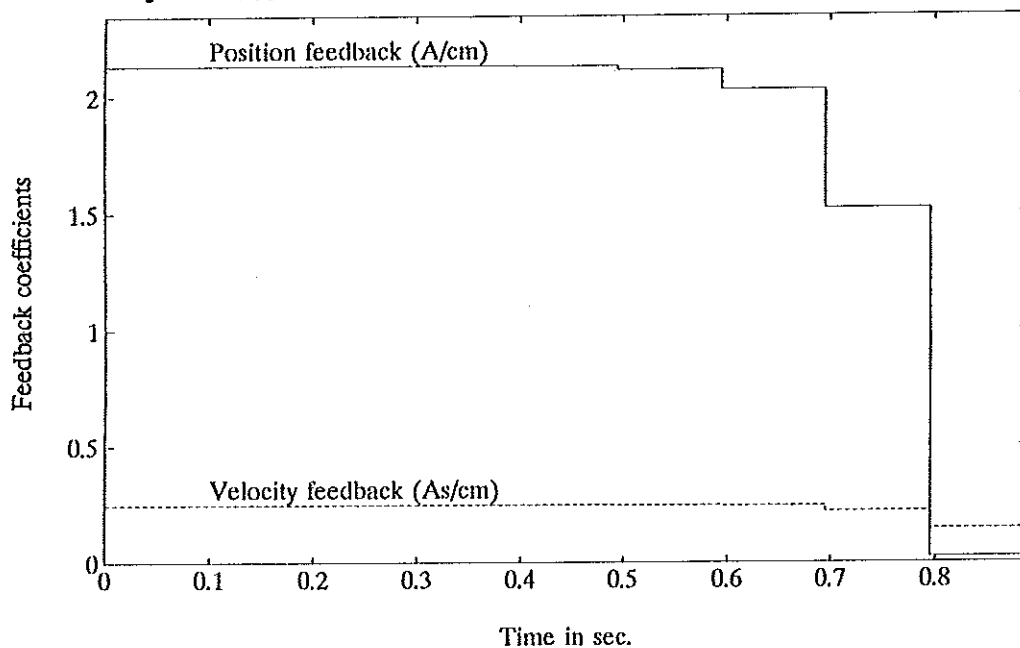


Figure 3.4d Feedback ax2 for final 0.89 seconds

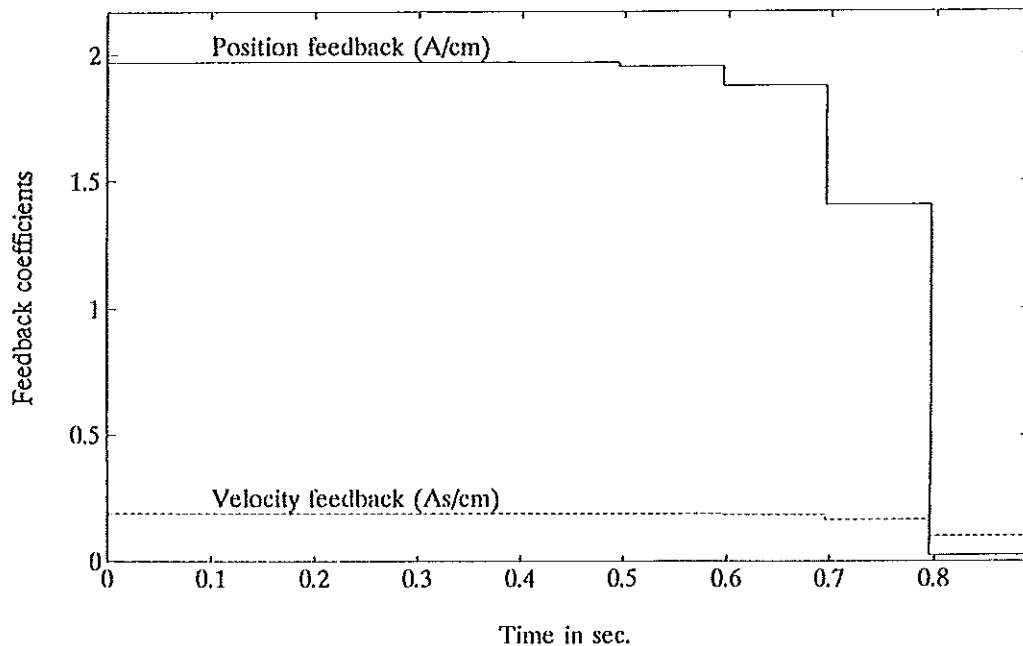


Figure 3.5a Prescribed and actual (broken line) translation ax1

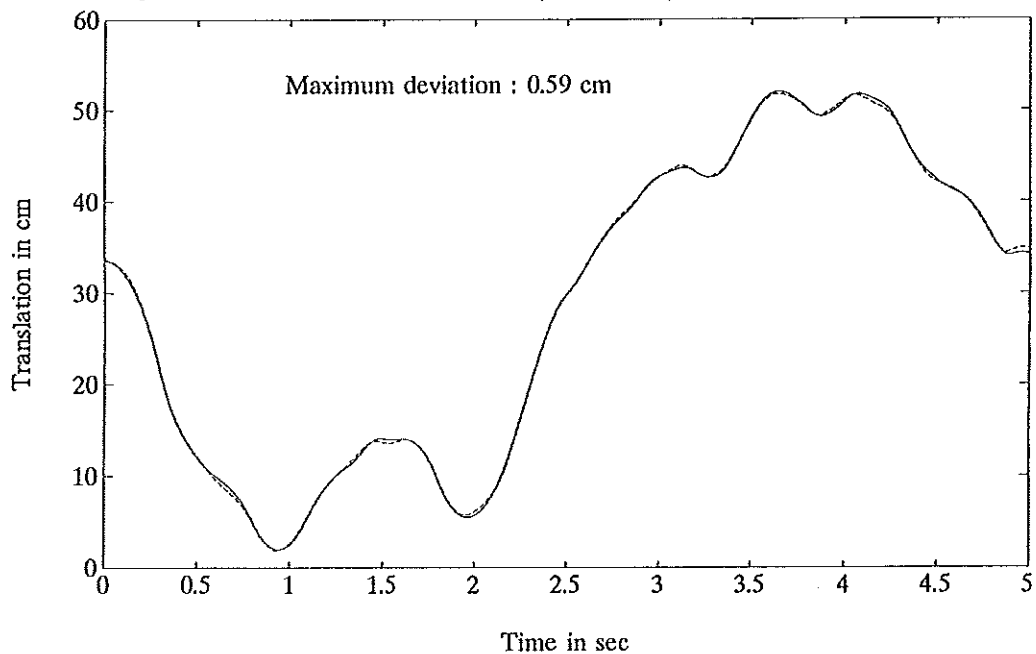


Figure 3.5b Prescribed and actual (broken line) translation ax2

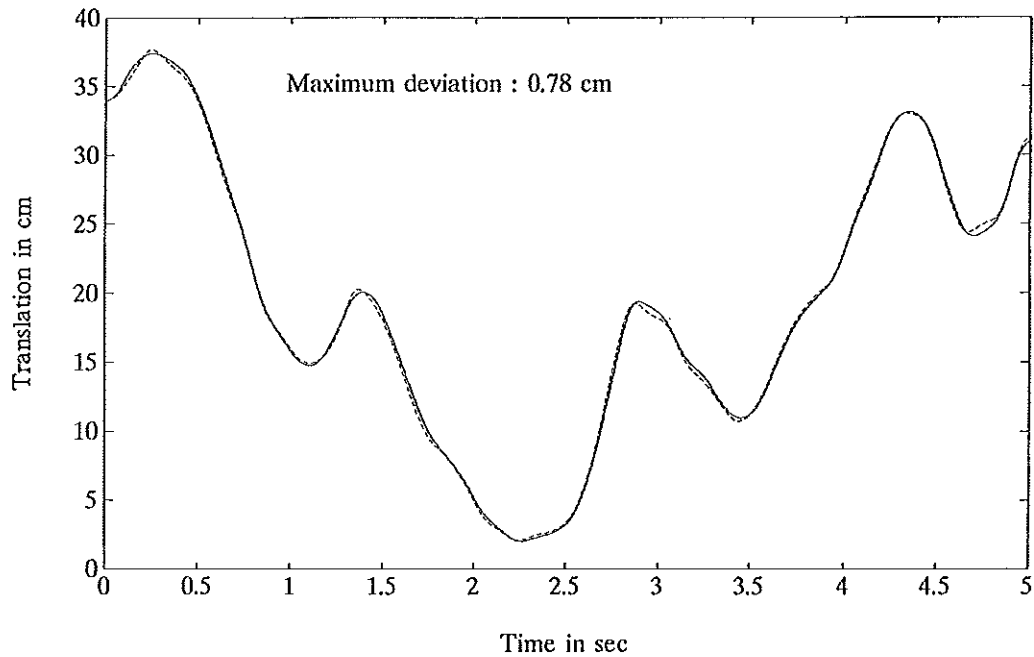


Figure 3.5c Prescribed and actual (broken line) speed ax1

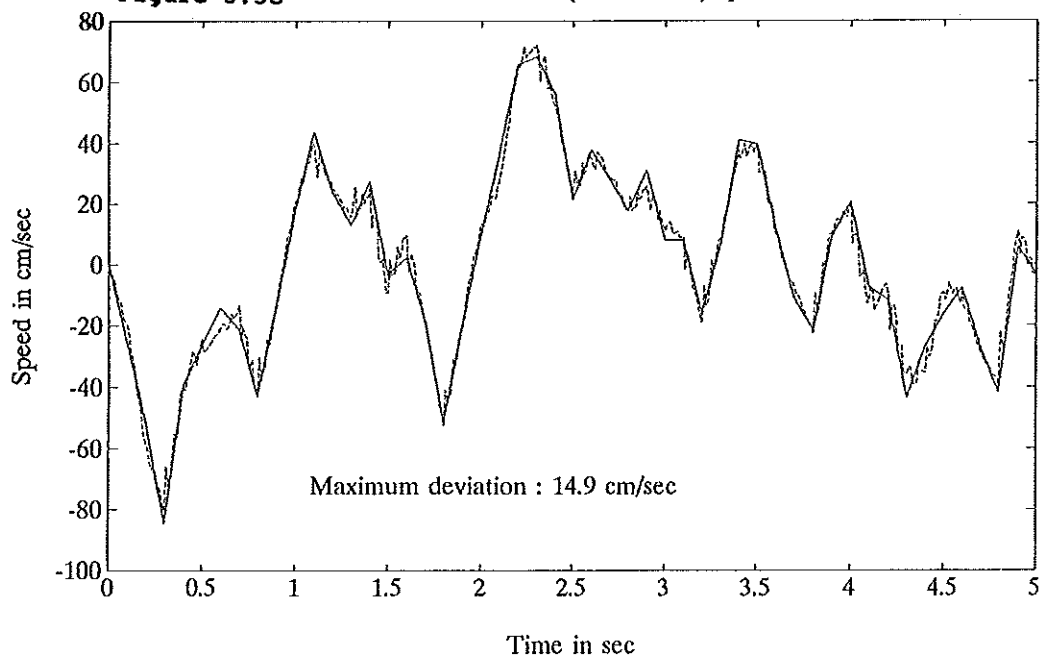


Figure 3.5d Prescribed and actual (broken line) speed ax2

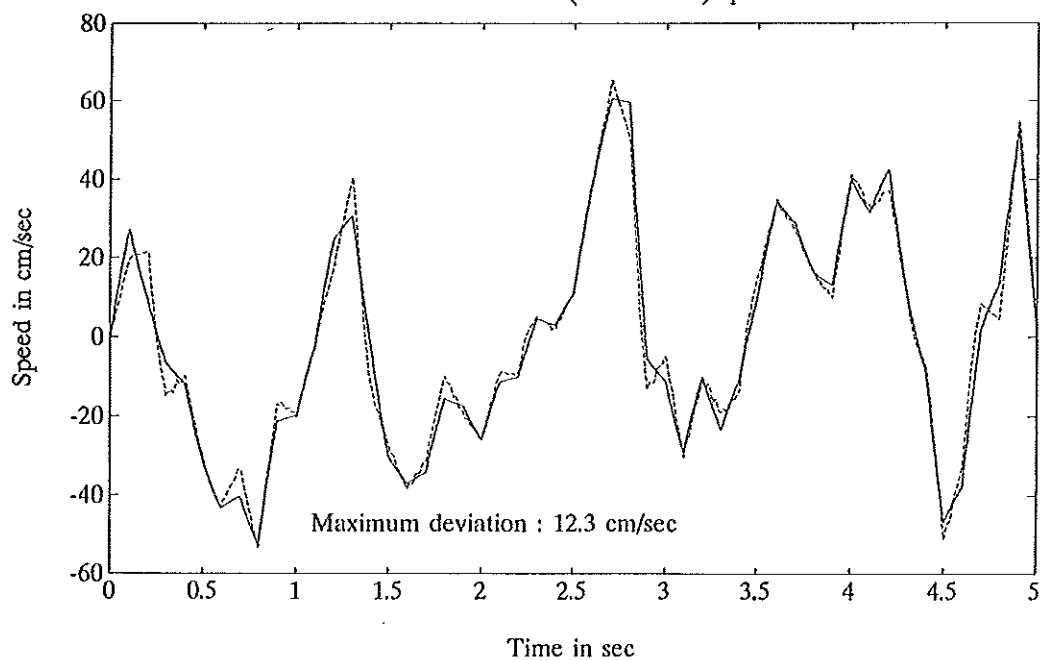


Figure 3.5e Prescribed and actual (broken line) control ax1

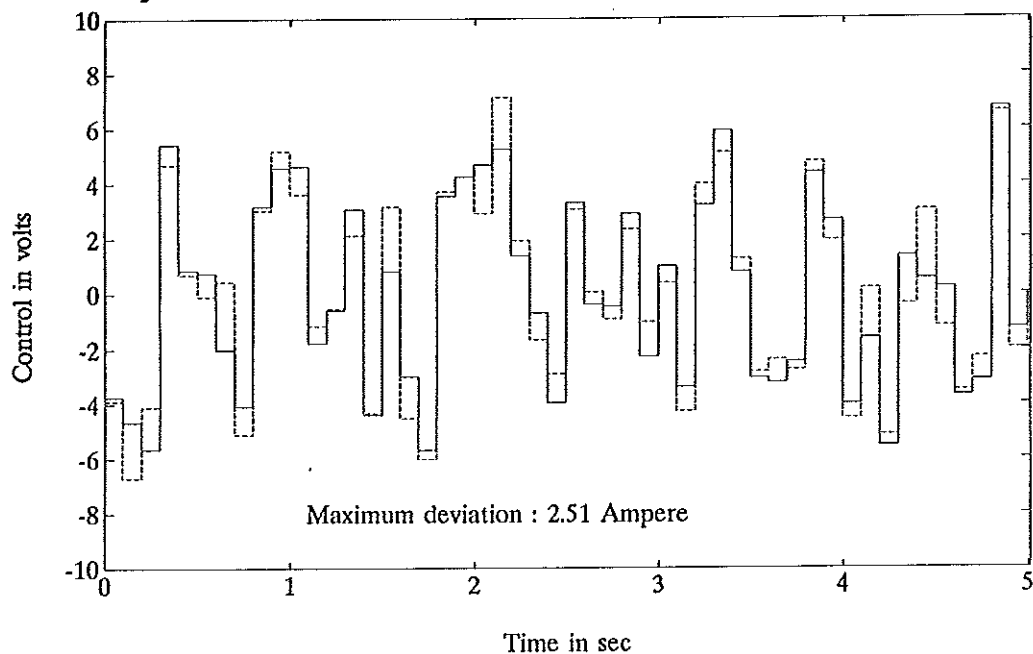


Figure 3.5f Prescribed and actual (broken line) control ax2

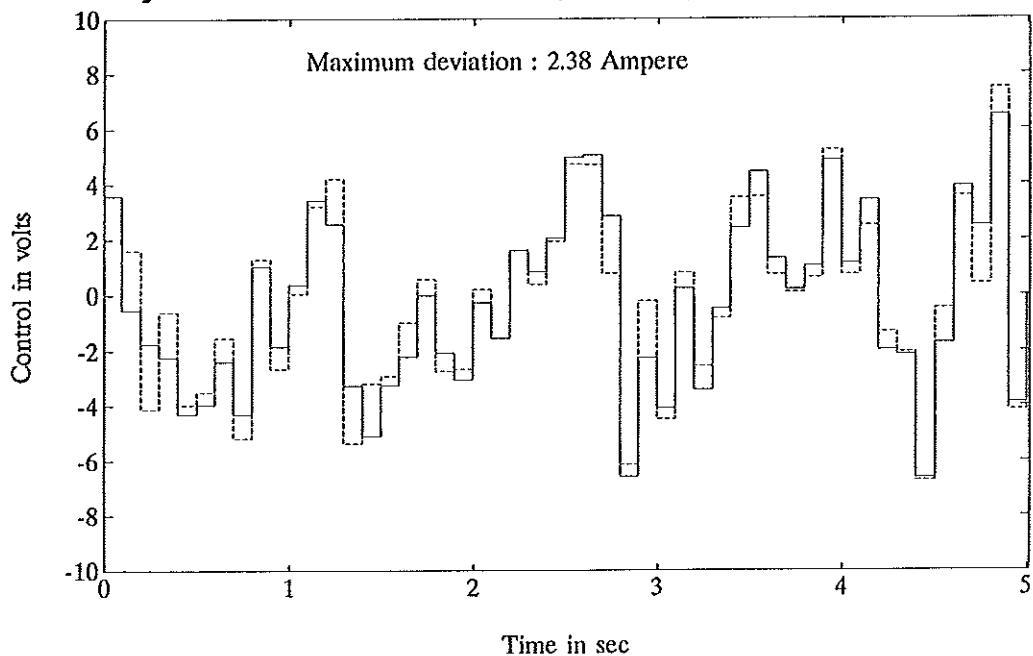


Figure 3.6a Prescribed and actual (broken line) translation ax1

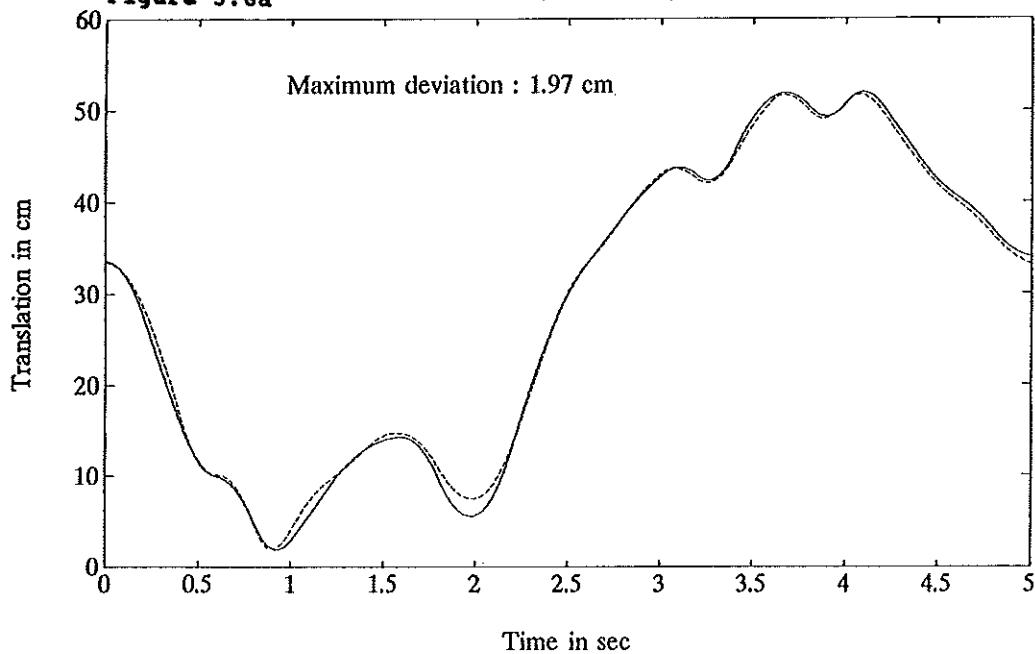


Figure 3.6b Prescribed and actual (broken line) translation ax2

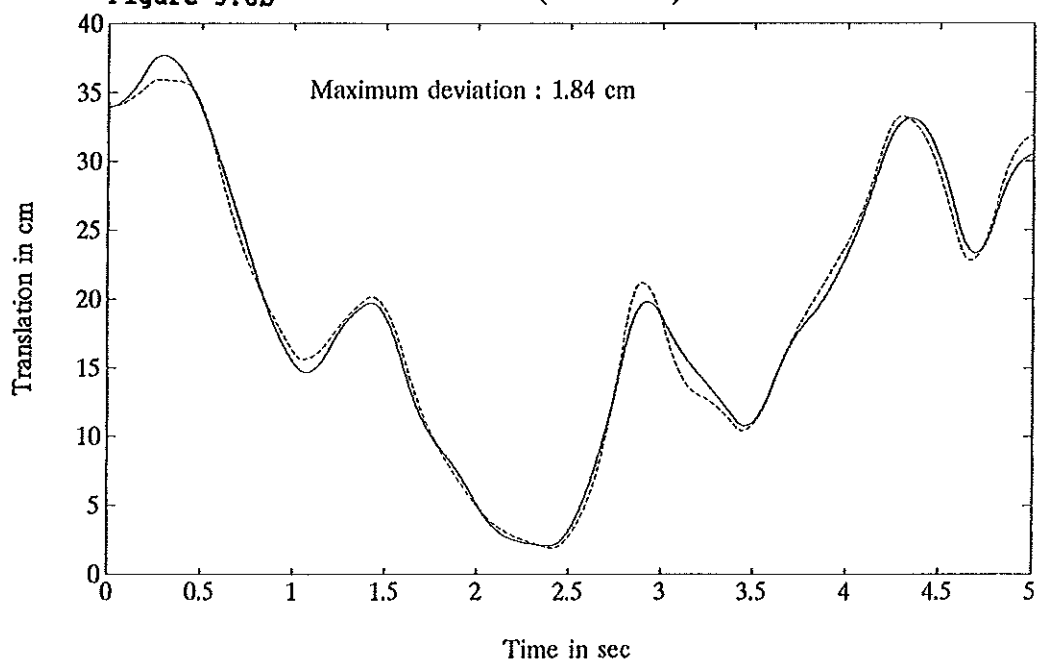


Figure 3.6c Prescribed and actual (broken line) speed ax1

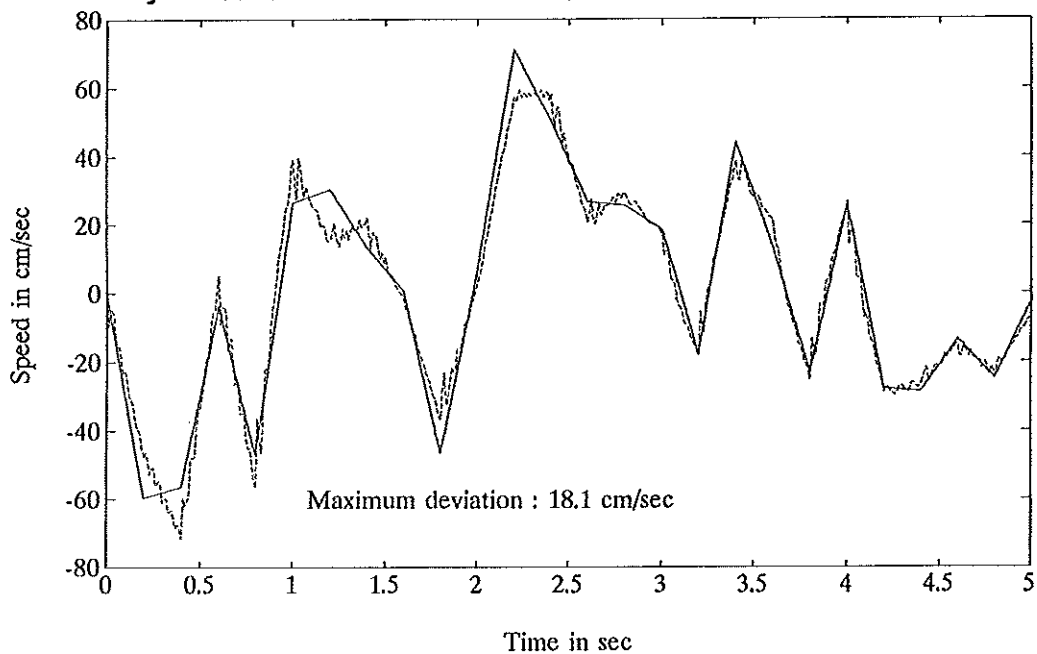


Figure 3.6d Prescribed and actual (broken line) speed ax2

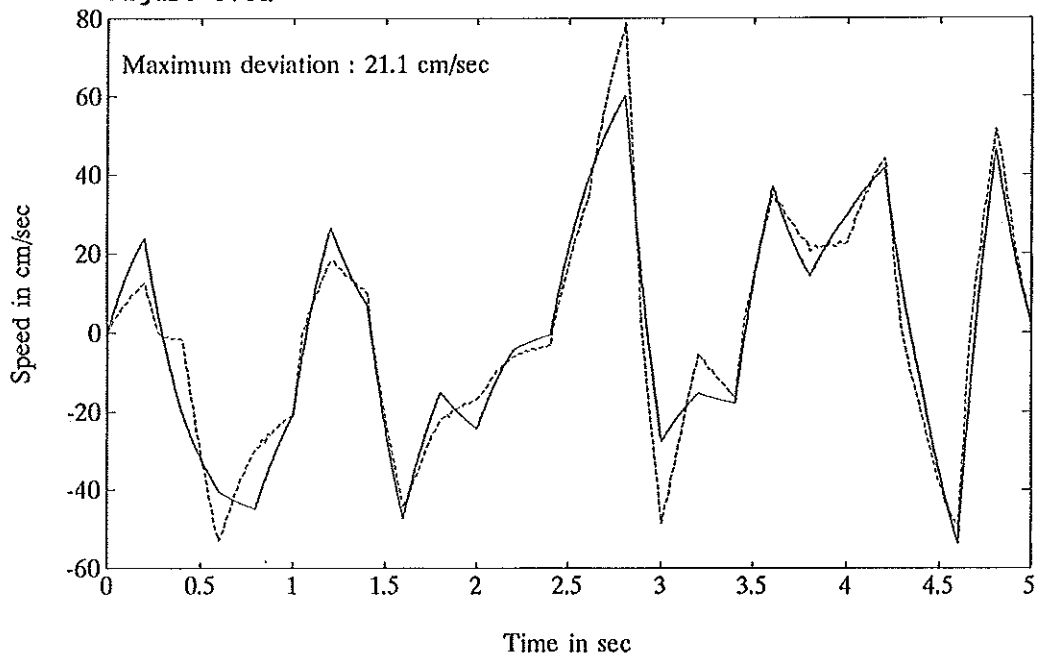


Figure 3.6e Prescribed and actual (broken line) control ax1

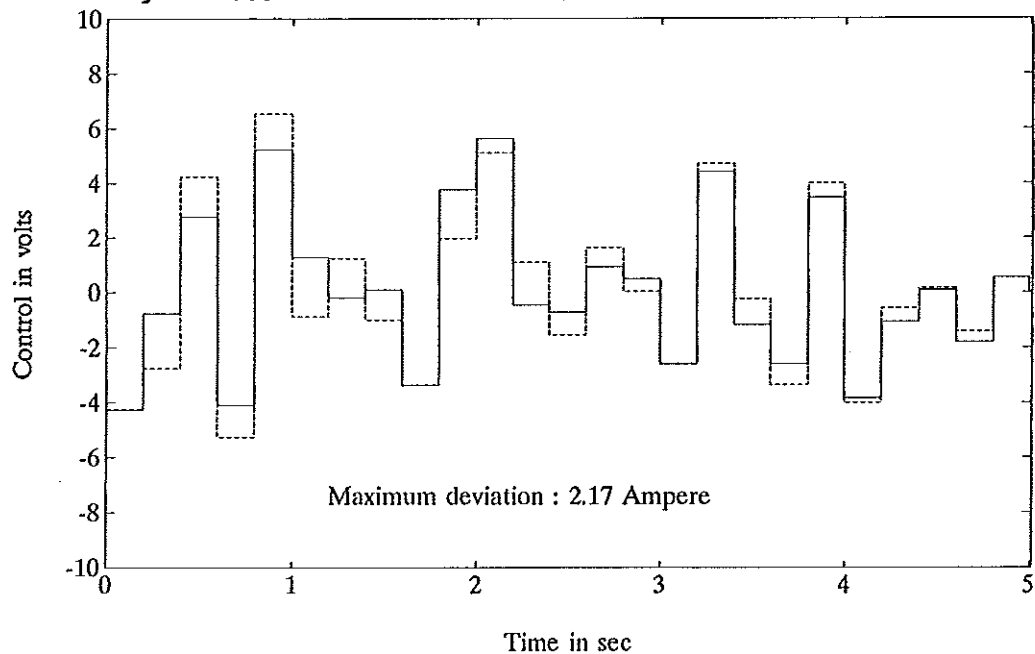


Figure 3.6f Prescribed and actual (broken line) control ax2

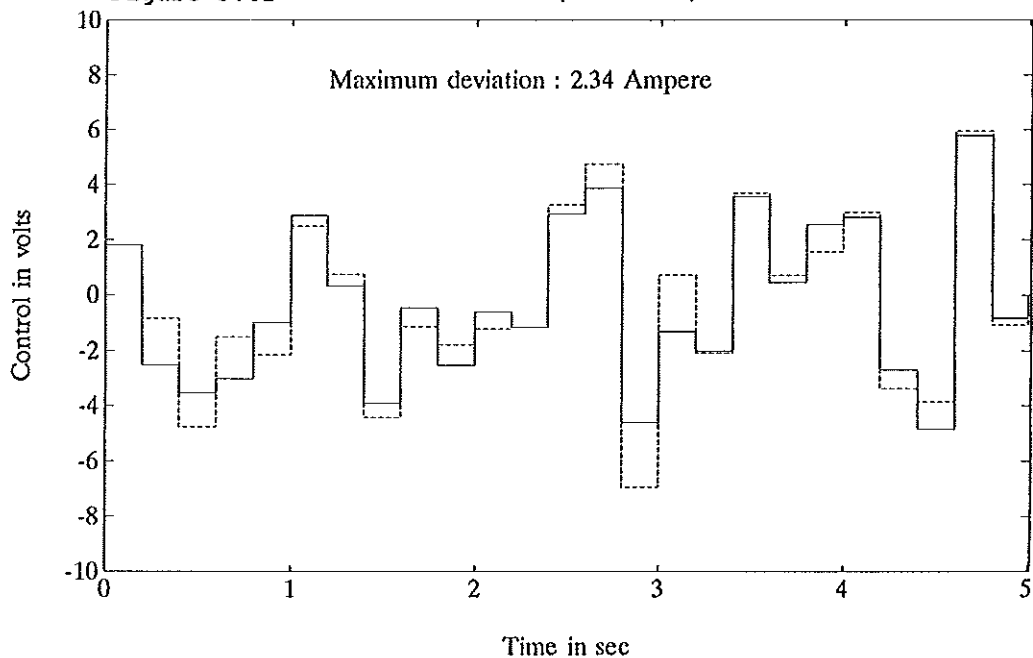


Figure 3.7a Feedback ax1 for final 0.95 seconds

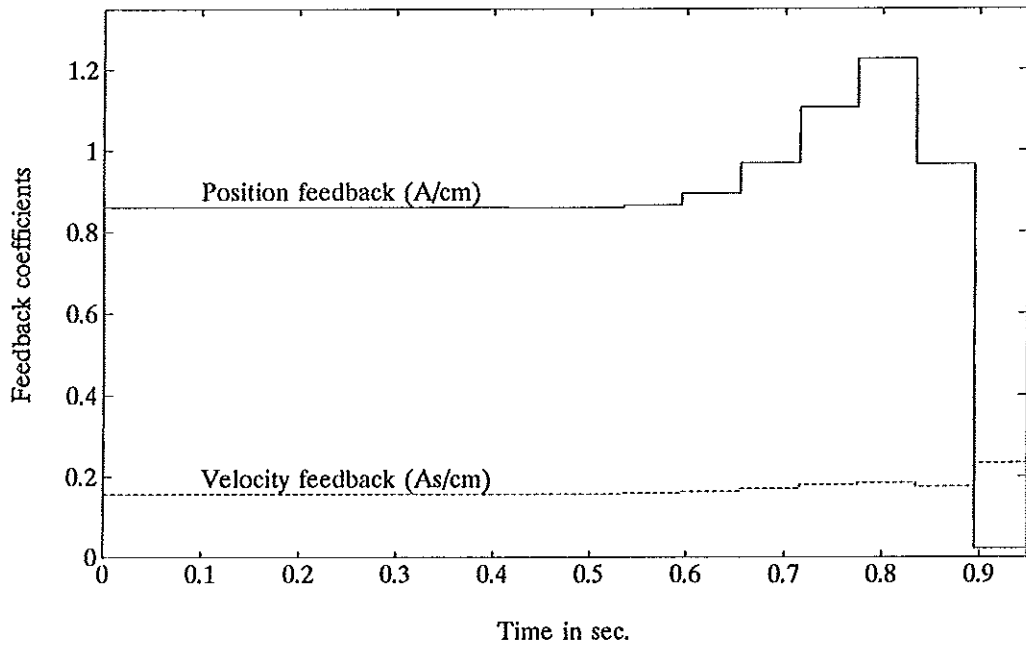


Figure 3.7b Feedback ax2 for final 0.95 seconds

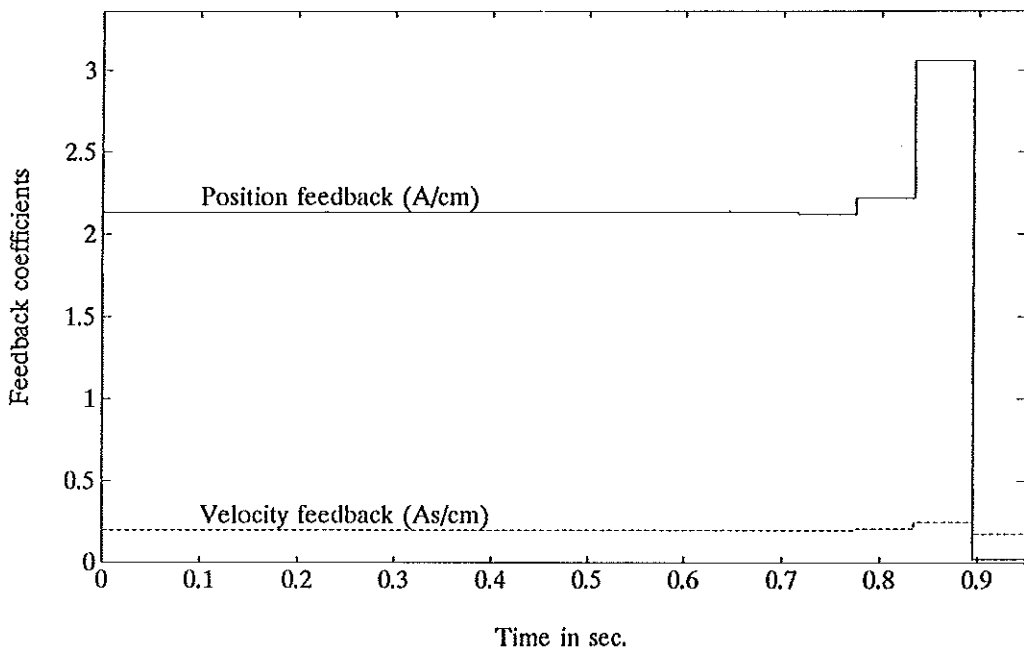


Figure 3.7c Prescribed and actual (broken line) translation ax1

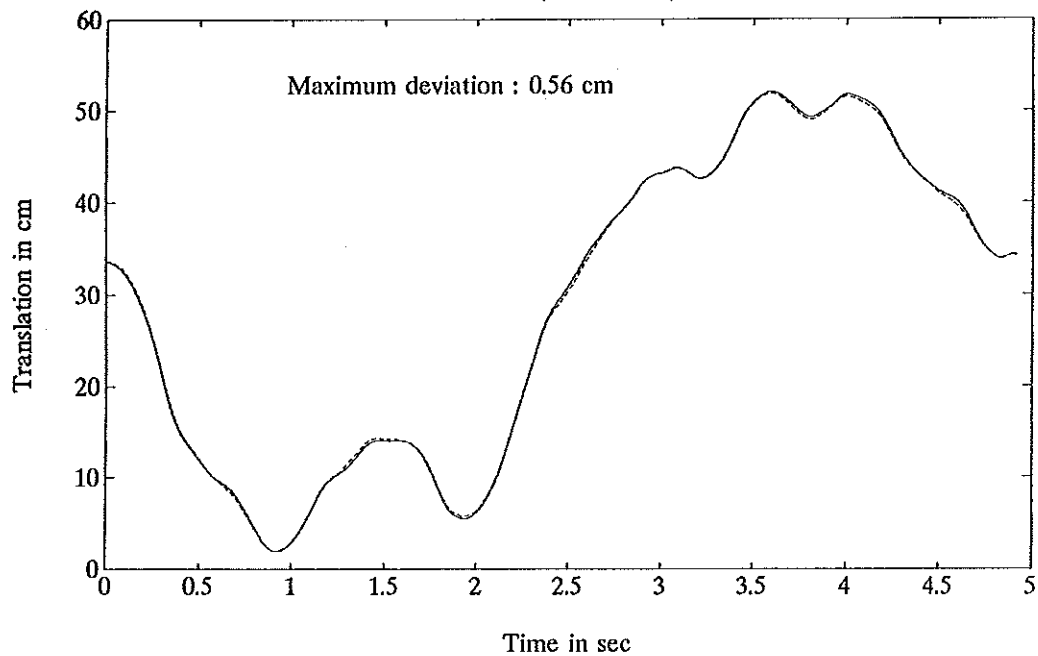


Figure 3.7d Prescribed and actual (broken line) translation ax2

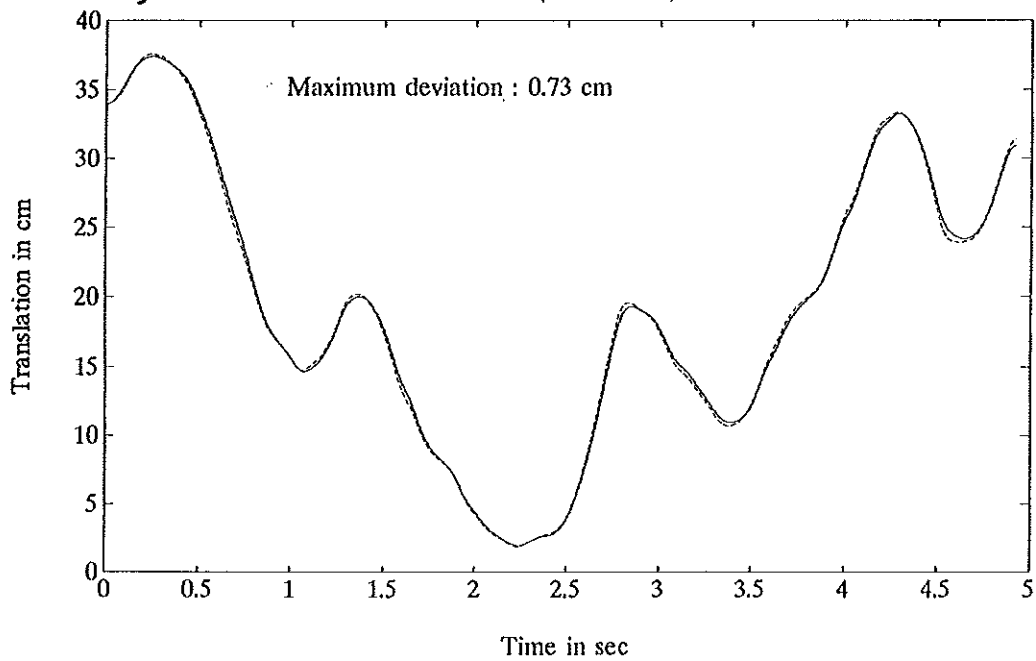


Figure 3.7e Prescribed and actual (broken line) speed ax1

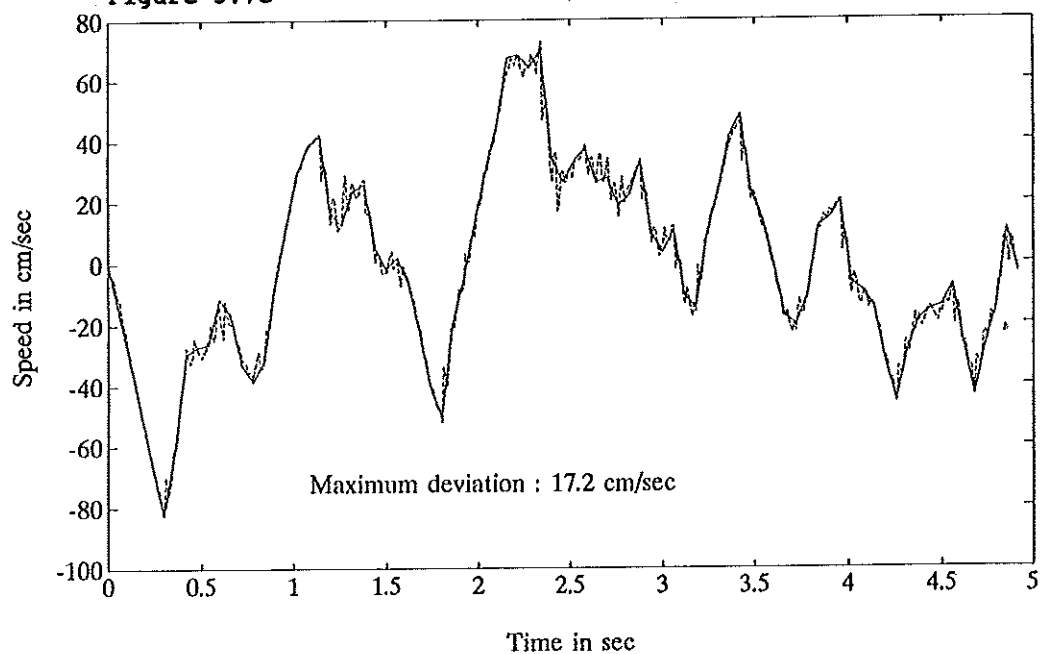


Figure 3.7f Prescribed and actual (broken line) speed ax2

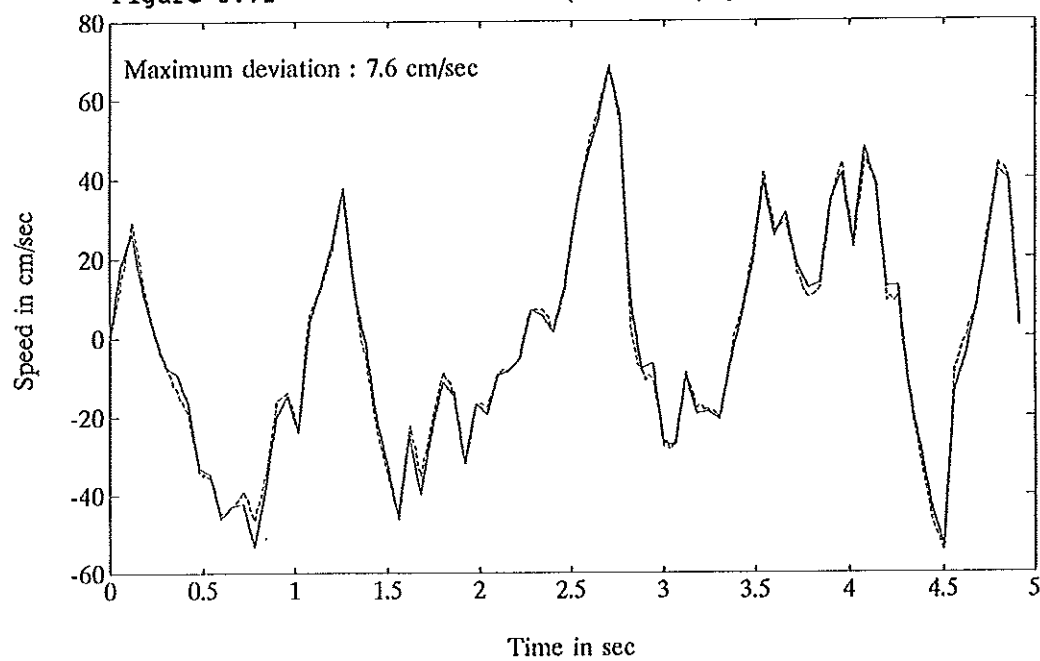


Figure 3.7g Prescribed and actual (broken line) control ax1

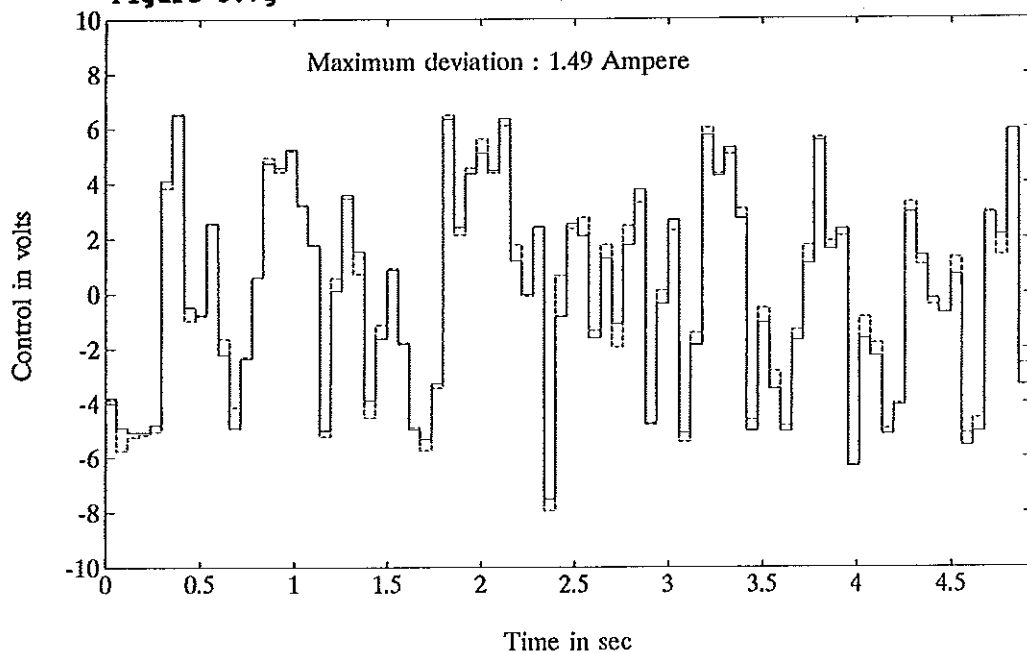


Figure 3.7h Prescribed and actual (broken line) control ax2

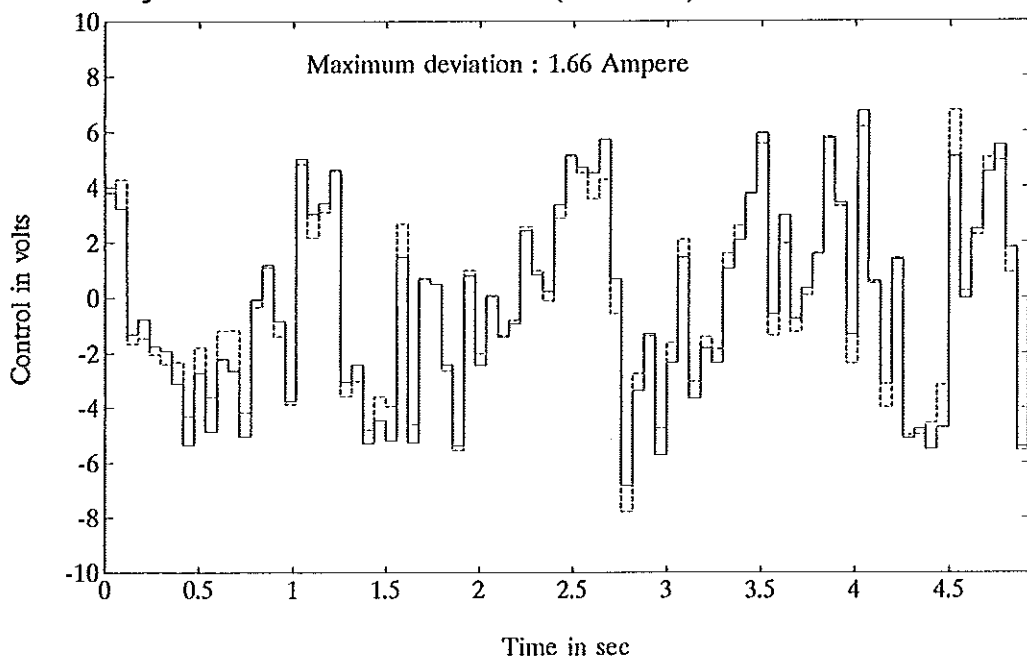


Figure 3.8a Prescribed and actual (broken line) translation ax1

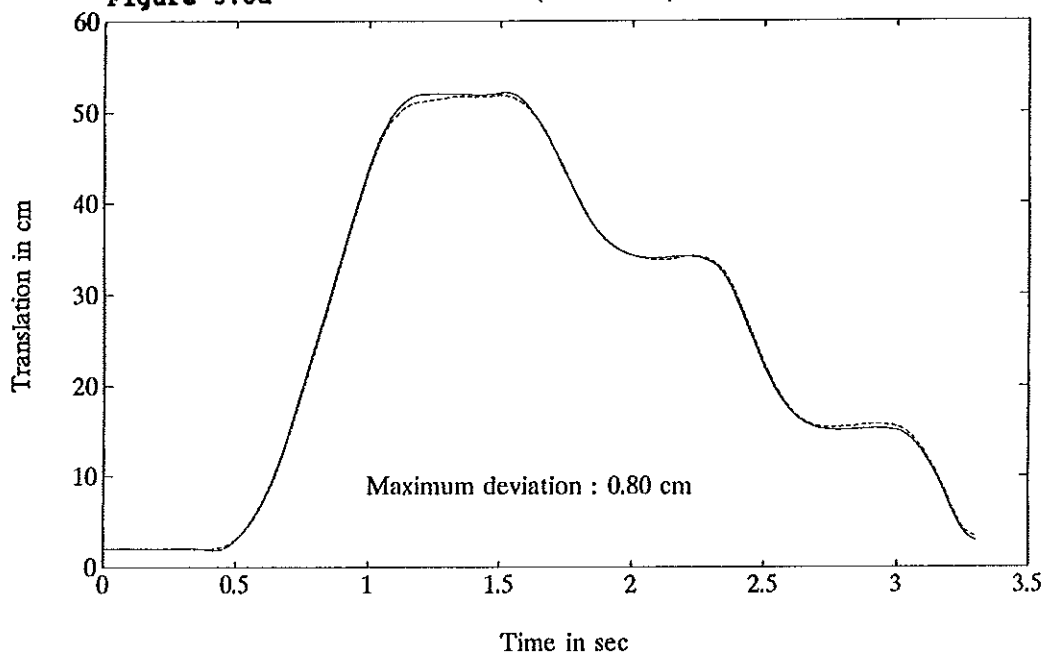


Figure 3.8b Prescribed and actual (broken line) translation ax2

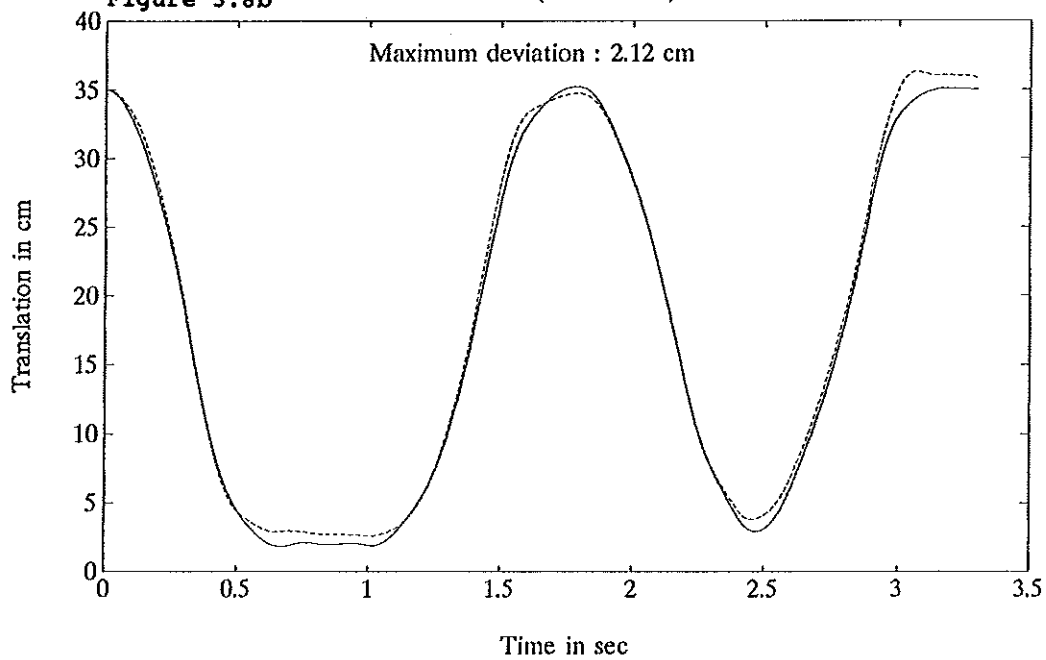


Figure 3.8c Prescribed and actual (broken line) speed ax1

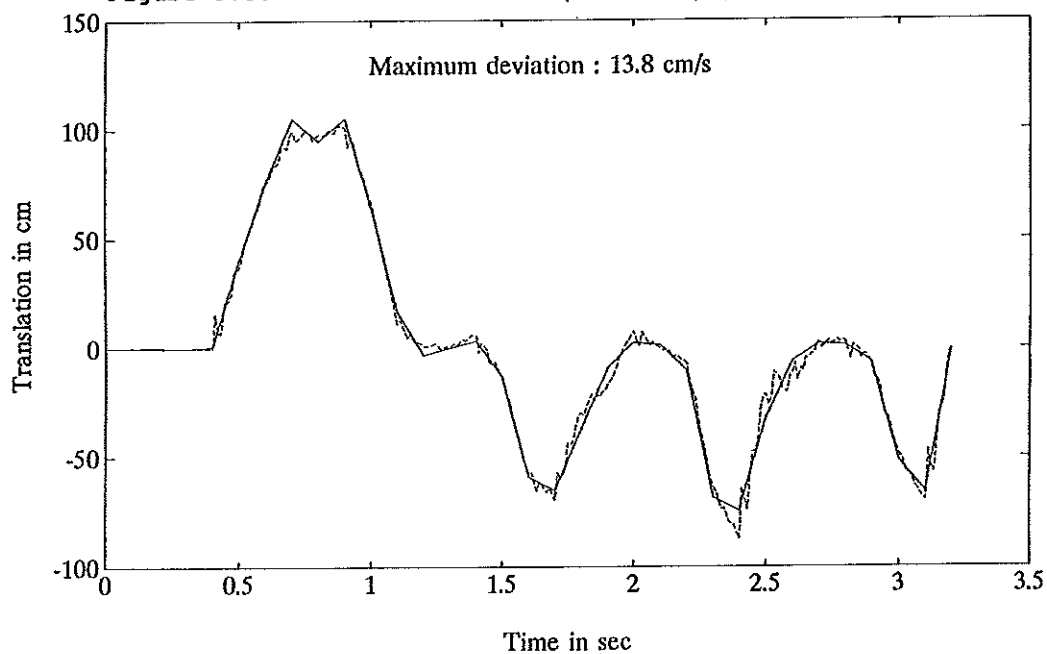


Figure 3.8d Prescribed and actual (broken line) speed ax2

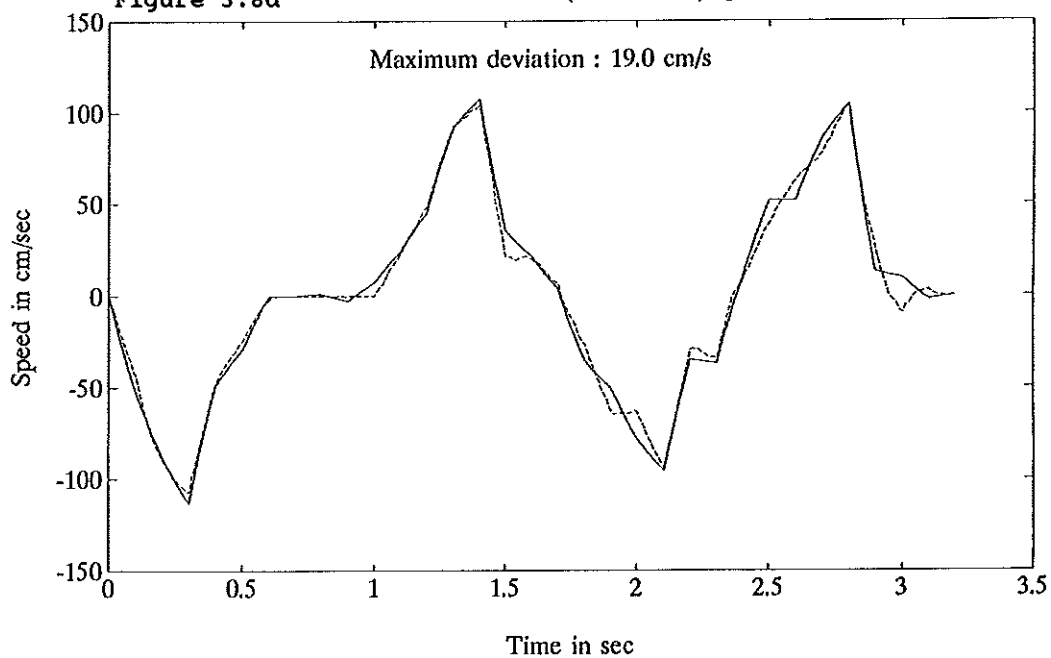


Figure 3.8e Prescribed and actual (broken line) control ax1

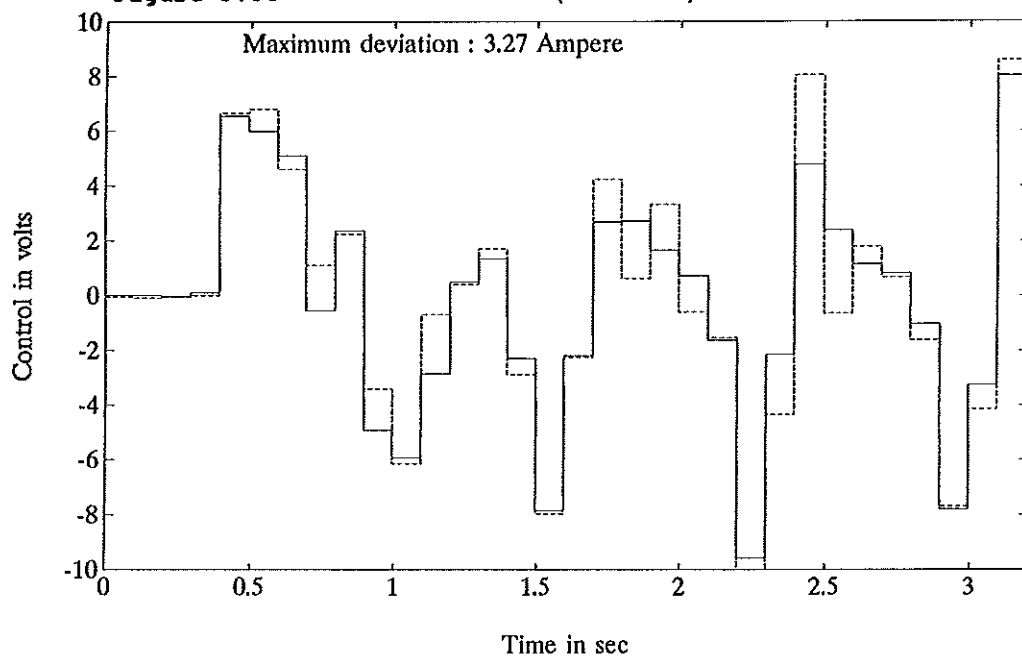
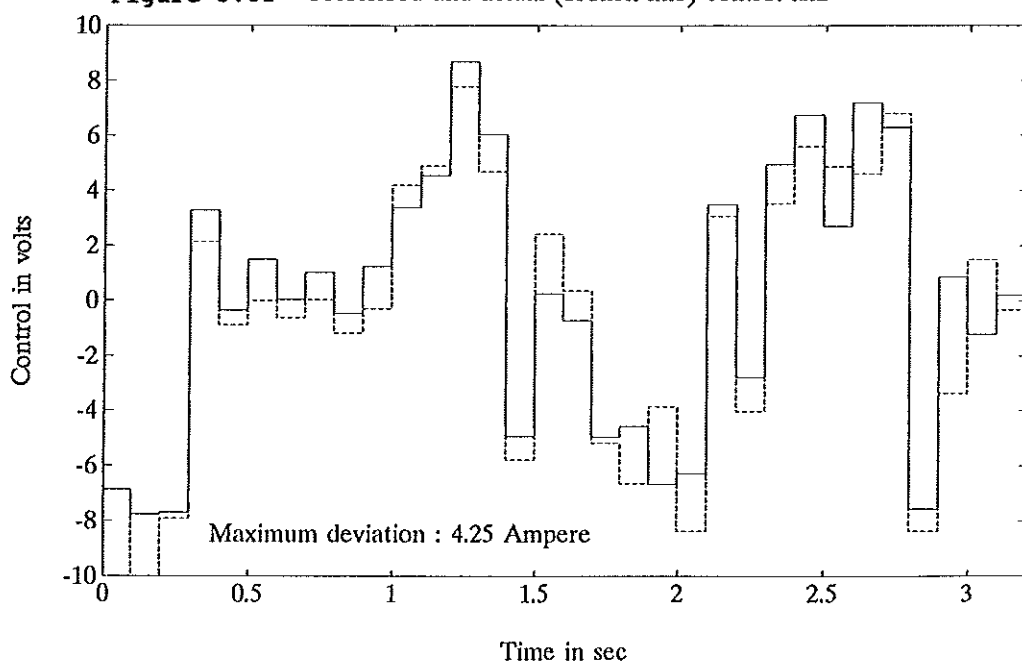


Figure 3.8f Prescribed and actual (broken line) control ax2



CHAPTER 3

COMPUTATION OF TIME-OPTIMAL CONTROLS APPLIED TO RIGID MANIPULATORS WITH FRICTION (co author R.P.H. Loop)

-Abstract-

In this paper we present a numerical procedure to compute non-singular time-optimal solutions for nonlinear systems, linear in the control, with fixed initial and final state and bounded control. Part of our procedure is a new numerical test, which determines whether bang-bang solutions satisfy Pontryagin's Minimum Principle. This test reveals the new important fact, that for a nonlinear systems, linear in the control and with dimension n , the probability that a bang-bang solution with more than $n-1$ switches satisfies Pontryagin's Minimum Principle is almost zero. Using a parameter optimization procedure we search for bang-bang solutions with up to $n-1$ switches which transfer the system from the initial to the final state. If no controls with up to $n-1$ switches can be found to satisfy Pontryagin's Minimum Principle the problem is very likely singular. We apply our procedure to the time-optimal control problem for rigid manipulators where friction may be included in the dynamics. We will demonstrate that some solutions mentioned in the literature to satisfy Pontryagin's Minimum Principle do not. A class of time-optimal control problems turns out to be singular. To solve these problems we propose and demonstrate the method of control parameterization.

I. Introduction

An assembly task performed by robotic manipulators generally involves the transportation of an object or a tool from one location to another. This operation is called a "point to point motion" and is characterized by prescribed initial and final positions and velocities of the robot links. The link positions and velocities may be considered as the state variables of the robotic manipulator. To maximize productivity the objective is to

perform the "point to point motion" in minimum time. This minimum time is limited since the actuation torques of the links are limited. The problem of performing a "point to point motion" in minimum time therefore constitutes a time-optimal control problem with fixed initial and final state, and bounded control, and is of great importance.

For an extensive review of earlier work on this subject we refer the reader to Chernousko et. al. (1989). We may roughly divide the work into three categories. One category uses linear models of which the solution to the time-optimal control problem may be computed. Some approximate the nonlinear robot dynamics, which are linear in the control, by a linear model (Kahn and Roth 1971, Kim and Shin 1985, Wen and Desrocher 1986, Nijmeyer et. al. 1988), others use feedback to compensate for nonlinear terms (Freund 1975, Katupitiya 1986) to arrive at a linear model. This is possible since robotic manipulators constitute so called feedback linearizable systems. The disadvantage of the latter is that due to the feedback the bounds on the control variables become state-dependent and have to be approximated by constants.

A second category (Sahar and Hollerbach 1985, Rajan 1985, Shiller and Dubowsky 1989) uses the solution of the time-optimal control problem along a prescribed path (Bobrow, Dubowsky and Gibson 1985, Shin and Mc Kay 1986, Van Willigenburg 1990). Using some optimization technique a path which connects the initial and final state is searched for that possesses the smallest minimum travelling time. A disadvantage of this method is that an assumption has to be made concerning the shape of the path, while the solution to the problem turns out to be very sensitive to the shape of the path.

The third category, like the second, considers the "true" nonlinear dynamics but except for Van Willigenburg (1990a) neglect friction (Ailon and Langholtz 1985, Sontag and Sussmann 1985, 1986, Wen 1986, Geering et. al. 1986, Chen 1989). In this category no assumptions concerning the solution have to be made.

Pontryagin's Minimum Principle, which states necessary conditions for a time-optimal control, is used to investigate the time-optimal control problem. However, except for Geering et. al. (1986), no procedures to compute time-optimal solutions have been presented within this category. The publications only state results concerning the form of the solution. Sontag and Sussmann (1985, 1986) demonstrate that the problem may be singular.

In this paper we will present a numerical procedure to compute time-optimal controls for nonlinear systems, linear in the control. If the time-optimal control problem is non-singular the time optimal control according to Pontryagin's Minimum Principle is of bang-bang type. Our procedure uses a parameter optimization routine to compute bang-bang controls which transfer the system from the initial to the final state using a penalty for deviations from the final state to force the final state to be reached. The parameters to be optimized are the switch times and the final time. However, bang-bang solutions that transfer the system from the initial to the final state, do not necessarily satisfy Pontryagin's Minimum Principle. A new numerical test, derived in this paper, is applied to the solution and determines whether or not bang-bang solutions satisfy Pontryagin's Minimum Principle. This test reveals a new important fact, concerning time-optimal solutions for nonlinear systems, linear in the control. For such a system with dimension n , the probability that a certain bang-bang solution with more than $n-1$ switches satisfies Pontryagin's Minimum Principle is almost zero.

As an example we will apply our numerical procedure to the IBM 7535 B 04 robot. Geering et. al. (1986) computed time-optimal solutions for this robot. Their work initially served as a reference for ours. We demonstrate that we find exactly the same bang-bang solutions transferring the robot from the initial to the final state. Although Geering et. al. (1986) state that they all satisfy Pontryagin's Minimum Principle our numerical test reveals that some of them do not. Finally we demonstrate that a method based on control parameterization (Goh and Teo 1988, Teo, Goh and

Lim 1989) generates solutions for non-singular problems involving the IBM 7535 B 04 robot, that are very close to the optimum. The method based on control parameterization can be applied to both singular and non-singular problems. For robotic manipulators it is in both cases expected to generate solutions that are very close to the optimum. The method explicitly considers the control to be piecewise constant. This is a realistic assumption since robotic manipulators are controlled by digital computers. Furthermore it allows for the inclusion of bounds on the individual link velocities which should be considered in practice as well (Van Willigenburg, 1990b). Finally we note that our numerical procedure, as well as the method based on control parameterization, allow for the inclusion of gravity and friction in the robot dynamics.

II. Dynamics of rigid manipulators with friction

The dynamics of a rigid N-link manipulator with friction can be written as (Asada and Slotine, 1986)

$$\tau = M(\theta)\ddot{\theta} + V(\theta, \dot{\theta}) + F(\theta, \dot{\theta}), \quad [1a]$$

where

$$\theta = (\theta_1, \theta_2, \dots, \theta_N)^T \quad [1b]$$

is an $N \times 1$ vector containing the joint angles of the links and

$$\tau = (\tau_1, \tau_2, \dots, \tau_N)^T \quad [1c]$$

is an $N \times 1$ vector containing the actuation torques, which are considered to be the control variables. $M(\theta)$ is an $N \times 1$ positive-definite inertia matrix, $V(\theta, \dot{\theta})$ is an $N \times 1$ vector representing centrifugal and Coriolis forces, $G(\theta)$ is an $N \times 1$ vector of forces due to gravity and $F(\theta, \dot{\theta})$ is an $N \times 1$ vector of friction terms.

To investigate the time-optimal control problem we will write the nonlinear system (1) in state space form, the state and control vector being $(\theta^T, \dot{\theta}^T)^T$ and τ , respectively. Since $M(\theta)$ is positive definite we obtain from (1)

$$\ddot{\theta} = M^{-1}(\theta) [\tau - V(\theta, \dot{\theta}) - G(\theta) - F(\theta, \dot{\theta})]. \quad [2]$$

Introducing

$$x_1 = \theta \quad [3a]$$

$$x_2 = \dot{\theta} \quad [3b]$$

$$x = \begin{bmatrix} x_1 \\ x_2 \end{bmatrix} \quad [3c]$$

$$u = \tau \quad [3d]$$

$$T = V + G + F \quad [3e]$$

(2) can be written in state space form using (3)

$$\dot{x}_1 = x_2 \quad [4a]$$

$$\dot{x}_2 = -M^{-1}(x_1)T(x) + M^{-1}(x_1)u. \quad [4b]$$

Observe that the dynamics (4) are linear in the control. In the sequel the index i will refer to the i -th component if it is associated with a row or column vector and to the i -th column in case of matrices.

Each component of the control vector u is assumed to be bounded.

$$|u_i| \leq b_i, \quad i = 1, \dots, N \quad [5]$$

If for instance the manipulator is actuated by current controlled DC-motors, the torque is proportional to the motor current, which

is limited in case of DC-motors.

III. The Time-optimal Control Problem

Consider a nonlinear time-optimal control problem, linear in the control. Given the system

$$\dot{x} = f(x) + B(x)u, \quad [6a]$$

where $x \in \mathbb{R}^n$, $u \in \mathbb{R}^r$, $r \leq n$, with fixed initial state

$$x(t_0) = x_0 \quad [6b]$$

and bounded control

$$|u_i| \leq a_i, \quad i = 1, \dots, r. \quad [7]$$

Minimize the cost criterion

$$J(t_0) = \int_{t_0}^{t_f} (1) dt, \quad [8]$$

subjected to the final state constraint

$$x(t_f) = x_f \quad [9]$$

where x_f is fixed and t_f is free.

The Hamiltonian for the system (6a) and the cost criterion (8) is given by

$$H(x, u, \lambda) = 1 + \lambda^T [f(x) + B(x)u], \quad [10]$$

where λ is the costate of the system (6a). The costate variables satisfy the adjoint differential equation

$$-\dot{\lambda} = \frac{\delta H}{\delta x} \quad [11]$$

Pontryagin's Minimum Principle states that a necessary condition for an optimal control is that it minimizes the Hamiltonian for optimal values of the state and costate, i.e. (Lewis, 1986)

$$H(x^*, u^*, \lambda^*) \leq H(x^*, u, \lambda^*) \quad \text{all admissible } u, \quad [12]$$

where the superscript * denotes an optimal quantity. Since (10) is linear in the control, we obtain from (10) and (12) the following control law

$$u_1^*(t) = \begin{cases} +a_1 & \text{if } [\lambda^T(t)B]_1 < 0, \\ -a_1 & \text{if } [\lambda^T(t)B]_1 > 0, \end{cases} \quad t_0 \leq t \leq t_f \quad [13]$$

where for obvious reasons $[\lambda^T(t)B]_1$, $t_0 \leq t \leq t_f$ is called the switching function corresponding to the control variable $u_1(t)$. If one or several of the switching functions are equal to zero over some time interval the control law (13) does not determine a solution. The time optimal control problem is called singular in this case. If the switching functions equal zero at isolated times only (13) determines a solution and the problem is called non-singular. For the moment we will only consider non-singular time optimal control problems. In case of a non-singular time optimal control problem we observe from (13) that almost everywhere each control variable takes on an extreme value. This type of control is called a bang-bang control.

The solution of the time-optimal control problem (6)-(9) is determined by (6), (9), (11) and (13) and constitutes a two point boundary value problem (TPBVP) where the boundary conditions are given by (6b) and (9) and in addition we have the boundary condition (Lewis, 1986)

$$H(t_f) = 0. \quad [14]$$

Since the system (6a) and the integrand of the cost criterion (8) do not explicitly depend on time, the Hamiltonian (10) is not an explicit function of time. So we have (Lewis, 1986)

$$\dot{H} = 0 \quad [15]$$

and together with (14)

$$H(t) = 0 \quad t_0 \leq t \leq t_f. \quad [16]$$

The TPBVP (6), (9), (11) and (13) is very difficult to solve numerically since except from (16) no information concerning values of the costate is available. In addition we experienced that the solution is very sensitive to changes in the costate. The usual approach is to search for bang-bang controls which transfer the system from the initial to the final state and to assume that the one with the smallest transition time satisfies Pontryagin's Minimum Principle. We will demonstrate that dependent on the solution this assumption may not be correct. In section 4 we will present a numerical test to verify whether bang-bang solutions satisfy Pontryagin's Minimum Principle.

As an introduction to section 4 let us finally look at the time optimal control problem from a different point of view. Given an initial costate

$$\lambda(t_0) = \lambda_0, \quad [17]$$

which according to (16) must satisfy

$$H(t_0) = 0, \quad [18]$$

the system (6a), the adjoint system (11) and the control law (13), when integrated from the initial conditions (6b) and (17), generate time optimal solutions satisfying Pontryagin's Minimum Principle. The final state in this case depends on the initial

costate (17) and the time at which the integration is stopped. So given a fixed final state (9) the time optimal control problem may be regarded as an initial value problem for the costate. Again however, this initial value problem is very difficult to solve numerically since except from (18) we have no information concerning the initial costate, while in addition we experienced the problem to be very sensitive to changes in the initial costate. Since furthermore the final time is unknown, during integration we constantly have to check whether we come across the fixed final state. In section 4 however we will demonstrate that given a bang-bang control we may compute whether or not an initial costate exists which generates this bang-bang control. If it exists the solution satisfies Pontryagin's Minimum Principle otherwise it does not. When the initial costate exists we are able to compute it and thereby compute the evolution of the costate and the switching functions corresponding to the time optimal control and state trajectory.

IV. A Numerical Test to Verify Whether Bang-bang Solutions Satisfy Pontryagin's Minimum Principle.

The state and costate equations for the time-optimal control problem are given by (6a) and (11). Pontryagin's Minimum Principle states that a necessary condition for a time-optimal solution is

$$u_1(t) = -a_1 \operatorname{sgn} [\lambda^T(t)B]_1 \quad t_0 \leq t \leq t_f. \quad [19]$$

In the sequel a time-optimal solution will denote a solution satisfying Pontryagin's Minimum Principle, i.e. equation (19). Assume we have a bang-bang control

$$u_b(t) \quad t_0 \leq t \leq t_f \quad [20]$$

which transfers the system from the initial to the final state, i.e.

$$x_b(t_0) = x_0 \quad [21a]$$

$$x_b(t_f) = x_f \quad [21b]$$

where x_b is the state trajectory of the system (6a) generated by the control (20). The question whether this control is time-optimal comes down to the question whether an initial costate vector $\lambda(t_0)$ exists which by (6a), (11) and (19) generates this bang-bang control. Equation (19) demands that at each switching instant the corresponding switching function is equal to zero. We will demonstrate that this condition can be transformed into p computable linear relationships between the n components of the initial costate vector, where p is the number of switches.

The solution to the linear adjoint differential equation (11) is given by

$$\lambda(t) = \Phi(t, t_0) \lambda(t_0), \quad [22]$$

where Φ is the fundamental matrix associated with (11). Note that since both x_b and u_b are known $\Phi(t, t_0)$ can be computed. If the i -th control variable switches from one extreme value to the other at time t_s , the corresponding switching function must be equal to zero. So we must have

$$[\lambda^T(t_s) B(t_s)]_i = 0. \quad [23]$$

From (22) and (23) we must therefore have

$$\lambda^T(t_0) \Xi_i(t_s) = 0 \quad [24a]$$

where

$$\Xi_i(t_s) = \Phi^T(t_s, t_0) B_i(t_s). \quad [24b]$$

Equation (24) constitutes a linear relationship between the n components of the initial costate vector. With p switching times

we obtain p linear relationships between the components of the initial costate vector. According to equations (10) and (18), the initial costate must also satisfy

$$\lambda^T(t_0) [f(x_0) + B(x_0)u(t_0)] = -1. \quad [25]$$

Equation (24), which holds at each switching instant and equation (25) define a nonhomogeneous system of $p+1$ linear equations with n unknowns. When $p+1 = n$, the system has a unique solution, if these $p+1$ equations are linearly independent. If $p+1 > n$, then at least $p+1-n$ equations must be linearly dependent for the system to have a solution, otherwise the system has no solution. If $p+1 < n$, a set of solutions exists.

The nonhomogeneous system of $p+1$ equations constitutes necessary conditions for the initial costate. If the system has no solution, the bang-bang control is not time-optimal. If the system has one or several solutions, we have to check if (19) is satisfied for all $t \in [t_0, t_f]$. This can be done by numerical integration of (6a), (11) and (19), given $x(t_0)$ and $\lambda(t_0)$.

V. The Time-optimal Control Problem for a Two-link Robotic Manipulator

V.I Introduction

In order to demonstrate our approach we will investigate the industrial IBM 7535 B 04 robot, treated by Geering et al. This is one of few papers, in which actual numerical calculation of the time-optimal controls is performed. Since Geering et al. also use Pontryagin's Minimum Principle to investigate the time-optimal control problem, this paper serves as a reference for our approach. We will show that some solutions presented in this publication to be time-optimal are not.

V.II Dynamic model of the IBM 7535 B 04 robot

The industrial IBM 7535 B 04 robot is sketched in figure 1. This robot consists of two links, which move in a horizontal plane. A third link which allows for vertical translations is mounted at the end of the second link. To perform various tasks a gripper which may hold a load during operations is mounted at the end of the third link. The vertical motion is completely decoupled from the horizontal motion of the first two links and is not treated here. The dynamics of this robotic manipulator as presented in Geering et al. are quite unaccessible and do not allow for easy extension to include gravity and friction terms. As we will demonstrate in appendix A, this robot can be fully described by the closed form dynamics of a two-link robotic manipulator (Asada and Slotine 1986). The third link, the gripper and the load are then considered as an integral part of the second link. The numerical values for the parameters of the IBM 7535 B 04 robot, given by Geering et al. can still be used after appropriate transformation. We will now present the closed form dynamics of the two-link robotic manipulator and give the actual values of the parameters. For a detailed description of the matching of the closed form dynamics with the model and data presented by Geering et al. we refer to appendix A.

Consider a common two-link robotic manipulator, which suffers from viscous and Coulomb friction. This is a robot with a geometry as sketched in figure 1 without a third link. The robot motion may be considered either in a horizontal or in a vertical plane. Let m_1 and l_1 be the mass and the length of the first link and m_2 and l_2 the mass and the length of the second link. The moments of inertia about the centroids are given by I_1 and I_2 . The angular rotation θ_2 of the second link is measured relative to the first link. The distances between the centroids of links and the joint axes are denoted by l_{c1} and l_{c2} .

The closed form dynamics are given by (Asada and Slotine, 1986)

$$\tau_1 = M_{11}\ddot{\theta}_1 + M_{12}\ddot{\theta}_2 - h\dot{\theta}_2^2 - 2h\dot{\theta}_1\dot{\theta}_2 + G_1 + F_1 \quad [26a]$$

$$\tau_2 = M_{12}\ddot{\theta}_1 + M_{22}\ddot{\theta}_2 - h\dot{\theta}_1^2 + G_2 + F_2 \quad [26b]$$

where

$$M_{11} = m_1 l_{c1}^2 + I_1 + m_2[l_1^2 + l_{c2}^2 + 2l_1 l_{c2} \cos(\theta_2)] + I_2 \quad [27a]$$

$$M_{12} = m_2 l_1 l_{c2} \cos(\theta_2) + m_2 l_{c2}^2 + I_2 \quad [27b]$$

$$M_{22} = m_2 l_{c2}^2 + I_2 \quad [27c]$$

$$h = m_2 l_1 l_{c2} \sin(\theta_2) \quad [27d]$$

$$G_1 = m_1 l_{c1} g \cos(\theta_1) + m_2 g \{l_{c2} \cos(\theta_1 + \theta_2) + l_1 \cos(\theta_1)\} \quad [27e]$$

$$G_2 = m_2 l_{c2} g \cos(\theta_1 + \theta_2) \quad [27f]$$

$$F_1 = c_1 \operatorname{sgn}(\dot{\theta}_1) + v_1 \dot{\theta}_1 \quad [27g]$$

$$F_2 = c_2 \operatorname{sgn}(\dot{\theta}_2) + v_2 \dot{\theta}_2 \quad [27h]$$

The terms G_1 and G_2 account for the effect of gravity, while the terms F_1 and F_2 which are not considered by Asada and Slotine represent both Coulomb and viscous friction.

If we consider the robot to move in a horizontal plane, we must exclude gravity terms, because then this force is orthogonal to the robot motion. If we consider the robot motion in a vertical plane, the gravity terms (27e) and (27f) play a major role in the dynamics.

The values of the parameters of the IBM 7535 B 04 robot, computed from the parameter values presented by Geering et al. are given below.

$$l_1 = 0.4 \text{ m} \quad l_2 = 0.25 \text{ m} \quad l_{c2} = 0.161 \text{ m}$$

$$\begin{aligned}
 m_2 &= 21 \text{ kg} & I_1 + m_1 l_{c1}^2 &= 1.6 \text{ m}^2\text{kg} & I_2 &= 0.273 \text{ m}^2\text{kg} \\
 c_1 &= 0.05 \text{ Nm} & v_1 &= 0.025 \text{ Nms}^{-1} & c_2 &= 0.15 \text{ Nm} & v_2 &= 0.005 \text{ Nms}^{-1} \\
 b_1 &= 25 \text{ Nm} & b_2 &= 9 \text{ Nm} & & & & [28]
 \end{aligned}$$

For the computation of these parameter values we refer to appendix A.

V.III Time-optimal solutions

The Hamiltonian (10) is affine in the controls u_i . Pontryagin's Minimum Principle then yields that the controls are of bang-bang type or may be singular. In case we have a bang-bang control that transfers the manipulator from the initial state to the final state, we are able to check whether or not this bang-bang solution satisfies Pontryagin's Minimum Principle. In order to find such a bang-bang control, we assume an initial control vector and we assume that the number of switching times equals p . Then we use a parameter optimization method to optimize the p switching times and the final time, using a penalty for deviations from the final state to force the final state to be reached.

Geering et al. treat several types of solutions for the special case in which the links are stretched in both the initial and final configuration. We find exactly the same bang-bang solutions, proving that we concern ourselves with exactly the same robot dynamics. To demonstrate this we give our computations of some of the robot motions presented by Geering et al. Furthermore we will check whether or not the computed solutions satisfy Pontryagin's Minimum Principle. Some solutions presented by Geering et al. as time-optimal turn out to be not time-optimal.

In section 4 we already noted that for a bang-bang solution with p

switching times to satisfy Pontryagin's Minimum Principle we have to consider a nonhomogeneous system of $p+1$ linear equations with n unknowns. Therefore it seems natural to look at first for a bang-bang solution with $n-1$ switching times, for then we have to solve a system of n linear equations with n unknowns, n being 4 in case of a two-link manipulator. Geering et al. also find time-optimal solutions with 3 switching times, designated as type A_0 .

The actuation torque u_2 of the second link acts on the first link too. If the sign of u_2 is opposite to the sign of u_1 at the beginning of the robot motion, u_2 increases the accelerating effect of u_1 . It seems natural for the initial control vector to have the first component positive and the second component negative. We will however try other initial control vectors as well.

For a robot motion with initial state

$$x_0 = [0 \ 0 \ 0 \ 0]^T \quad [29a]$$

and final state

$$x_f = [0.975 \ 0 \ 0 \ 0]^T, \quad [29b]$$

assuming three switch times, parameter optimization, performed by the routine BCPOL from the IMSL library, yields the bang-bang control shown figure 3 which transfers the system from the initial to the final state as shown in figure 2. Now we have to check whether this bang-bang control satisfies Pontryagin's Minimum Principle. This is done by calculating an initial costate following the lines of section 4. Then we numerically integrate the system (6a), (11) and (19), given $x(t_0)$ and $\lambda(t_0)$ from the initial time to the final time to check whether (19) is satisfied for all $t \in [t_0, t_f]$.

For the robot motion (29) the bang-bang solution satisfies

Pontryagin's Minimum Principle as can be seen from figure 3. In this figure both the optimized bang-bang control and the bang-bang control generated by the switching functions are sketched, which are identical in this case.

Next we present in figure 4 our results for a robot motion with initial state

$$x_0 = [0 \ 0 \ 0 \ 0]^T \quad [30a]$$

and final state

$$x_f = [1.5 \ 0 \ 0 \ 0]^T, \quad [30b]$$

the control again having three switches. Obviously the computed control and the control generated by the switching function do not match, so this control is not time optimal. The initial costate, which constitutes the unique solution to the necessary conditions (24) and (25) does not yield the desired bang-bang control.

For $\theta_1(t_f) > 0.98$ bang-bang controls with three switches do not satisfy Pontryagin's Minimum Principle. Next we assume four switching times in order to try and find time-optimal controls which transfer the robot to a configuration with $\theta_1(t_f) > 0.98$. Geering et al. find this type of solution and denote it as type A_1 . We will now demonstrate that this bang-bang control with two switches for each torque does not satisfy Pontryagin's Minimum Principle, i.e. these solutions are not time-optimal!

The results for a robot motion with the control switching four times given the initial state

$$x_0 = [0 \ 0 \ 0 \ 0]^T \quad [31a]$$

and the final state

$$x_f = [1.0 \ 0 \ 0 \ 0]^T \quad [31b]$$

are shown in figure 5. An initial costate is calculated from the first three switching times, which determine a unique solution for the initial costate. Integrating the system yields that the calculated bang-bang solution does not satisfy Pontryagin's Minimum Principle, as can be seen from Figure 5b.

Next we compute a time-optimal bang-bang control with four switching times. In section 3 we noted that in this case there must be a linear dependency in the nonhomogeneous system which determines the initial costate. We consider a solution with the second link swinging through, u_1 switching three times and u_2 once. Geering et al. denote this type of solution as B_0 . The results are depicted in figure 6 for the robot motion from the initial state

$$x_0 = [0 \ 0 \ 0 \ 0]^T \quad [32a]$$

to the final state

$$x_f = [0.76 \ -2\pi \ 0 \ 0]^T. \quad [32b]$$

As can be seen from figure 7, although the solution has more than $n-1$ switching times, the computed bang-bang control with four switching times satisfies Pontryagin's Minimum Principle! In general the probability that a solution with more than $n-1$ switching times satisfies Pontryagin's Minimum Principle is almost zero, since the probability of the necessary conditions (24), (25) for the initial costate being linearly dependent is almost zero. Therefore there must be an explanation why we find the complete class of time-optimal control problems of type B_0 having time-optimal solutions with n switching times. This can be explained by the symmetry of the switching functions, which causes linear dependence in the necessary conditions (24), (25) for the initial costate. The symmetry of the switching functions for time-optimal control problems of type B_0 is explicitly contained in the robot dynamics. For detailed analysis we refer to appendix

B. Once however we introduce friction into the robot dynamics, this symmetry immediately vanishes. We will show this by evaluating the same robot motion of type B_0 as above, now only with addition of small Coulomb and viscous friction terms as described in equations (27g) and (27h) with parameter values given by equation (28). The results are presented in figure 8. In this case the switching functions are only nearly symmetric, the symmetry, which causes the linear dependence in the necessary conditions (24), (25) for the initial costate, therefore is lost and the solution does not satisfy Pontryagin's Minimum Principle. Also if we consider the robot motion in a vertical plane the influence of gravity destroys the symmetry. We want to make the point here that the solutions of type B_0 , when we disregard friction and gravity, constitute a very special class of time-optimal control problems for which a solution with more than $n-1$ switches satisfies Pontryagin's Minimum Principle. In other words, if we consider an arbitrary initial and final state, then the probability that the time-optimal control consists of a bang-bang control with more than $n-1$ switches is almost to zero.

Therefore to solve the time-optimal control problem for a given initial and final state, we search for a bang-bang control with no more than $n-1$ switches which satisfies Pontryagin's Minimum Principle. If such a bang-bang control can not be found the time-optimal control problem is very likely singular.

The procedure described above can be applied to robot motions in vertical planes as well. Although we computed several, we will not actually include examples in which gravity is contained.

VI. Sub-Time-Optimal Solutions computed by Control Parameterization

From section 5 we observe that the time-optimal control problem is non-singular only for a limited class of initial and final states. For singular problems Pontryagin's Minimum Principle

COMPUTATION OF TIME-OPTIMAL CONTROLS

does not yield an optimal control. In this section we will demonstrate that the method of control parameterization can be used to compute sub-optimal controls. The control parameterization will be based on the assumption that the control is of piecewise constant nature which is a *realistic* assumption when using a digital controller. We will show that for a non-singular time-optimal control problem solutions computed by means of control parameterization transfer the manipulator in near minimum time from the initial to the final state. Since for singular time-optimal control problems the optimum is very flat solutions found by control parameterization are expected to be near time-optimal as well.

Consider the system (6) and the cost functional (8). The control parameterization is given by

$$u_i(t) = u_i(t_k), \quad t \in [t_k, t_{k+1}), \quad i = 1, \dots, r \quad k = 0, 1, \dots, N \quad [33]$$

where, although not necessary, we assume t_k are equidistant time instants and $t_{N+1} = t_f$. The controls are assumed to be bounded

$$|u_i(t_k)| \leq A_i \quad i = 1, \dots, r \quad k = 0, 1, \dots, N. \quad [34]$$

The control parameterization (33) and (34) constitutes a bounded piecewise constant control. The time-optimal control problem now is to find a control $u(t)$ satisfying (33) and (34) which transfers the manipulator from the initial to the final state, such that the cost functional (8) is minimized. As can be observed from (33) the control variable u_i is a function of $N+1$ parameters, the parameters being the amplitudes of the control variable. By a parameter optimization method, i.e. the routine BCPOL from the IMSL library, the amplitudes are varied in order to find a control which drives the system from the initial to the final state, using a penalty for deviations from the final state in order to force the final state to be reached. A final time is assumed, and when a solution is found the final time is decreased otherwise it is increased and the process is repeated until changes in the final

time become insignificant.

For non-singular time-optimal control problems we are able to compute time-optimal solutions. Therefore the minimum transition time is known. We will demonstrate that the method of control parameterization yields near time optimal controls which differ significantly from the time-optimal bang-bang controls demonstrating that the cost functional has a weak minimum.

For the robot motion with initial and final state given by (29) we computed a time-optimal solution with a minimum transition time of 1.085 s, shown in figures 2 and 3. We applied control parameterization using 20 equidistant time-intervals. We find a piecewise constant control which transfers the robot from the initial to the final state in 1.095 s, as shown in figures 9 and 10.

Next we apply control parameterization to the singular problem presented in figure 4, i.e. a robot motion with initial and final state given by (30). The results are depicted in figures 11 and 12. We observe that the final time found by control parameterization is equal to 1.225 s. Previously we obtained a bang-bang solution with 3 switches and a final time of 1.28 s. Based type A_1 of Geering et al. we computed a bang-bang control with 4 switches yielding a final time of 1.235 s. Control parameterization obviously gives the smallest transition time for this problem.

Summarizing the method of control parameterization seems to be well suited to solve both non-singular and singular problems.

VII. Conclusions

For nonlinear systems, linear in the control, we presented a new numerical test which determines whether bang-bang solutions satisfy Pontryagin's Minimum Principle. The test reveals the new

important fact that if we consider such a system with dimension n , the probability that a certain bang-bang solution, with more than $n-1$ switches, satisfies Pontryagin's Minimum Principle, is almost zero. Given an arbitrary initial and final state we therefore search for bang-bang solutions with up to $n-1$ switches, which transfer the system from the initial to the final state. The search constitutes a parameter optimization procedure where the parameters are the switch times and the final time. A penalty for deviations from the final state is used to force the final state to be reached. The numerical test is applied to verify whether or not these solutions satisfy Pontryagin's Minimum Principle. If no solutions with up to $n-1$ switches can be found transferring the system from the initial to the final state while satisfying Pontryagin's Minimum Principle, the problem is very likely singular. In that case we use an optimization procedure, based on control parameterization, to compute sub-optimal solutions.

Our method can be applied to rigid robotic manipulators, where both friction and the effect of gravity may be included in the robot dynamics. We computed time-optimal solutions for an IBM 7535 B 04 robot, which can be modeled as a two-link manipulator. We demonstrated that for this robot some numerical solutions mentioned in the literature to satisfy Pontryagin's Minimum Principle, do not. Furthermore we demonstrated that for non-singular problems the method based on control parameterization generates sub-optimal solutions for this robot, which are very close to the optimum. Since for singular problems the minimum is very flat, in these cases we expect the method based on control parameterization to generate sub-optimal solutions that are very close to the optimum as well. Summarizing the method of control parameterization seems to be very well suited to solve general time-optimal control problems for rigid manipulators. The method explicitly assumes the control to be piecewise constant, which is a realistic assumption, since robots are controlled by digital computers. Bounds on the individual link velocities, which have to be considered in practice as well, are also easily included in the problem. The solutions are in open-loop form but, when

conservative bounds on the control variables are used, can be implemented in conjunction with a perturbation controller, the result yielding a time-optimal feedback controller (Van Willigenburg 1990c).

We have not gone into detail with respect to the computations involved in the numerical test to verify whether bang-bang solutions satisfy Pontryagin's Minimum Principle. In a future paper we plan to treat the numerical computation of the test, together with the influence of numerical errors, in detail. For instance, the numerical determination whether or not a nonhomogeneous set of equations is linearly dependent presents a problem. Furthermore the errors introduced by numerical integration, which plays a crucial role in the computation of the numerical test, have to be considered. Questions concerning numerical errors are related to questions concerning the sub-optimality of solutions. Questions concerning sub-optimality are interesting since they may answer the question to what extend solutions generated by control parameterization are optimal. Furthermore they are of interest since the application of bang-bang controls in practice increases wear. One generally prefers a more smooth control. The question concerning the sub-optimality of solutions will also be a subject of future research.

References

- AILON A., LANGHOLTZ G., 'On the Existence of Time-Optimal Control of Mechanical Manipulators', J Opt. Th. Appl., 46, 1, 1-20.
- ASADA H., SLOTINE J.-J.E., 1986, Robot Analysis and Control, Wiley
- CHEN Y.C., 1989, 'On the Structure of the Time-Optimal Controls for Robotic Manipulators', IEEE Trans. Aut. Cont., 34, 1, 115-116.
- CHERNOUSKO F.L., AKULENKO L.D., BOLOTNIK N.N., 1989, 'Time-optimal control for robotic manipulators', Optimal Cont. Appl. and Meth., 10, 293-311.
- CRAIG J.J., 1986, Introduction to Robotics, Addison and Wesley
- FREUND E., 1975, 'The structure of decoupled nonlinear systems',

COMPUTATION OF TIME-OPTIMAL CONTROLS

Int. J. Cont., 21, 443-450.

GEERING H.P., GUZELLA L., HEPNER S.A.R., ONDER C.H., 'Time-Optimal Motions of Robots in Assembly Tasks', IEEE Trans. Aut. Cont., AC-31, 6, 512-518.

GOH C.J., TEO K.L., 1988, 'Control Parameterization: a Unified Approach to Optimal Control Problems with General Constraints', Automatica, 24, 3-18.

KAHN M.E., ROTH B., 1971, 'The near-minimum-time control of open loop articulated kinematic chains', Trans. ASME J. Dyn. Sys. Meas. and Contr., 93, 164-172.

KAPITUYA J., 1986, Vision assisted tracking and the time-optimal acquisition of moving objects using a manipulator, PHD thesis, Dept. of Mechanical Engineering, Leuven.

LEWIS F.L., 1986, Optimal Control, Wiley

NIJMEYER H., ROODHARDT P., LOHNBURG P., 'On the Time-Suboptimal Control of Two-Link Horizontal Robot Arms with Friction', Internal Report no. 88R011, Control Systems and Computer Engineering Laboratory, Department of Electrical Engineering, University of Twente, The Netherlands.

RAJAN V.T., 1985, 'Minimum time trajectory planning', IEEE Int. Conf. on Rob. and Aut., St. Louis MO, 759-764.

SAHAR G., HOLLERBACH J.M., 1985, 'Planning of minimum-time trajectories for robot-arms', IEEE Int. Conf. on Rob. and Aut., St. Louis MO, 751-758.

SONTAG E.D., SUSSMANN, H.J., 1985, 'Remarks on the time-optimal control of two link manipulators', Proc. Conf. on Decision and Control, Ft. Lauderdale, 1646-1652.

SONTAG E.D., SUSSMANN, H.J., 1986, 'Time-optimal control of manipulators', IEEE Int. Conf. on Rob. and Aut., San Francisco 1692-1697.

TEO K.L., GOH C.J., LIM C.C., 1989, 'A Computational Method for a Class of Dynamical Optimization Problems in which the Terminal Time is Conditionally Free', IMA J. of Math. Cont. and Inf.

VAN WILLIGENBURG L.G., 1990a, 'First order controllability and the time optimal control problem for rigid articulated arm robots with friction', Int. J. Cont., 51, 6, 1159-1171.

VAN WILLIGENBURG L.G., 1990b, 'Design, computation and

implementation of digital optimal controllers for cartesian robots', Submitted for publication.

VAN WILLIGENBURG L.G., 1990c, 'Digital optimal control of nonlinear uncertain systems applied to rigid manipulators', to appear

WEN J., DESROCHER A., 1986, 'Sub-time-optimal control strategies for robotic manipulators', IEEE Conf. on Rob. and Aut., San Francisco CA, 402-406.

WEN J., 1986, 'On Minimum Time Control for Robotic Manipulators', Recent Trends in Robotics, Elsevier.

Appendix A

We can easily include the effects of the third link, the gripper and the load in the closed form dynamics of the two-link manipulator by integrating the third link, the gripper and the load in the second link. Since the third link moves perpendicular to the second link the centroid of the third link, the gripper and the load may be located at the end of the second link. Assume the third link, the gripper and the load have a total mass m_3 and a moment of inertia I_3 . The second link as a whole will have a mass m'_2 , a centroid l'_{c2} and a moment of inertia I'_2 , which can all be calculated from the masses and moments of inertia of the second link and the third link together with the gripper and the load by application of Steiner's Translation Theorem.

Application of Steiner's Theorem yields

$$m'_2 = m_2 + m_3, \quad [A1]$$

$$l'_{c2} = \frac{m_2 l_{c2} + m_3 l_3}{m_2 + m_3}, \quad [A2]$$

$$I'_2 = I_2 + I_3 + \frac{m_2 m_3}{m_2 + m_3} (l_2 - l_{c2})^2 \quad [A3]$$

Equations [26] and [27] still hold in case of a third link with a gripper and a load at the end of the second link, but must be transformed by setting $m_2 = m'_2$, $l_{C2} = l'_{C2}$ and $I_2 = I'_2$.

Geering et al. use the moment of inertia ξ with respect to the joint axes, while I in our equations denotes the moment of inertia about the centroid of the link. These descriptions can be related using Steiner's Theorem. For example we have for the first link

$$\xi_1 = I_1 + m_1 l_{C1}^2 \quad [A4]$$

As can be seen in equations [26] and [27], the parameter m_1 does not occur in the closed form dynamics in case we consider the robot motion in a horizontal plane if we use [A4]. If however we consider the robot motion in a vertical plane, m_1 should be known since it occurs in the gravity term.

Geering et al. locate the center of gravity of the second link in the middle of the second link, so

$$l_{C2} = \frac{1}{2} l_2. \quad [A5]$$

The above yields the following numerical values for the IBM 7535 B 04 robot in terms of the closed form dynamics of a two-link robot.

$$l_1 = 0.4 \text{ m} \quad l_2 = 0.25 \text{ m} \quad l'_{C2} = 0.161 \text{ m}$$

$$m'_2 = 21 \text{ kg} \quad \xi_1 = 1.6 \text{ m}^2\text{kg} \quad I'_2 = 0.273 \text{ m}^2\text{kg}$$

$$c_1 = 0.05 \text{ Nm} \quad v_1 = 0.025 \text{ Nms}^{-1} \quad c_2 = 0.15 \text{ Nm} \quad v_2 = 0.005 \text{ Nms}^{-1}$$

$$b_1 = 25 \text{ Nm} \quad b_2 = 9 \text{ Nm}, \quad [A6]$$

Friction will play only a minor role in the dynamics, as can be seen from the values in (A6). In modern robots in which significant gearing is typical, friction forces can be actually

quite large, up to 25% of the torque required to move the manipulator (Craig, 1986).

Appendix B

In this appendix we demonstrate that the symmetry and anti-symmetry in figures (6) and (7) is explicitly contained in the robot dynamics for the robot motion of type B_0 , where gravity and friction terms are not taken into account.

From the closed form dynamics (26) we observe

$$\ddot{\theta}_1 = f_1(\theta_2, \dot{\theta}_1, \dot{\theta}_2, \tau) \quad [B1]$$

$$\ddot{\theta}_2 = f_2(\theta_2, \dot{\theta}_1, \dot{\theta}_2, \tau). \quad [B2]$$

By inspection of the closed form dynamics we have

$$f_1(-\pi + \theta_2, \dot{\theta}_1, \dot{\theta}_2, \tau) = -f_1(-\pi - \theta_2, \dot{\theta}_1, \dot{\theta}_2, -\tau) \quad [B3]$$

$$f_2(-\pi + \theta_2, \dot{\theta}_1, \dot{\theta}_2, \tau) = -f_2(-\pi - \theta_2, \dot{\theta}_1, \dot{\theta}_2, -\tau). \quad [B4]$$

Starting at a configuration where $\theta_2 = -\pi$ equations (B1)-(B4) imply that the behavior of $\dot{\theta}_1$ and $\dot{\theta}_2$ forward in time is equal to the behavior backward in time, if the controls have opposite sign. This explains the symmetry of $\dot{\theta}_1$ and $\dot{\theta}_2$ and the anti-symmetry of θ_1 and θ_2 in figures (6) and (7).

From the costate equation (11) using (B1) and (B2) we obtain the following equations for the costate

$$\begin{aligned}
 \dot{\lambda}_1 &= 0 \\
 -\dot{\lambda}_2 &= \frac{\delta f_1}{\delta \theta_2} \lambda_3 + \frac{\delta f_2}{\delta \theta_2} \lambda_4 \\
 -\dot{\lambda}_3 &= \lambda_1 + \frac{\delta f_1}{\delta \dot{\theta}_1} \lambda_3 + \frac{\delta f_2}{\delta \dot{\theta}_1} \lambda_4 \\
 -\dot{\lambda}_4 &= \lambda_2 + \frac{\delta f_1}{\delta \dot{\theta}_2} \lambda_3 + \frac{\delta f_2}{\delta \dot{\theta}_2} \lambda_4
 \end{aligned} \tag{B5}$$

The symmetry of $\dot{\theta}_1$ and $\dot{\theta}_2$ and the anti-symmetry of f_1 , f_2 and θ_2 with respect to $\theta_2 = -\pi$ imply the symmetry of λ_1 and λ_2 and the anti-symmetry of λ_3 and λ_4 , assuming λ_3 and λ_4 are equal to zero when $\theta_2 = -\pi$. When $\theta_2 = -\pi$ both control variables switch, which implies that both switching functions must be equal to zero. Given (4), (10) and (13) this implies that

$$[\lambda_3 \ \lambda_4] M^{-1} = 0 \tag{B6}$$

Since M^{-1} is a positive definite matrix this implies that both $\lambda_3 = 0$ and $\lambda_4 = 0$ when $\theta_2 = -\pi$.

Finally from the closed form dynamics (26) we observe that

$$M(-\pi + \theta_2) = M(-\pi - \theta_2) \tag{B7}$$

So M is symmetric with respect to $\theta_2 = -\pi$ and therefore M^{-1} is also. The symmetry of M^{-1} and the anti-symmetry of λ_3 and λ_4 imply that the switching functions are anti-symmetric. Given this anti-symmetry a switching point on one side of $\theta_2 = -\pi$ automatically implies a switching point on the other side.

Summarizing, the linear dependency of the non-homogeneous system of $p+1$ equations for the initial costate is explicitly contained in the robot dynamics.

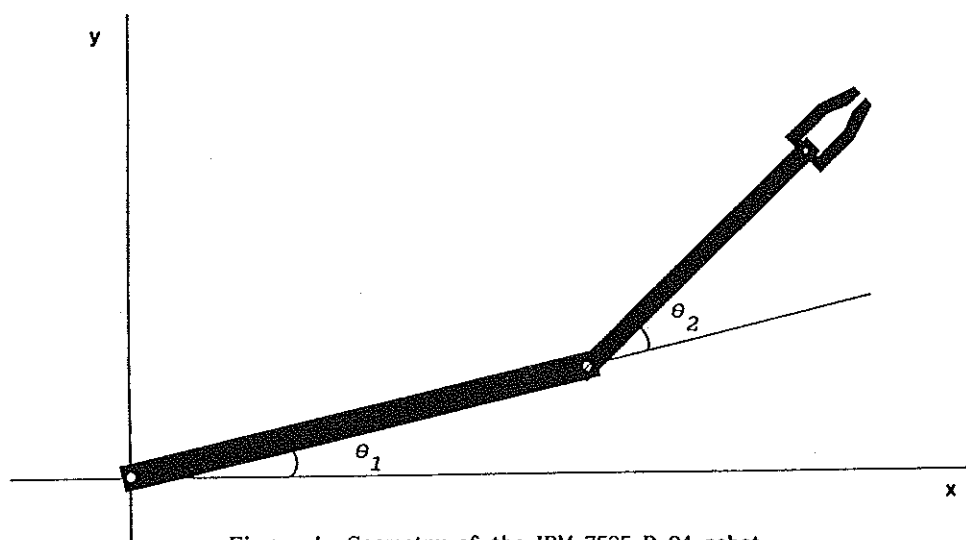


Figure 1. Geometry of the IBM 7535 B 04 robot

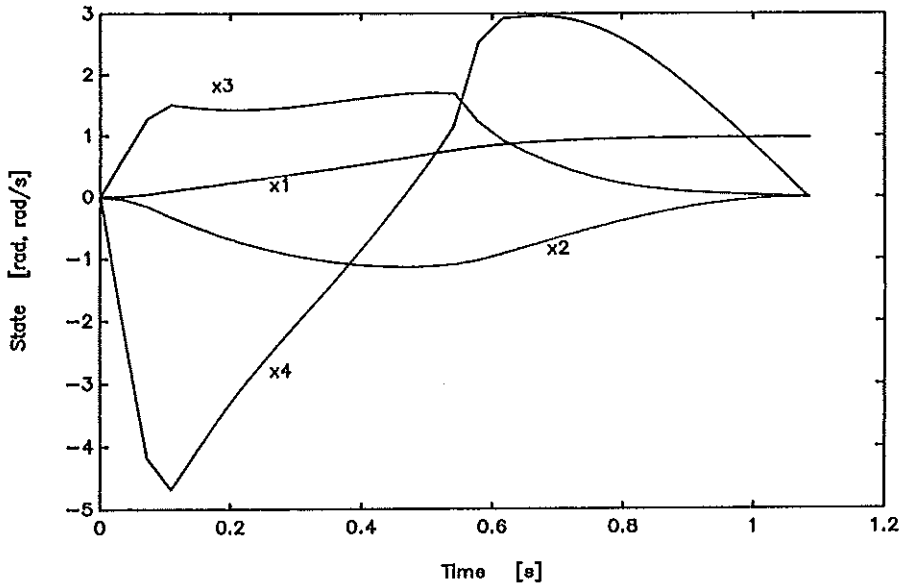


Figure 2. Time-optimal state trajectory for a robot motion with stretched initial and final configuration; $\theta_1(t_f) = 0.975 \text{ rad}$, $\theta_2(t_f) = 0 \text{ rad}$.

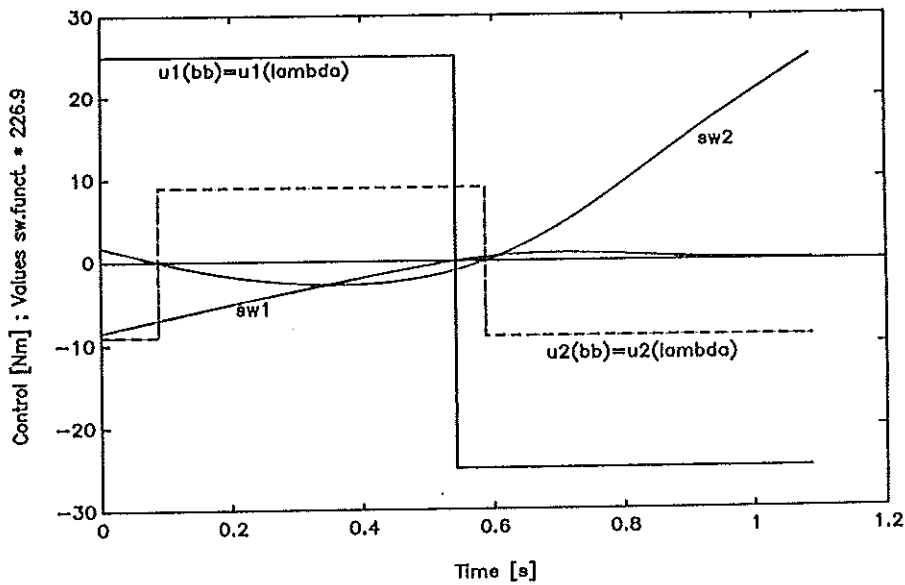


Figure 3. Time-optimal control for the robot motion in fig.2; u_1 switches at 0.5423 s, u_2 switches at 0.088 s and 0.588 s and the final time $t_f = 1.085 \text{ s}$. The bang-bang control and the control generated by the switching functions match. The switching functions are scaled as indicated.

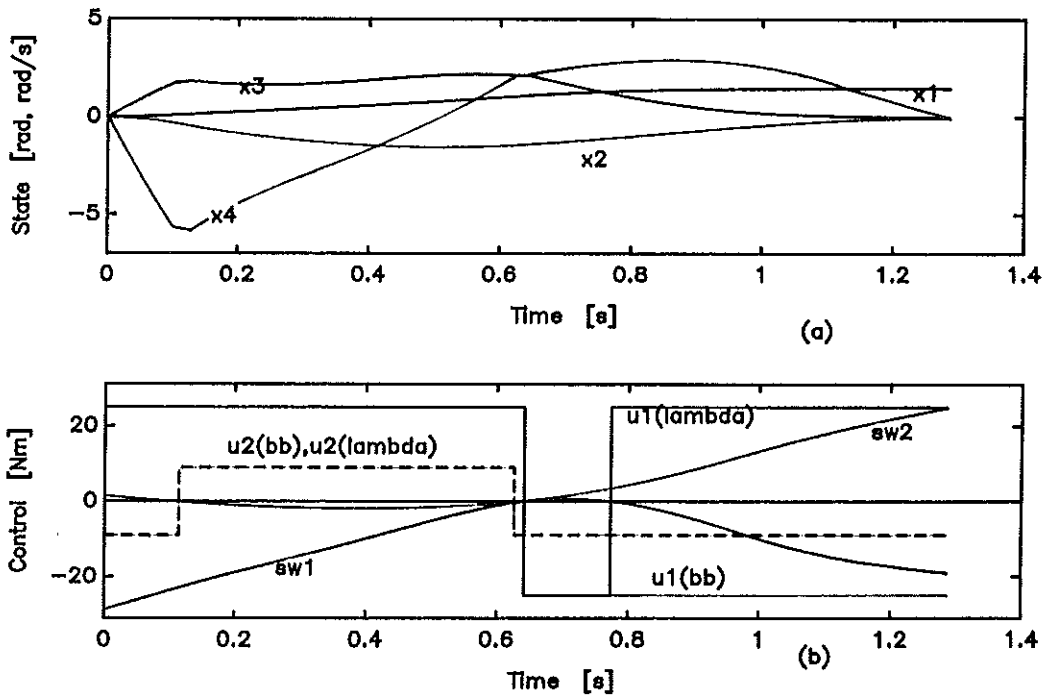


Figure 4. (a) State trajectory for a robot motion with stretched initial and final configuration; $\theta_1(t_f) = 1.5 \text{ rad}$, $\theta_2(t_f) = 0 \text{ rad}$ and $t_f = 1.28 \text{ s}$. (b) The bang-bang control with 3 switches and the control generated by the switching functions do not match. The first switching function is scaled by 140.8 and the second switching function by 802.6 .

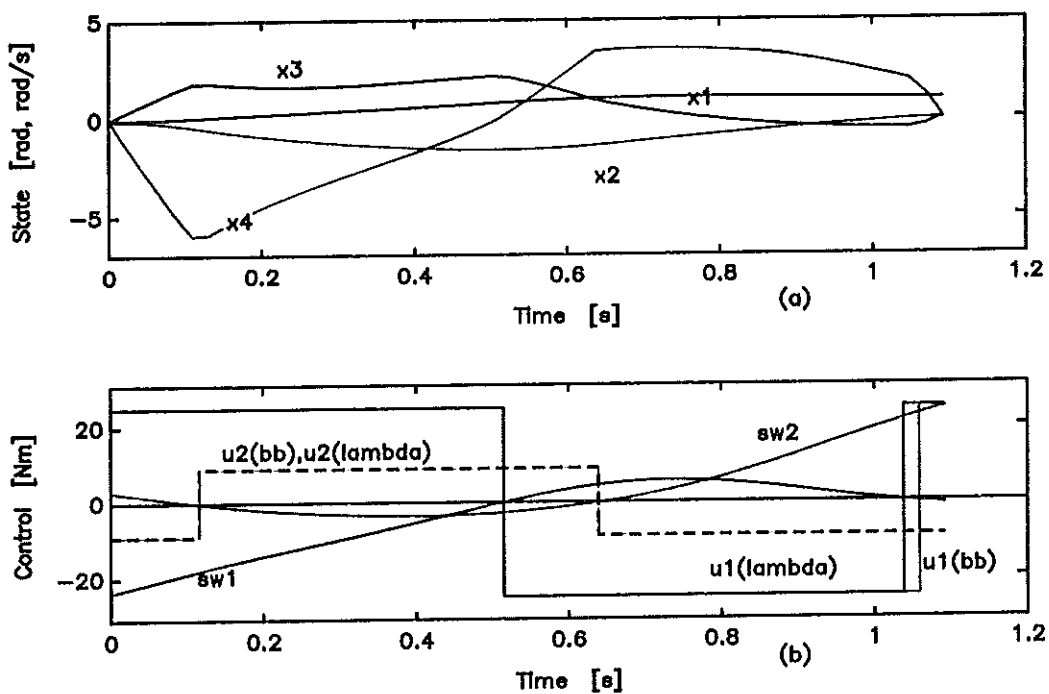


Figure 5. (a) State trajectory for a robot motion with stretched initial and final configuration; $\theta_1(t_f) = 1.0 \text{ rad}$, $\theta_2(t_f) = 0 \text{ rad}$ and $t_f = 1.09 \text{ s}$. (b) The bang-bang control with 4 switches and the control generated by the switching functions do not match. The first switching function is scaled by 225.3 and the second switching function by 675.9 .

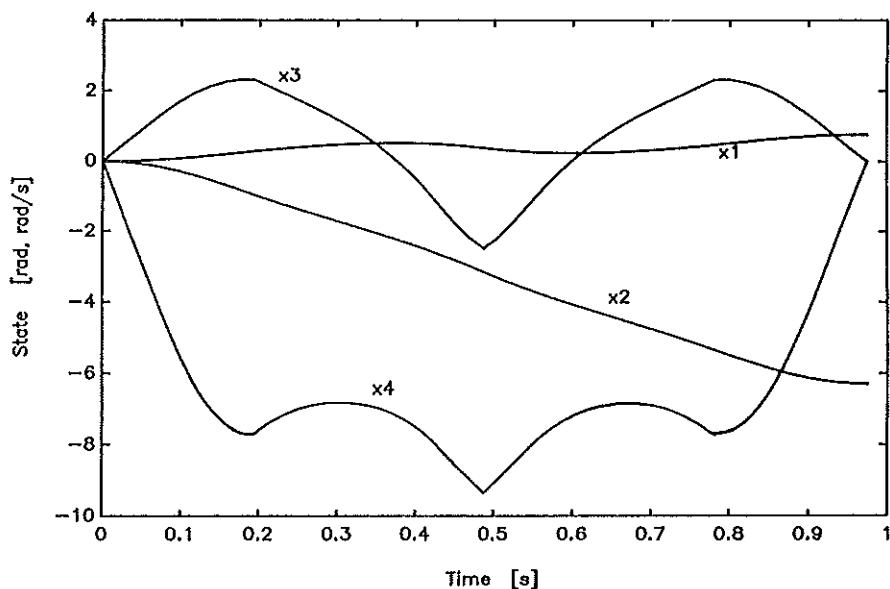


Figure 6. Time-optimal state trajectory for a robot motion with stretched initial and final configuration, the second link swinging through; $\theta_1(t_f) = 0.76 \text{ rad}$, $\theta_2(t_f) = -2\pi \text{ rad}$ and $t_f = 0.975 \text{ s}$.

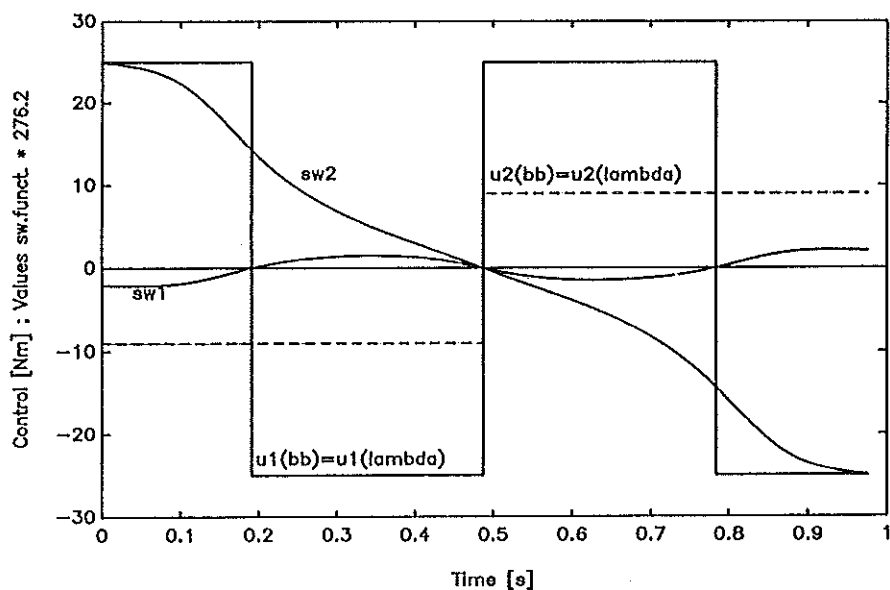


Figure 7. Time-optimal control for the robot motion in fig.6; u_1 switches at 0.191 s , 0.4873 s and 0.784 s , u_2 switches at 0.4873 s and the final time $t_f = 0.975 \text{ s}$. The bang-bang control with 4 switches and the control generated by the switching functions match. The switching functions are scaled as indicated.

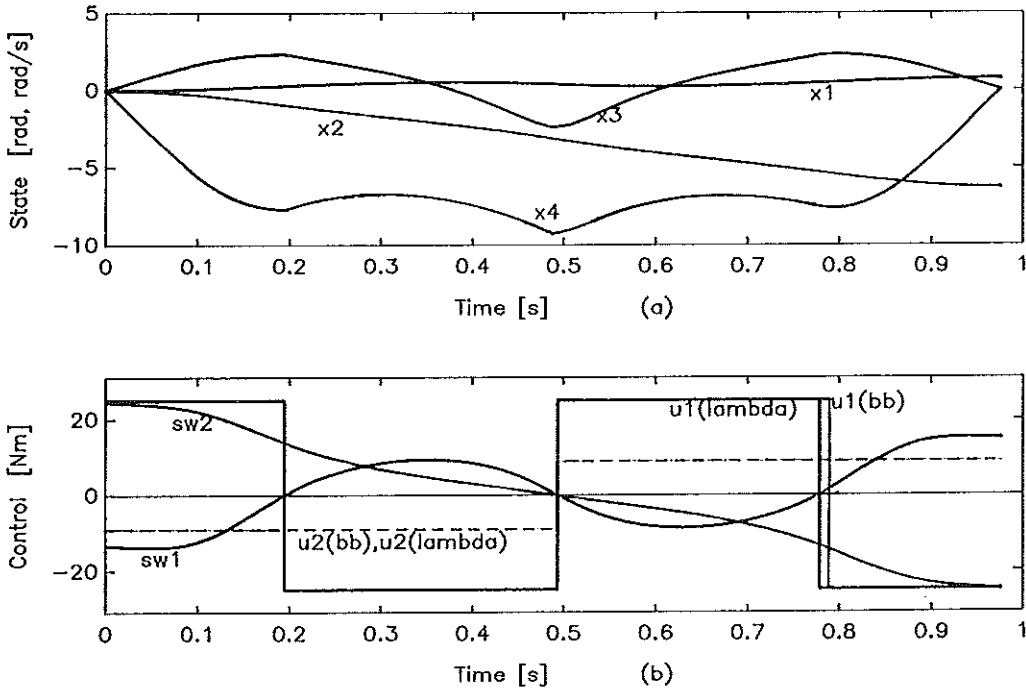


Figure 8. (a) State trajectory for a robot motion with stretched initial and final configuration with friction, the second link swinging through; $\theta_1(t_f) = 0.76 \text{ rad}$, $\theta_2(t_f) = -2\pi \text{ rad}$ and $t_f = 0.976 \text{ s}$. (b) The bang-bang control with 4 switches and the control generated by the switching functions do not match. The first switching function is scaled by 271.6 and the second switching function by 1765.4

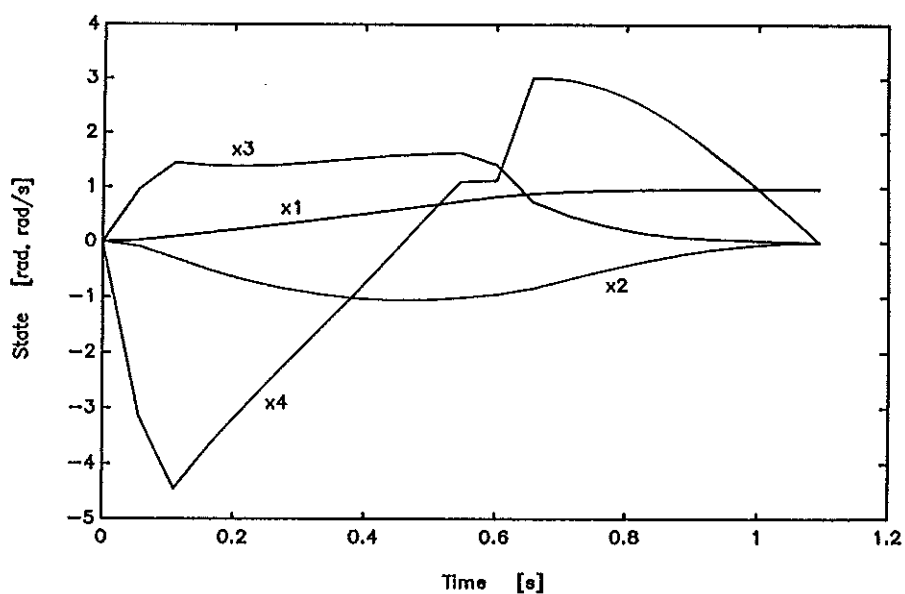


Figure 9. State trajectory for a robot motion with stretched initial and final configuration ; $\theta_1(t_f) = 0.975$ rad, $\theta_2(t_f) = 0$ rad.

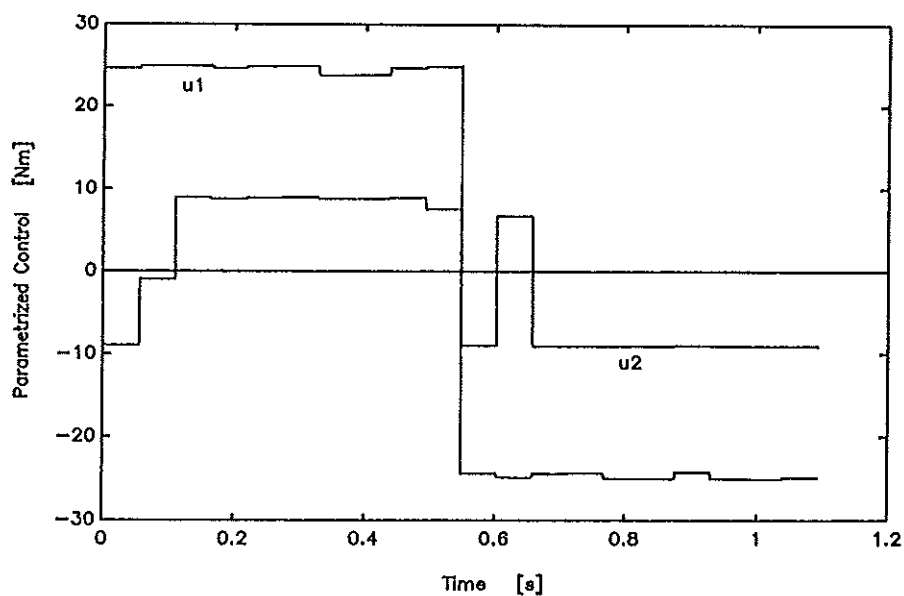


Figure 10. Parametrized control for the robot motion in fig.9; the number of time intervals is 20 and the final time $t_f = 1.095$ s.

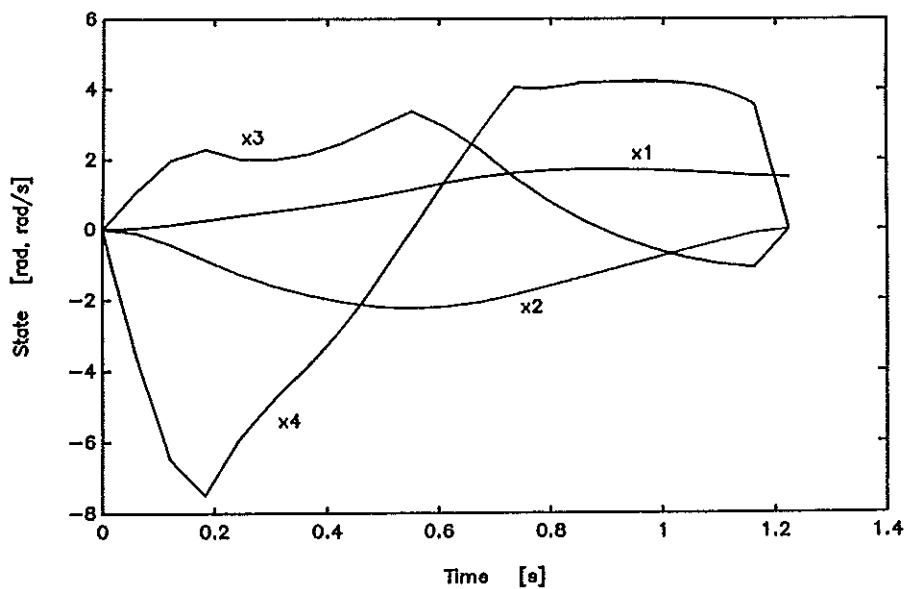


Figure 11. State trajectory for a robot motion with stretched initial and final configuration ; $\theta_1(t_f) = 1.5 \text{ rad}$, $\theta_2(t_f) = 0 \text{ rad}$.

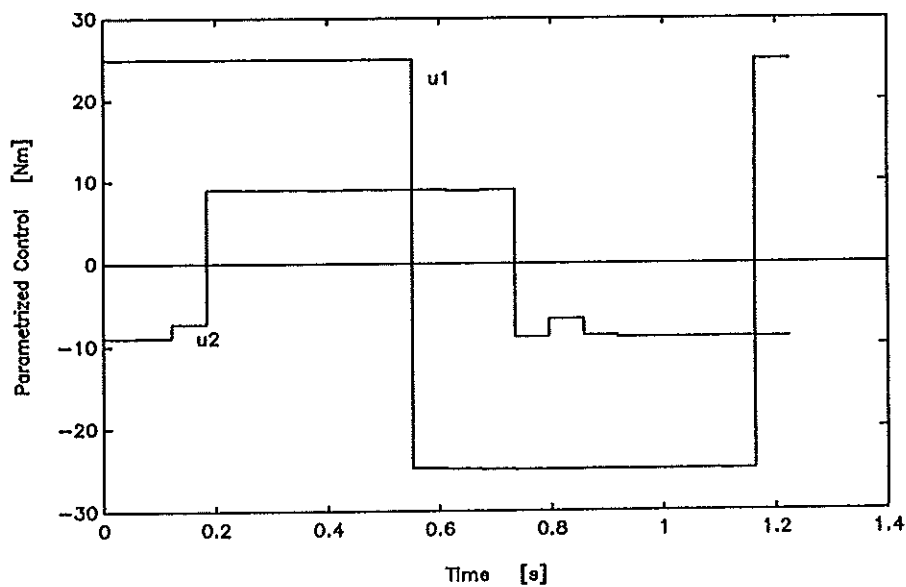


Figure 12. Parametrized control for the robot motion in fig.11; the number of time intervals is 20 and the final time $t_f = 1.225 \text{ s}$.

L.G. VAN WILLIGENBURG

DIGITAL OPTIMAL CONTROL OF NONLINEAR UNCERTAIN SYSTEMS APPLIED TO
RIGID MANIPULATORS

Abstract

Based on the recently developed numerical solution of the sampled-data (digital) LQG problem for linear time-varying systems we will treat the design and computation of *implementable digital compensators* for continuous-time nonlinear uncertain systems. A compensator is used to control the system about a so called ideal input-state response. The ideal input-state response is computed off-line through optimization and represents the desired system behavior. In this paper both the compensator design and the optimization are characterized by the fact that the *continuous-time system behavior and the digital nature of the controller are explicitly considered* in both problems. Usual controller designs *neglect the inter-sample behavior or the digital nature of the controller*. The digital controllers that result from our design procedure need only a very small number of on-line computations to be performed. As an example we compute and simulate digital controllers for a robotic manipulator.

1. Introduction

Industrial processes very often constitute continuous-time systems. The automatic control of industrial processes is generally performed by digital computers. In these cases the automatic control system is a digital control system that can be schematically represented by figure 1. The continuous-time system has a sampler at the output and a sampler and zero order hold circuit at the input.

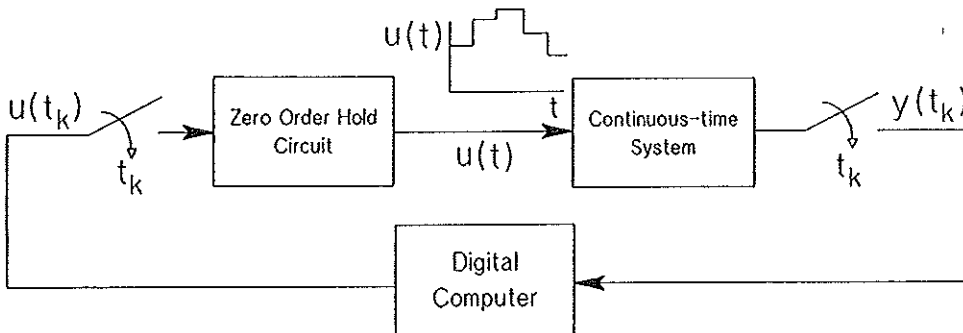


Figure 1: Digital Control System

The design of a digital controller for a continuous-time system is often referred to as a *digital control problem*. The term *digital* throughout this paper will refer to the facts that

- a) We have sampled measurements since a computer cannot deal with continuous-time measurements
- b) The control is of piecewise constant nature (a stair case function), since a sampler and zero order hold circuit connect the computer to the input of the system
- c) We consider the continuous-time behavior of the system.

Although these seem all very straightforward considerations, much to surprise, very often at least one of these considerations is not met in the design of digital controllers for continuous-time systems. Very often the design only considers the system behavior at the sampling instants, *completely disregarding the inter-sample behavior* (Ackerman 1985, Astrom and Wittenmark 1984, Franklin and Powell 1980). So in that case consideration c) is not met. In other cases continuous-time control algorithms are designed, which then somehow have to be approximated by a digital controller

(Athans 1971). In these cases both consideration a) and b) are not met. In both cases there is a demand for a "small" sampling time, in the former case to prevent undesirable inter-sample behavior, in the latter case to properly approximate the continuous-time algorithm. This demand, for instance in the case of robot control where the computational burden on the computer is high, results in computational difficulties. Even if the sampling time is chosen to be "small" the digital controllers will only constitute approximate solutions.

Over the years only a few publications have appeared which consider digital control problems in the proper context just described (Levis, Schlueter and Athans 1971, Nour Eldin 1971, Halyo and Caglayan 1976, De Koning 1980,1984, Stengel 1986, Van Willigenburg and De Koning 1990 a,b). From these publications it is apparent that it hardly takes extra effort to solve digital control problems in the proper context.

Since most industrial processes are nonlinear in this paper we will deal with the design of digital controllers for continuous-time nonlinear uncertain systems where the uncertainty consists of additive white system and measurement noise. Based on the solution to the digital LQG problem (Van Willigenburg and De Koning 1990b) and a numerical procedure to compute it (Van Willigenburg 1990a) we will treat the design and computation of a digital compensator which is used to control a nonlinear system about an off-line determined so called ideal input-state response. This response defines the desired system behavior. The computation of the ideal input-state response will also be treated. The design procedure may be compared to the one presented by Athans (1971). He considered the design of continuous-time controllers where we consider the design of implementable digital controllers. The digital controllers that result are characterized by the fact that the number of on-line computations to be performed is very small.

As an example we will present the design and simulation of digital controllers for the IBM 7535 B 04 robot, which constitutes a

highly nonlinear system. Using our approach we will demonstrate that proper results are obtained with controllers that have a sampling time of 70mS, which is generally considered too large for robot control (Craig 1986).

2. Continuous-time optimal control of nonlinear uncertain systems

Athans (1971) has excellently described the use of the solution to the continuous-time LQG problem to control continuous-time nonlinear uncertain systems about an ideal input-state response, that defines the desired system behavior. The ideal input-state response will often be referred to as the trajectory. The uncertainty is modeled by additive white gaussian system and measurement noise and the behavior is considered over a finite time interval $[t_0, t_f]$. The dynamics of the continuous-time nonlinear uncertain system are therefore given by

$$\dot{x}(t) = f(x(t), u(t), t) + \xi(t), \quad t \in [t_0, t_f] \quad [1a]$$

$$y(t) = g(x(t), u(t), t) + \theta(t), \quad t \in [t_0, t_f] \quad [1b]$$

where f is a nonlinear function and also g may be a nonlinear function. ξ and θ represent the additive white system and measurement noise. Based on the linearized dynamics about the trajectory, which approximately describe the dynamic behavior of small deviations from the trajectory, the solution of the continuous-time LQG problem, which constitutes a compensator, is used to control deviations from the trajectory to zero. The continuous time control system is schematically represented in figure 2.

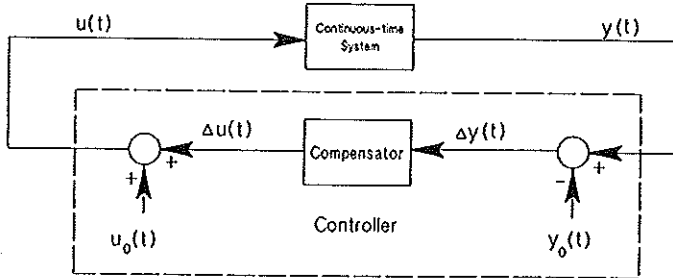


Figure 2: Continuous-time control system
with a compensator
based on linearized dynamics

Athans divides the controller design procedure into five parts, each part involving several steps.

Part A: Deterministic Modeling.

Step 1: Determination of the deterministic part of the nonlinear system equation (1a), i.e. $f(x(t), u(t), t)$.

Step 2: Determination of the deterministic part of the output equation (1b), i.e. $g(x(t), u(t), t)$.

Step 3: Based on the deterministic version of the model (1), i.e.

$$\dot{x} = f(x(t), u(t), t) \quad [2a]$$

$$y(t) = g(x(t), u(t), t) \quad [2b]$$

determine a so called ideal input-state-output

response,

$u_0(t)$: ideal input, [3a]

$x_0(t)$: ideal state response, [3b]

$y_0(t)$: ideal output response. [3c]

The ideal input-state response reflects how we actually want the system to behave. $u_0(t)$ and $x_0(t)$ are related through equation (2a) and constitute the trajectory about which we want to control the system. The ideal input-state response, i.e. the trajectory, may be the outcome of a deterministic optimization problem constrained by the nonlinear dynamics (2a). The ideal output response via (2b) directly follows from the ideal state response.

Part B: Stochastic Modeling.

Step 4: Modeling of uncertainty in the initial state of the system (1).

Selection of the mean $\bar{x}(t_0)$.

Selection of the covariance

$$\Sigma_0 = \text{cov}[x(t_0); x(t_0)]. \quad [4]$$

Step 5: Modeling of uncertainty in the system (1).

Selection of the covariance

$$\Xi(t)\delta(t-\tau) = \text{cov}[\xi(t); \xi(\tau)] \quad [5]$$

where $\xi(t)$ is the additive white system noise in (1a).

Step 6: Modeling of measurement uncertainty.

Selection of the covariance

$$\Theta(t)\delta(t-\tau) = \text{cov}[\theta(t); \theta(\tau)] \quad [6]$$

where $\theta(t)$ is the additive white measurement noise in (1b).

Part C: Linearization modeling.

Step 7: Establishing of the linearized model

$$\delta \dot{x}(t) = A_0(t) \delta x(t) + B_0(t) \delta u(t), \quad [7a]$$

$$\delta y(t) = C_0(t) \delta x(t), \quad [7b]$$

about the ideal input-state response $u_0(t)$, $x_0(t)$, below referred to by 0, i.e.

$$A_0(t) = \left. \frac{\partial f}{\partial x(t)} \right|_0, \quad B_0(t) = \left. \frac{\partial f}{\partial u(t)} \right|_0, \quad C_0(t) = \left. \frac{\partial g}{\partial x(t)} \right|_0, \quad [7c]$$

which approximately describes the dynamic behavior of the perturbation variables

$$\delta u(t) = u(t) - u_0(t), \quad [8a]$$

$$\delta x(t) = x(t) - x_0(t), \quad [8b]$$

$$\delta y(t) = y(t) - y_0(t), \quad [8c]$$

as long as they are small.

Step 8: With due consideration of Σ_0 , $\Xi(t)$ and $\Theta(t)$ and depending on the degree of nonlinearity of the system (1) select the cost weighting matrices $Q_0(t)$, $R_0(t)$ and F_0 of the cost criterion

$$J(u) = \delta x^T(t_f) F_0 \delta x(t_f) + \int_{t_0}^{t_f} \delta x^T(t) Q_0(t) \delta x(t) +$$

$$\delta u^T(t) R_0(t) \delta u(t) dt. \quad [9]$$

which is used to keep the perturbation variables, i.e. deviations from the trajectory, small.

Part D: Control problem computation.

Step 9: Given the matrices established in steps 7 and 8, solve the linear regulator problem [8], [9], i.e. solve backward in time the control Ricatti equation,

$$\begin{aligned} \dot{K}_0(t) = & -K_0(t)A_0(t) - A_0^T(t)K_0(t) - Q_0(t) + \\ & K_0(t)B_0(t)R_0^{-1}(t)B_0^T(t)K_0(t), \quad K_0(t_f) = F_0. \end{aligned} \quad [10]$$

Step 10: From the solution $K_0(t)$, determine the feedback gain matrix,

$$G_0(t) = R_0^{-1}(t)B_0^T(t)K_0(t). \quad [11]$$

Part E: Filtering problem computation.

Step 11: Given the matrices established in steps 4,5 and 6 solve forward in time the filter Ricatti equation,

$$\begin{aligned} \dot{\Sigma}_0(t) = & A_0(t)\Sigma_0(t) + \Sigma_0(t)A_0^T(t) + \Xi(t) - \\ & \Sigma_0(t)C_0(t)\Theta_0^{-1}(t)C_0^T(t)\Sigma_0(t), \quad \Sigma_0(t_0) = \Sigma_0 \end{aligned} \quad [12]$$

Step 12: From the solution $\Sigma_0(t)$, determine the filter gain matrix,

$$H_0(t) = \Sigma_0(t)C_0^T(t)\Theta_0^{-1}(t). \quad [13]$$

Part F: Construction of the linearized dynamic compensator.

Step 13: The linearized dynamic compensator is given by

$$\begin{aligned} \delta \dot{\hat{x}}(t) = & [A_0(t) - B_0(t)G_0(t) - H_0(t)C_0(t)] \delta \hat{x}(t) \\ & + H_0(t)\delta y(t), \quad \delta \hat{x}(t_0) = \bar{x}_0 - x_0(t_0), \end{aligned} \quad [14a]$$

$$\delta u(t) = -G_0(t) \delta \hat{x}(t) \quad [14b]$$

where $\delta \hat{x}(t)$ is the minimum variance estimate of $\delta x(t)$, generated by the filter.

Since all matrices appearing in the compensator equation (14) can be computed off-line we observe that the number of on-line computations to be performed is very small which is a very attractive property. Athans stresses the importance of part A and B and step 8 of part C since these all involve modeling issues, where the ability of the engineer is crucial, since no recipes exist to translate the "real world" into a mathematical model. The other steps Athans calls mechanical since a variety of computational techniques to solve the Ricatti differential equation were already available then.

Concerning the implementation Athans suggest the implementation of an approximation of (14) on a digital computer. The exact implementation of the continuous-time control algorithm (14) on a digital computer is impossible since the digital nature prevents the ability to deal with continuous-time measurements as well as it prevents the generation of a control which is adjusted continuously in time.

3. Digital (sampled-data) optimal control of nonlinear uncertain systems

Since the compensator (14) cannot be implemented in a digital computer approximations have to be made, or we have to incorporate

the digital nature of the computer into the control problem. Consider the general digital control system depicted in figure 1 with a sampler at the output and a sampler and zero order hold at the input of the continuous-time system. The sampling process is characterized by

- a) sampling instants $t_0 < t_1 < t_2 < \dots < t_N$
- b) sampling periods $T_k = t_{k+1} - t_k, k=0, 1, 2, \dots, N-1$
- c) sampling intervals $[t_{k+1}, t_k), k=0, 1, 2, \dots, N-1$

The tasks to be performed by the computer during the sampling interval $[t_{k+1}, t_k)$ are schematically represented by figure 3. At time t_k the computer must adjust the control $u(t_k)$ and observe the output $y(t_k)$. Within $[t_{k+1}, t_k)$ the next control $u(t_{k+1})$ must be computed.

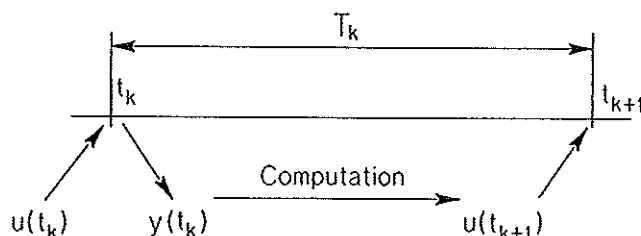


Figure 3: Task sequence of the computer

Observe that the sampling instants are not necessarily equidistant. Because of the sampler and the zero order hold at the input of the continuous-time system the continuous-time control is now of the following form

$$u(t) = u(t_k), \quad t \in [t_k, t_{k+1}), \quad k=0, 1, 2, \dots, N-1 \quad [15]$$

The continuous-time control (15) is called a piecewise constant control and is uniquely determined by the finite sequence

$$u(t_k), \quad k=0, 1, 2, \dots, N-1 \quad [16]$$

DIGITAL OPTIMAL CONTROL OF NONLINEAR UNCERTAIN SYSTEMS

Because of the sampler at the output we now obtain a finite discrete-time sequence of measurements given by

$$y_k = y(t_k) \quad k=0,1,2,\dots,N-1 \quad [17]$$

Summarizing instead of continuous-time measurements we now have a finite discrete-time sequence of measurements (17) and instead of an unconstrained continuous-time control we now have a piecewise constant control (15). Finally we assume the final sampling instant to satisfy

$$t_N = t_f \quad [18]$$

where t_f is given by (1).

The piecewise constant nature of the control restricts the choice of the ideal input $u_0(t)$ determined in step 3. When considered over the finite time interval $[t_0, t_f]$, unconstrained continuous-time controls constitute an infinite dimensional space, while piecewise constant controls constitute a finite dimensional space, since they are uniquely determined by the finite sequence (16).

Consider the ideal input-state response in step 3 to be the outcome of an optimization problem. This problem is of the following general form (Lewis 1986). Given the deterministic initial state

$$x(t_0) = x_0 \quad [19]$$

of the deterministic system (2) minimize the integral criterion

$$J(x,u) = \Psi(x(t_f), t_f) + \int_{t_0}^{t_f} L(x,u,t) dt \quad [20]$$

constrained by the dynamics (2) and some additional state and control constraints,

$$x(t) \in X, \quad t \in [t_0, t_f] \quad [21a]$$

$$u(t) \in U, \quad t \in [t_0, t_f] \quad [21b]$$

Note that any admissible control, i.e. a control satisfying (21b) via (2) and (19) uniquely determines the value of the integral criterion (20). So the optimization problem constitutes an optimal control problem, i.e. the problem of finding a control satisfying (21b) which minimizes (20) such that (21a) is satisfied. If the control constraints (21b) limit the controls to belong to a finite dimensional space, each control is uniquely determined by a finite sequence. An example is the piecewise constant constrained (15) on the control, each piecewise constant control being uniquely determined by the finite sequence (16). In these cases the optimal control problem may be regarded as the problem of minimizing the generally nonlinear function (20) of a finite sequence, i.e. the sequence (16) in case of a piecewise constant constrained on the control. Summarizing in these cases the optimal control problem may be regarded as the constrained minimization of a nonlinear function of a finite number of variables (Goh and Teo 1988). This problem is generally much more easy to solve than the original one. The nonlinear function value can be computed by numerical integration of equation (2a) and (20) given the control (15). In other words, to account for the piecewise constant constrained on the control *simplifies* the determination of the ideal input-state response through optimization. Very often however, the optimization is performed without considering the piecewise constant constrained on $u_0(t)$!

Obviously the fact that we now have a finite discrete-time sequence of measurements and a piecewise constant constraint on the control also affects the compensator (14). We now obtain a digital control system schematically represented by figure 4.

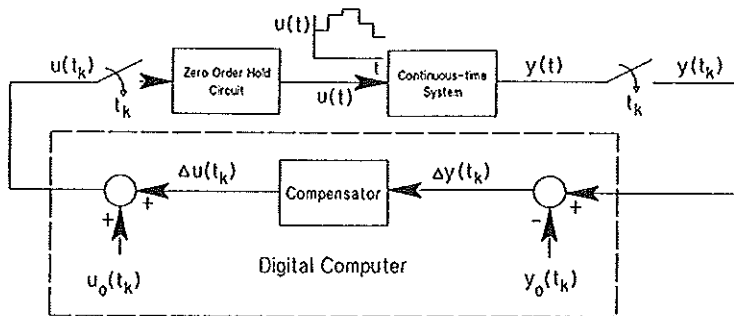


Figure 4: Digital control system
with a digital compensator
based on linearized dynamics

We now have to solve a different LQG problem, called the sampled-data LQG problem (Halyo and Caglayan 1976) or the digital LQG problem (Van Willigenburg and De Koning 1990b). Halyo and Caglayan only partially solved the sampled-data LQG problem since they did not present expressions for the minimum cost of the problem. Expressions for the minimum cost, explicit in the system and criterion matrices, were presented by Van Willigenburg and De Koning, who solved both the digital regulator and tracking problem completely. Both publications however were not concerned with the numerical computation of the solution. The numerical computation is not straightforward since it for instance involves the computation and integration of expressions involving the state-transition matrix of time-varying linear systems. These problems were solved by Van Willigenburg (1990a) who presented a numerical solution to the digital LQG problem.

If we incorporate the digital nature of the control system into the control problem, we have to replace the solution of the continuous-time LQG problem by the solution of the digital (sampled-data) LQG problem. Considering the design procedure presented in the previous paragraph only Part D,E and F, i.e. only

the mechanical part of the design changes. So the modeling issues, where the ability of the engineer is crucial, are not at all affected! Although the modeling issues are unchanged we do have to reconsider step 3, and as a result the mechanical step 7, since step 3 is affected by the piecewise constant constraint on the control. Still using the same models and reconsidering step 3, and as a result step 7, by replacing the numerical tools to compute the solution to the continuous-time LQG problem by tools to compute the solution to the digital LQG problem (Van Willigenburg 1990a) we design a *truly implementable digital controller*. The new versions of part D,E and F of the design procedure are given below

Part D: Control problem computation.

Step 9: Given the matrices established in steps 7 and 8, solve the digital regulator problem associated with [8], [9], and the digital control system in figure 1, i.e. solve the discrete-time control Ricatti equation,

$$S_k = (\Phi'_k - \Gamma_k G_k)^T S_{k+1} (\Phi'_k - \Gamma_k G_k) + G_k^T R_k G_k + Q'_k, \quad S_N = F_0. \quad [22]$$

where the index k refers to values at the sampling instant t_k . The matrices in equation (22) are given by

$$\Phi'_k = \Phi_k - \Gamma_k R_k^{-1} M_k^T, \quad [23a]$$

$$Q'_k = Q_k - M_k R_k^{-1} M_k^T, \quad [23b]$$

$$G_k = (\Gamma_k S_{k+1} \Gamma_k + R_k)^{-1} \Gamma_k^T S_{k+1} \Phi'_k, \quad [23c]$$

where

$$Q_k = \int_{t_k}^{t_{k+1}} \Phi^T(t, t_k) Q_0(t) \Phi(t, t_k) dt, \quad [23d]$$

$$M_k = \int_{t_k}^{t_{k+1}} \Phi^T(t, t_k) Q_0(t) \Gamma(t, t_k) dt, \quad [23e]$$

$$R_k = \int_{t_k}^{t_{k+1}} [R_0(t) + \Gamma^T(t, t_k) Q_0(t) \Gamma(t, t_k)] dt, \quad [23f]$$

$$\Gamma_k = \Gamma(t_{k+1}, t_k), \quad [23g]$$

in which

$$\Gamma(t, t_k) = \int_{t_k}^t \Phi(t, s) B_0(s) ds, \quad [23h]$$

$$\Phi_k = \Phi(t_{k+1}, t_k), \quad [23i]$$

Φ being the state transition matrix of the linearized system (7a).

Step 10: The feedback gain matrices are given by (23c) so

$$G_k = (\Gamma_k S_{k+1} \Gamma_k + R_k)^{-1} \Gamma_k^T S_{k+1} \Phi_k', \quad k=0, 1, 2, \dots, N-1 \quad [24]$$

Part E: Estimator problem computation.

Step 11: Given the matrices established in steps 4,5 and 6 solve forward in time the discrete-time predictor Ricatti equation,

$$P_{k+1} = (\Phi_k - H_k C_k) P_k (\Phi_k - H_k C_k)^T + H_k \Theta_k H_k^T + \Xi_k, \quad P_0 = \Sigma_0(t_0) \quad [25]$$

where again the index k refers to the values at the sampling instants t_k and

$$H_k = \Phi_k P_k C_k^T (C_k P_k C_k^T + \Theta_k)^{-1} \quad [26a]$$

and finally

$$C_k = C_0(t_k). \quad [26b]$$

Step 12: The Kalman one step ahead predictor gain matrices are given by (26a) so

$$H_k = \Phi_k P_k C_k^T (C_k P_k C_k^T + \Theta_k)^{-1}. \quad [27]$$

Part F: Construction of the linearized dynamic compensator.

Step 13: The linearized dynamic compensator is given by

$$\begin{aligned} \delta \hat{x}(t_{k+1}) &= [\Phi_k - H_k C_k] \delta \hat{x}(t_k) + H_k \delta y(t_k) + \Gamma_k \delta u(t_k), \\ \delta \hat{x}_0 &= x(t_0) - \bar{x}_0, \end{aligned} \quad [28a]$$

$$\delta u(t_k) = -G_k \delta \hat{x}(t_k) \quad [28b]$$

where $\delta \hat{x}(t_k)$ is the minimum variance estimate of $\delta x(t_k)$, generated by the one step ahead predictor.

Part F from the continuous-time Kalman Filter now turns into the discrete-time Kalman one step ahead predictor (Van Willigenburg and De Koning 1990b), which is very well known. Part D from the continuous-time linear optimal regulator turns into the digital optimal regulator (Van Willigenburg and De Koning 1990b) or sampled-data optimal regulator (Halyo and Caglayan 1976). This regulator problem considers the minimization of a *continuous-time quadratic criterion* of the form (9) by means of a *piecewise constant control* given *complete state information* at the *sampling instants*. Since this problem is of vital importance in the context of digital control of continuous-time systems it is rather surprising, to say the least, that this regulator problem has only received minor attention. The reason is that instead the solution

to the discrete-time regulator problem is used. However, this regulator problem minimizes a discrete-time quadratic criterion which only considers the continuous-time behavior of the perturbation variables (8a,b) at the sampling instants. It therefore constitutes only an *approximate solution* to the problem since it *completely disregards the inter-sample behavior*! This creates the demand for a "small" sampling time to prevent undesirable inter-sample behavior. The discrete-time criterion furthermore must be selected to generate a desired continuous-time behavior!

4. First order controllability and reconstructibility of a nonlinear continuous-time system about a trajectory

A first order approximation, i.e. the linearized model (7), is used to approximate the dynamic behavior of the perturbation variables $\delta x(t)$ and $\delta u(t)$. The error using this approximation is primarily determined by quadratic terms in $\delta x(t)$ and $\delta u(t)$ as long as these perturbation variables remain small. This justifies the use of the quadratic criterion (9) which tries to minimize quadratic terms in $\delta x(t)$ and $\delta u(t)$. Still the use of the quadratic criterion (9) does not guarantee that the perturbation variables remain small. If the linearized dynamics (7) are differentially uncontrollable over a time interval (t_1, t_2) within $[t_0, t_f]$ this implies that certain deviations $\delta x(t)$, $t \in (t_1, t_2)$ from the trajectory cannot be controlled to zero within (t_1, t_2) (Van Willigenburg 1990b). This however implies that those deviations $\delta x(t)$ are not influenced by the control during (t_1, t_2) , so they cannot in general be expected to remain small. Since the controller design is based on the idea that the perturbation variables do remain small, the differential controllability of the linearized dynamics is an important property considering the successful application of the controller presented in section 2. Van Willigenburg (1990b) demonstrated that for a rigid manipulator with friction, which we will consider in this paper as an example of a nonlinear system, any trajectory is first order controllable,

i.e. the linearized dynamics (7) about any trajectory are differentially controllable. In case of rigid manipulators the linearized dynamics about any trajectory are also differentially reconstructible. The property of differential reconstructibility is dual to the property of differential controllability (Van Willigenburg 1990b). Although not recognized as such by Van Willigenburg (1990b) the differential reconstructibility of the linearized dynamics about the trajectory, which may be called first order reconstructibility, presents another important property for the successful application of the controller in section 2. This can be intuitively understood since in case the linearized dynamics are differentially unreconstructible over a time interval (t_1, t_2) within $[t_0, t_f]$ certain deviations $\delta x(t)$ do not affect the measurements during (t_1, t_2) , and therefore $\delta \hat{x}(t)$ may become unreliable and we cannot in general expect $\delta x(t)$ to remain small within (t_1, t_2) .

In case of the digital controller of section 3, aspects of controllability and reconstructibility of the linearized dynamics about the trajectory should be reconsidered, since we have sampled measurements and a piecewise constant control. Because of this, loosely speaking, the system will always be less controllable and reconstructible, so compared to the controller of section 2, things will not improve. Concerning controllability of linear systems by means of piecewise constant controls there is the result of Furi et al. (1985), stating that complete controllability by means of continuous-time controls is equivalent to complete controllability by means of piecewise constant controls. Since we are interested in results over the finite time interval $[t_0, t_f]$ this is not the exact result we are looking for. In this paper we will not further concern ourselves with these problems, although they certainly are of interest. We will just apply the digital controller design procedure outlined in section 2 and 3 to a robotic manipulator and observe the result.

5. Digital optimal control of the IBM 7535 B 04 robotic

manipulator

In this section we present examples of the numerical computation of digital optimal controllers for the IBM 7535 B 04 robotic manipulator, designed according to the procedure described in section 2 and 3. Simulation results are also presented to demonstrate the behavior of the digital optimal robot control system.

We will use a dynamic model of the IBM 7535 B 04 robot taken from the literature (Geering et al. 1986, Van Willigenburg and Loop 1990). Before we present the examples we want to stress that our aim is not to apply these controllers in practice, our aim is merely to demonstrate how the design procedure works and that the numerically computed controllers, when applied to the nonlinear system disturbed by additive white noise, result in a proper performance. To be more specific, we will not be concerned with the careful choice of the design parameters, i.e. the covariance matrices (4), (5) and (6) and the matrices appearing in the cost criterion (9). If the aim is to apply the controller in practice the careful choice of the design parameters is essential, and that is where the ability of the engineer comes in.

Although the numerical solution to the digital LQG problem (Van Willigenburg 1990a) allows for the choice of time-varying covariance and criterion matrices we will chose both the covariance and the criterion matrices to be time-invariant to simplify the examples.

Step by step we will now follow the design steps, i.e. the parts A, B and C outlined in section 2.

Part A: Deterministic Modeling.

Step 1: Determination of $f(x(t), u(t), t)$.

The dynamics of a rigid N link manipulator with friction

are given by (Van Willigenburg and Loop 1990)

$$\dot{x}_1 = x_2 \quad [29a]$$

$$\dot{x}_2 = -M^{-1}(x_1)T(x_1, x_2) + M^{-1}(x_1)u. \quad [29b]$$

where x_1 is a vector of dimension N containing the joint angles of the links, x_2 is a vector of dimension N containing the joint angular velocities, $M(x_1)$ is a inertia matrix depending on the momentary configuration of the robot and $T(x_1, x_2)$ represents centrifugal, coriolis, gravity and friction forces. Finally u is the control vector of dimension N , containing the actuation torque applied to each joint. Since $T(x_1, x_2)$ in (29b) is highly nonlinear manipulators constitute nonlinear systems, while x_1 and x_2 constitute a natural choice for the state variables. Observe that the system is linear in the control. The dynamics of the IBM 7535 B 04 robotic manipulator can be modeled using the closed form dynamics of a rigid two link manipulator (Van Willigenburg and Loop 1990) given by Asada and Slotine (1986). In terms of equation (28) we obtain

$$x_1 = (\theta_1, \theta_2)^T, \quad [30a]$$

$$x_2 = (\dot{\theta}_1, \dot{\theta}_2)^T, \quad [30b]$$

where θ_1 and θ_2 are the joint angles of the links,

$$M(x_1) = \begin{bmatrix} M_{11} & M_{12} \\ M_{21} & M_{22} \end{bmatrix}, \quad [31]$$

where

$$M_{11} = m_1 l_{c1}^2 + I_1 + m_2 [l_1^2 + l_{c2}^2 + 2l_1 l_{c2} \cos(\theta_2)] + I_2, \quad [32a]$$

$$M_{12} = m_2 l_1 l_{c2} \cos(\theta_2) + m_2 l_{c2}^2 + I_2, \quad [32b]$$

$$M_{21} = M_{12}, \quad [32c]$$

$$M_{22} = m_2 l_{C2}^2 + I_2, \quad [32d]$$

and

$$T(x_1, x_2) = \begin{bmatrix} -h\dot{\theta}_2^2 - 2h\dot{\theta}_1\dot{\theta}_2 + G_1 + F_1 \\ -h\dot{\theta}_1^2 + G_2 + F_2 \end{bmatrix} \quad [33]$$

where

$$h = m_2 l_1 l_{C2} \sin(\theta_2), \quad [34a]$$

$$G_1 = m_1 l_{C1} g \cos(\theta_1) + m_2 g (l_{C2} \cos(\theta_1 + \theta_2) + l_1 \cos(\theta_1)), \quad [34b]$$

$$G_2 = m_2 l_{C2} g \cos(\theta_1 + \theta_2), \quad [34c]$$

$$F_1 = c_1 \operatorname{sgn}(\dot{\theta}_1) + v_1 \dot{\theta}_1, \quad [34d]$$

$$F_2 = c_2 \operatorname{sgn}(\dot{\theta}_2) + v_2 \dot{\theta}_2. \quad [34e]$$

I_1 and I_2 are the moments of inertia with respect to the center of mass, m_1 and m_2 are the total masses, l_{C1} and l_{C2} the distances between the center of mass and the joint, v_1 and v_2 the viscous friction coefficients and c_1 and c_2 are the coulomb friction coefficients of the corresponding link. Finally g is the acceleration due to gravity. Equations (33b) and (33c) represent gravity forces, in case the robot moves in a vertical plane. Since the IBM 7535 B 04 robot moves in a horizontal plane they should be disregarded. The Coulomb and viscous friction forces (33d) and (33e) are neglected in case of the IBM 7535 B 04 robot. The remaining parameter values appearing in (31) and (33) for the IBM 7535 B 04 robot are as follows (Geering et al. 1986, Van Willigenburg and Loop 1990)

$$l_1 = 0.4 \text{ m} \quad l_2 = 0.25 \text{ m} \quad l_{C2} = 0.161 \text{ m}$$

$$m_2 = 21 \text{ kg} \quad m_1 l_{c1}^2 + I_1 = 1.6 \text{ m}^2 \text{kg} \quad I_2 = 0.273 \text{ m}^2 \text{kg}. \quad [35]$$

Step 2: Determination of $g(x(t), u(t), t)$

Each joint angle of the manipulator is measured by an encoder, and often each joint angular velocity is measured by a tacho generator. We will consider both cases so we either assume the complete state is measured, i.e.

$$y(t) = C_o(t) x(t) \quad [36a]$$

where

$$C_o = \begin{bmatrix} 1 & 0 & 0 & 0 \\ 0 & 1 & 0 & 0 \\ 0 & 0 & 1 & 0 \\ 0 & 0 & 0 & 1 \end{bmatrix} \quad [36b]$$

or we assume

$$y(t) = C_1(t) x(t), \quad [37a]$$

where

$$C_1 = \begin{bmatrix} 1 & 0 & 0 & 0 \\ 0 & 1 & 0 & 0 \\ 0 & 0 & 0 & 0 \\ 0 & 0 & 0 & 0 \end{bmatrix} \quad [37b]$$

Step 3: Determination of ideal input-state-output response, $u_o(t)$, $x_o(t)$, $y_o(t)$.

As the ideal input-state response we take a time-optimal solution computed by Van Willigenburg and Loop (1990) who presented numerical procedures to compute time-optimal solutions

for rigid manipulators. The time-optimal control problem is to find the control which drives the manipulator from a fixed initial to a fixed final state in minimum time given bounds on the control variables and a deterministic dynamic model of the manipulator. We take a solution computed by a method based on control parameterization (Teo et al 1989). The control parameterization consists of the assumption that the control is piecewise constant, which is the necessary assumption to be made, in case of digital control. Furthermore the sampling times are assumed to be equidistant. Given the fixed initial state

$$x_0(t_0) = [0 \ 0 \ 0 \ 0]^T, \quad [38a]$$

the fixed final state

$$x_0(t_f) = [2.5 \ 0 \ 0 \ 0]^T, \quad [38b]$$

the bounds

$$|u_1(t)| \leq 25.0 \quad t \in [t_0, t_f], \quad [39a]$$

$$|u_2(t)| \leq 9.0 \quad t \in [t_0, t_f] \quad [39b]$$

on the control variables and the deterministic dynamics (30)-(35) of the IBM 7535 B 04 robot the time-optimal piecewise constant control is shown by the broken lines in figure 5b and the corresponding state-trajectory by the broken lines in figure 5a. The time-optimal solution presents the control in an open-loop fashion. To obtain a solution in feedback form, which we need in practice to overcome modeling and measurement errors and uncertainty, we need to recompute the solution on-line at every sampling instant. Since sampling times for robot manipulators are of the order of 10-100ms, even for very fast computers, this is impossible. Therefore we design a digital compensator, as described in sections 2 and 3, to control the system about the time-optimal input-state response. In this case the number of on-line computations is very small. To be able to control the

system about the time-optimal input-state response, the bounds (39) must constitute *conservative bounds*, since they must allow for control corrections $\delta u(t)$. This is the price one has to pay for the fact that we incorporate uncertainty into the time-optimal control problem.

Part B: Stochastic Modeling.

As already mentioned, our aim is not to design a controller which will be used in practice, but merely to demonstrate the controller design procedure. Therefore we will only briefly, or not at all, motivate the choice of the following design parameters. In practice the choice of the design parameters is essential and that is where the ability of the engineer comes in.

Step 4: Modeling of uncertainty in the initial state of the system (1).

We chose

$$\bar{x}(t_0) = x(t_0) \quad [40]$$

and

$$\Sigma_0 = \begin{bmatrix} 0.01 & 0 & 0 & 0 \\ 0 & 0.01 & 0 & 0 \\ 0 & 0 & 0.09 & 0 \\ 0 & 0 & 0 & 0.09 \end{bmatrix} \quad [41]$$

Equation (41) assumes the standard deviation in the initial joint angles to be 0.1 rad and the standard deviation in the initial joint velocities to be 0.3 rad/s. Finally it assumes the uncertainty in the initial values of the state variables to be uncorrelated.

Step 5: Modeling of uncertainty in the system (1).

We chose

$$\Xi(t) = \begin{bmatrix} .235 & 0 & 0 & 0 \\ 0 & .563 & 0 & 0 \\ 0 & 0 & 3.20 & 0 \\ 0 & 0 & 0 & 34.3 \end{bmatrix}, \quad t \in [t_0, t_f]. \quad [42]$$

This choice is such that at each time t the standard deviation of each component of $\dot{x}(t)$ equals 10 percent of the maximum value of the corresponding component of $f(x_0(t), u_0(t), t)$ over the interval $[t_0, t_f]$. The choice furthermore assumes the noise on each component of \dot{x} to be uncorrelated with the noise on the other components of \dot{x} .

Step 6: Modeling of measurement uncertainty.

We chose

$$\Theta(t) = \begin{bmatrix} 1e-4 & 0 & 0 & 0 \\ 0 & 1e-4 & 0 & 0 \\ 0 & 0 & 9e-2 & 0 \\ 0 & 0 & 0 & 9e-2 \end{bmatrix} \quad t \in [t_0, t_f] \quad [43]$$

in case the output equation (36) holds and we chose

$$\Theta(t) = \begin{bmatrix} 1e-4 & 0 \\ 0 & 1e-4 \end{bmatrix} \quad t \in [t_0, t_f] \quad [44]$$

in case the output equation (37) holds. This choice assumes the standard deviation of the joint angle measurements to be 0.01 rad. This low value reflects the fact that encoders, which measure the joint angles, give very accurate results. The standard deviation on the joint velocities, measured by tachogenerators is chosen to be 0.3 rad/s. Again the measurement noise on each output variable is assumed to be uncorrelated with the noise on the other

output variables.

Part C: Linearization modeling.

Step 7: Establishing of the linearized model

According to (7c) we have to compute

$$A_0(t) = \left. \frac{\partial f}{\partial x(t)} \right|_0, \quad B_0(t) = \left. \frac{\partial f}{\partial u(t)} \right|_0, \quad C_0(t) = \left. \frac{\partial g}{\partial x(t)} \right|_0.$$

The numerical algorithm to compute the solution to the digital LQG problem demands the evaluation of (7c) at a finite number of time-instants, depending on the number of integration steps performed during each sampling interval (Van Willigenburg 1990a). We perform the linearization (7c) numerically and chose 10 numerical integration steps during each sampling interval.

Step 8: Selection of $Q_0(t)$, $R_0(t)$ and F_0

We chose

$$Q_0(t) = \begin{bmatrix} 10.0 & 0 & 0 & 0 \\ 0 & 1.0 & 0 & 0 \\ 0 & 0 & 0.1 & 0 \\ 0 & 0 & 0 & 0.1 \end{bmatrix} \quad t \in [t_0, t_f], \quad [45]$$

$$R_0(t) = \begin{bmatrix} 0.1 & 0 \\ 0 & 0.1 \end{bmatrix} \quad t \in [t_0, t_f], \quad [46]$$

$$F_0 = \begin{bmatrix} 100.0 & 0 & 0 & 0 \\ 0 & 10.0 & 0 & 0 \\ 0 & 0 & 1.0 & 0 \\ 0 & 0 & 0 & 1.0 \end{bmatrix} \quad [47]$$

When we chose Q_0 , R_0 and F_0 to be diagonal matrices, as in (45)-(47) the feedback gain matrix is uniquely determined by the ratios of the diagonal elements of these matrices. Note that $F_0=10Q_0$ which reflects the fact that we want the final state to be reached closely, which corresponds to the objective of the time-optimal control problem. The other ratios were chosen experimentally using simulation results as the ones presented in the figures 5-8.

The simulation result in figure 5 is obtained with the digital robot controller designed using the above design parameter values. The simulation was performed using the *uncertain dynamics* (1) determined by (29)-(35), (40)-(42), (37), and (44). We simulated the white gaussian system and measurement noise using random number generators. To demonstrate the effect of the white gaussian system noise we included figure 9 which shows a response of the robot when we only apply the ideal input, i.e. the open loop control of figure 5b to the system. As expected, if we do not compensate for deviations, the system behavior becomes highly undesirable.

The ideal input-state response was obtained using the fifth and sixth order Runge Kutta integration algorithm IVPRK from the IMSL library (Van Willigenburg and Loop 1990) with a variable self adjustable step size. This routine can not be used to integrate an uncertain system since it repeats integration steps and compares the results to determine whether the accuracy is appropriate. Obviously the uncertainty prevents the results of repeated steps to match. We used a fourth order Runge Kutta integration routine, with a fixed step size equal to 1/10 of the sampling time. This proved to be sufficient to closely reobtain the ideal state response from the ideal input, demonstrating that the accuracy of integration is comparable to that of the routine IVPRK.

Since (1) constitutes an uncertain system figure 5 shows just one *realization* of the robot control system response. We have depicted

another in figure 6. Finally figure 7 and 8 show two realizations of the response of the robot control system when the complete state is measured, i.e. where equations (37) and (44) are replaced by (36) and (43).

The simulation results are merely presented to demonstrate that the design "works" and results in a "proper" system behavior given the uncertain dynamics (1). We do not intend here to specify what "proper" is neither compare it to other results. As already mentioned several times, the success of the digital LQG compensator design, depends very much on the ability of the engineer to translate the "real world" into the mathematical model (1) and the criterion (9). What can be said is that given the linearization (7) of the model (1), which approximately describes the dynamic behavior of small deviations $\delta x(t)$ and $\delta u(t)$, and given the criterion (9) the digital LQG compensator constitutes a truly implementable optimal solution to the digital control problem (7), (9).

Conclusions

Since automatic control is almost exclusively performed by digital computers it is rather surprising that the proper adaptation of the continuous-time LQG problem and solution, to incorporate the digital nature of the controller, has drawn very little attention over the years. In this paper we used a recently developed result to numerically compute the solution to the digital LQG problem, which does incorporate the digital nature of the controller properly, to treat the design and computation of truly implementable digital controllers for nonlinear uncertain systems. The design procedure may be compared to the one presented by Athans (1971) who treated the design of continuous-time controllers for nonlinear uncertain systems. It has been demonstrated in this paper that only the "mechanical" part of this design procedure has to be adjusted, i.e. the design parameters do not have to be adjusted!. We simply have to replace software to

compute continuous-time controllers by software to compute digital controllers. The software to compute the digital controllers has been recently developed.

Both the design of continuous-time and digital controllers presented in this paper is characterized by the fact that the controllers need only a very small number of computations to be performed on-line. Considering the control of robot manipulators, which constitute highly nonlinear systems where the computational burden on the computer is high since sampling times are often in between 10 and 40ms, this property is crucial. Again it is rather surprising that the design procedure based on the solution to the LQG problem has found very little application in this area. In this paper we computed digital controllers for an industrial robot. Through simulation we demonstrated that the demand for "small" sampling times, caused by in proper incorporation of the digital nature of the controller in the design, can be relaxed using our controller design procedure which incorporates the digital nature of the controller properly.

Concerning the applicability of the continuous-time controllers we have briefly mentioned the properties of differential controllability and reconstructibility of the linearized dynamics about the trajectory, called first order controllability and reconstructibility. In case these properties are not met questions remain how serious the proper behavior of the control system is affected. In case of digital controllers we also have to consider the effect of sampling on the controllability and reconstructibility of the linearized dynamics about the trajectory. Results are known with regard to complete controllability by means of piecewise constant controls (Furi et al. 1985), furthermore the reconstructibility of discrete-time systems is a well known property. However these properties are defined over an infinite time-interval. Our concern is with properties defined over a finite time-interval. This presents a new area of research.

References

- ACKERMANN J., 1985, 'Sampled data control-systems', Springer Verlag.
- ASADA H., SLOTINE J.-J.E., 1986, Robot Analysis and Control, Wiley
- ASTROM K.J., WITTENMARK B., 1984, Computer controlled systems, Englewood Cliffs, NJ: Prentice Hall
- ATHANS M., 1971, 'The Role and Use of the Stochastic Linear-Quadratic-Gaussian Problem in Control System Design', IEEE Trans. Aut. Cont., AC 16, 6, 529-552.
- CRAIG J.J., 1986, Introduction to Robotics, Addison and Wesley
- DE KONING W.L., 1980, 'Equivalent discrete optimal control problem for randomly sampled digital control systems', Int.J.Sys.Sci., 11, 841-855.
- DE KONING W.L., 1984, Digital Control Systems with Stochastic Parameters, PHD Thesis, Delft University Press
- FRANKLIN G.F., POWELL D., Digital control of dynamic systems, Addison and Wesley.
- FURI M., NISTRI P., PERA M.P., ZEZZA P.L., 1985, 'Linear Controllability by Piecewise Constant Controls with Assigned Switching Times', J. Opt. Th. Appl., 45, 2, 219-229
- GEERING H.P., GUZELLA L., HEPNER S.A.R., ONDER C.H., 'Time-Optimal Motions of Robots in Assembly Tasks', IEEE Trans. Aut. Cont., AC-31, 6, 512-518.
- GOH C.J., TEO K.L., 1988, 'Control Parameterization: a Unified Approach to Optimal Control Problems with General Constraints', Automatica, 24, 3-18.
- HALYO N, CAGLAYAN A.K., 1976, 'A separation theorem for the stochastic sampled-data LQG problem', Int. J. Cont., 23, 2, 237-244
- LEVIS A.H., SCHLUETER R.A., ATHANS M., 1971, 'On the behavior of optimal linear sampled data regulators', Int. J. Cont., 13, 343-361.
- LEWIS F.L., 1986, Optimal Control, Wiley
- NOUR ELDIN H.A., 1971, 'Optimierung linearer regelsysteme mit quadratischer zielfunction', Lect. Notes Oper. Res. Math. Sys., 47.

DIGITAL OPTIMAL CONTROL OF NONLINEAR UNCERTAIN SYSTEMS

- STENGEL R.F., 1986, Stochastic Optimal Control, Wiley
- TEO K.L., GOH C.J., LIM C.C., 1989, 'A Computational Method for a Class of Dynamical Optimization Problems in which the Terminal Time is Conditionally Free', IMA J. of Math. Cont. and Inf.
- VAN WILLIGENBURG L.G., DE KONING W.L., 1990a, 'The optimal digital regulator and tracker for deterministic linear time-varying systems', submitted for publication.
- VAN WILLIGENBURG L.G., DE KONING W.L., 1990b, 'The optimal digital regulator and tracker for stochastic linear time-varying systems', submitted for publication.
- VAN WILLIGENBURG L.G., LOOP R.P.H., 1990, 'Computation of time optimal controls applied to rigid manipulators with friction' submitted for publication.
- VAN WILLIGENBURG L.G., 1990a, 'Numerical procedures to compute the optimal digital regulator and tracker for linear time-varying systems', submitted for publication.
- VAN WILLIGENBURG L.G., 1990b, 'First order controllability and the time optimal control problem for rigid articulated arm robots with friction', Int. J. Cont., 51, 6, 1159-1171.

Figure 5a Trajectory and robot control system response

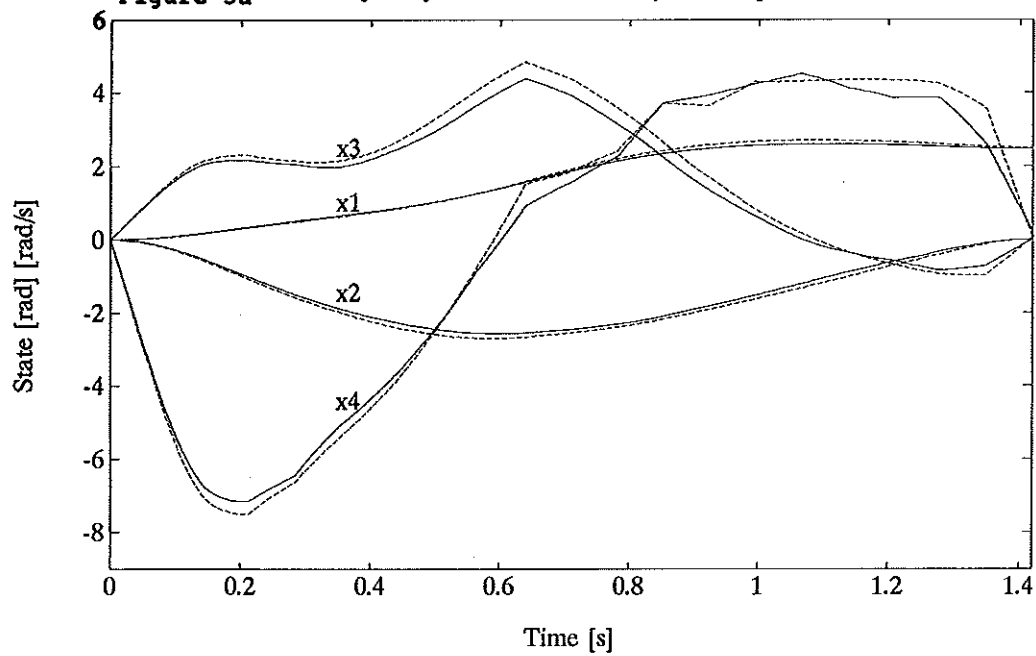


Figure 5b Ideal and actual control

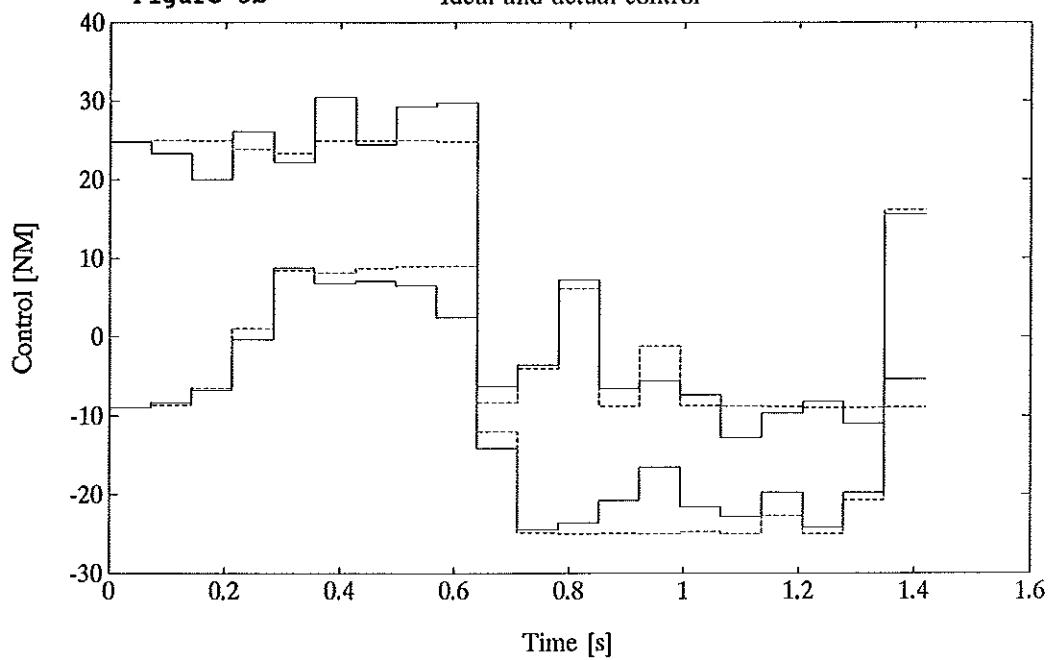


Figure 6a Trajectory and robot control system response

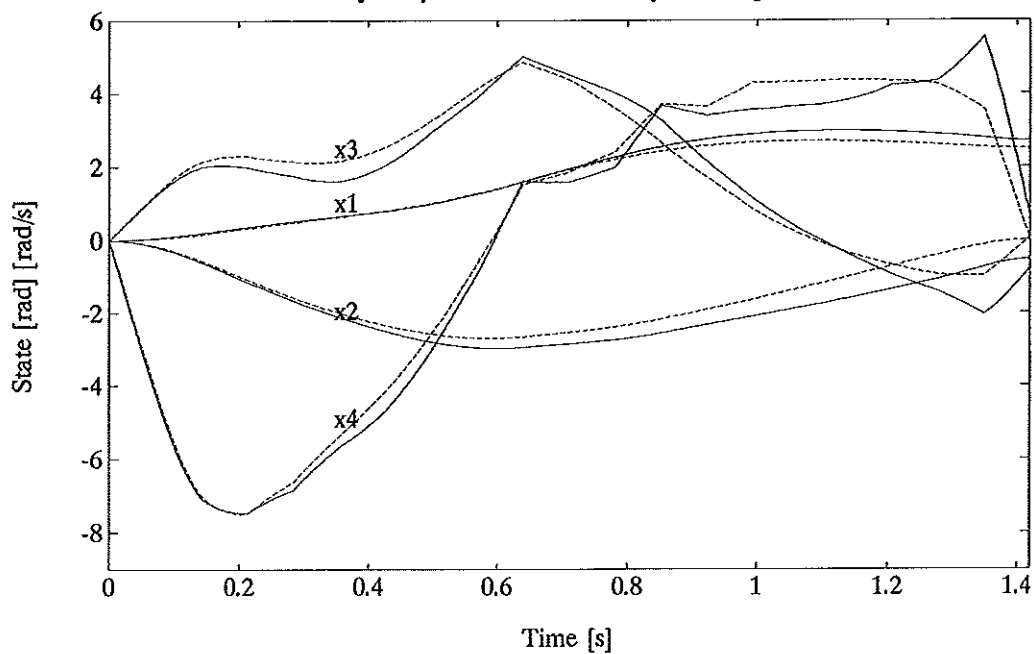


Figure 6b Ideal and actual control

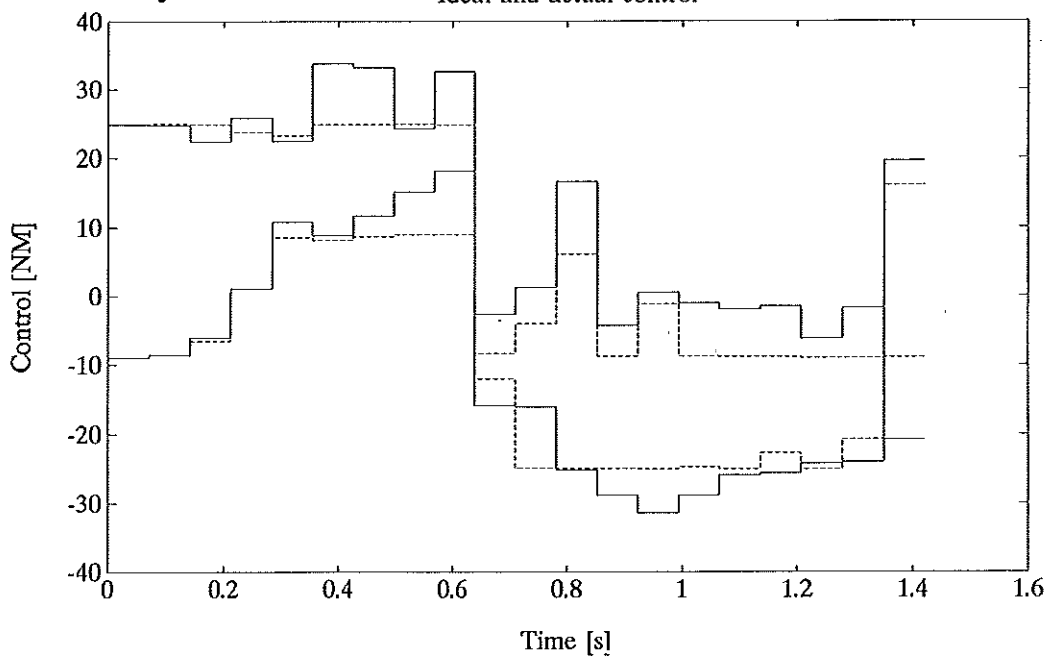


Figure 7a Trajectory and robot control system response

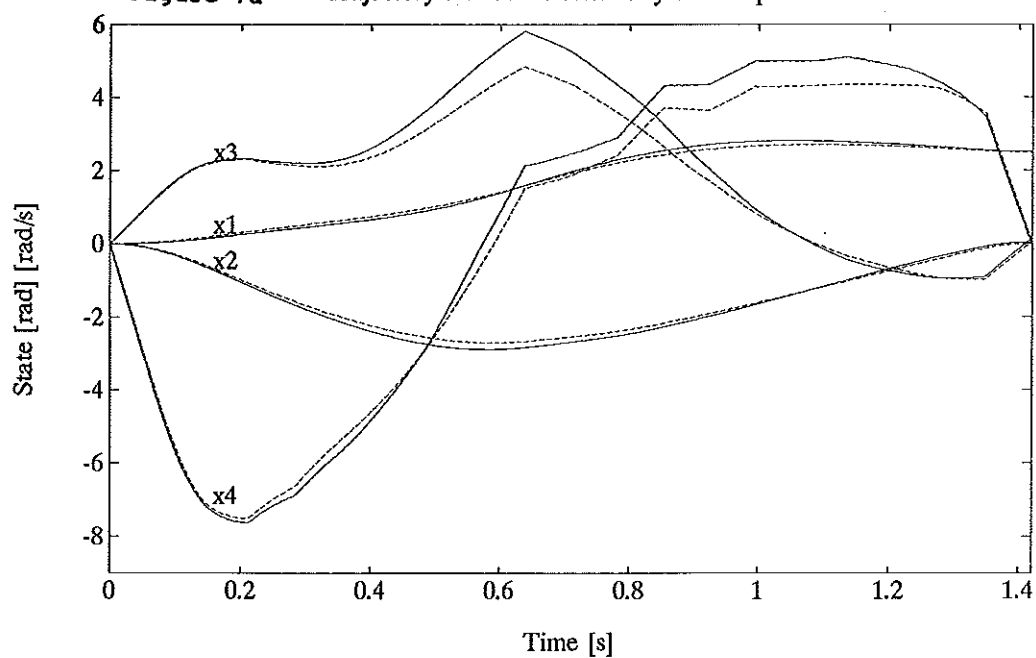


Figure 7b Ideal and actual control

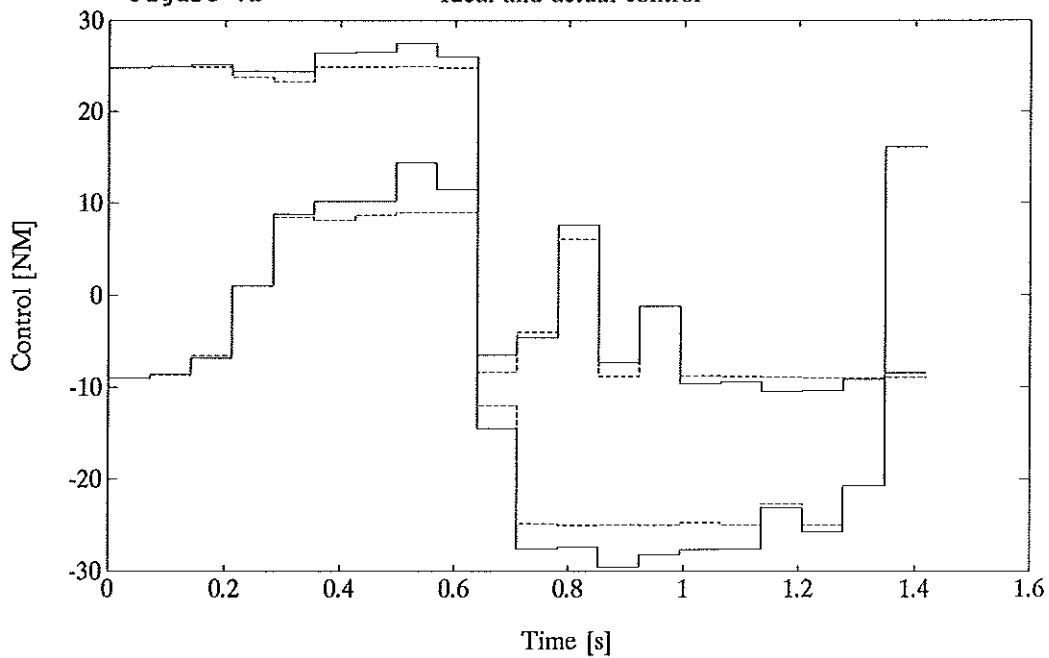


Figure 8a Trajectory and robot control system response

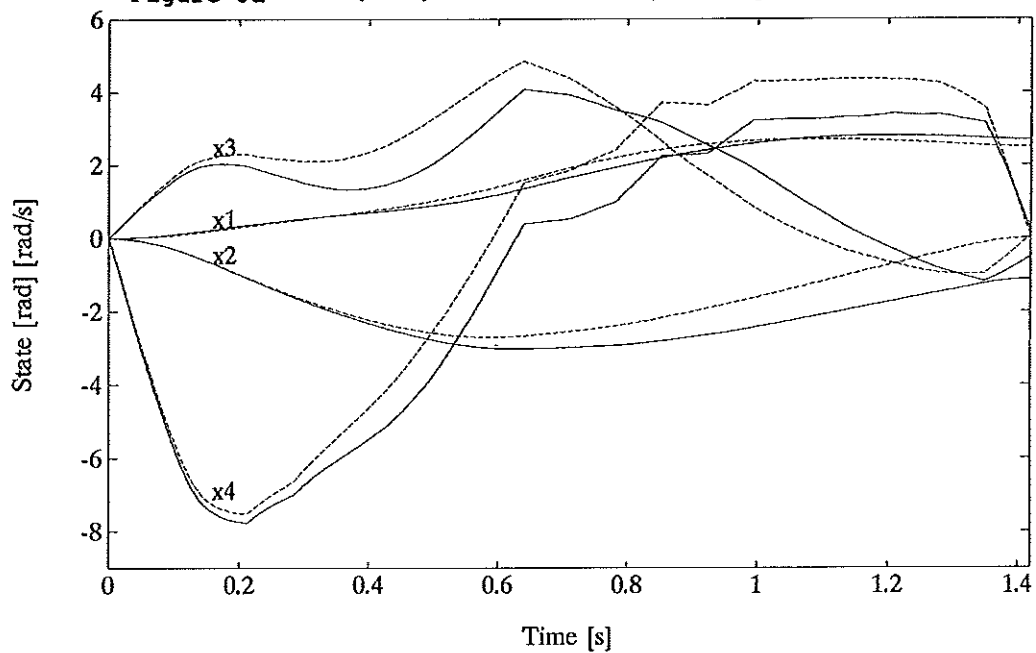


Figure 8b Ideal and actual control

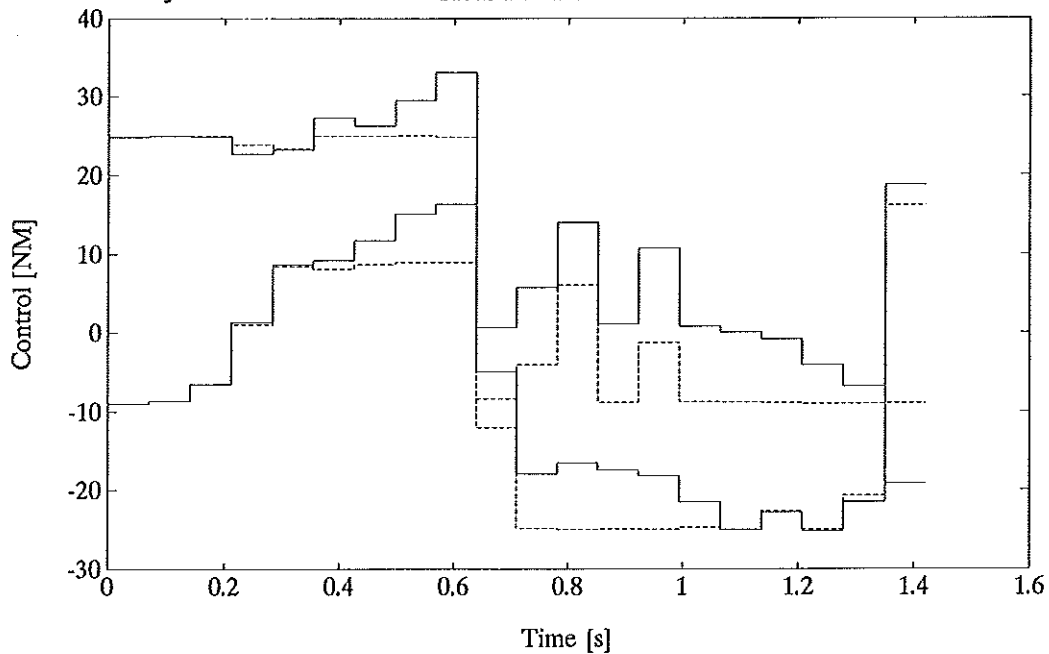
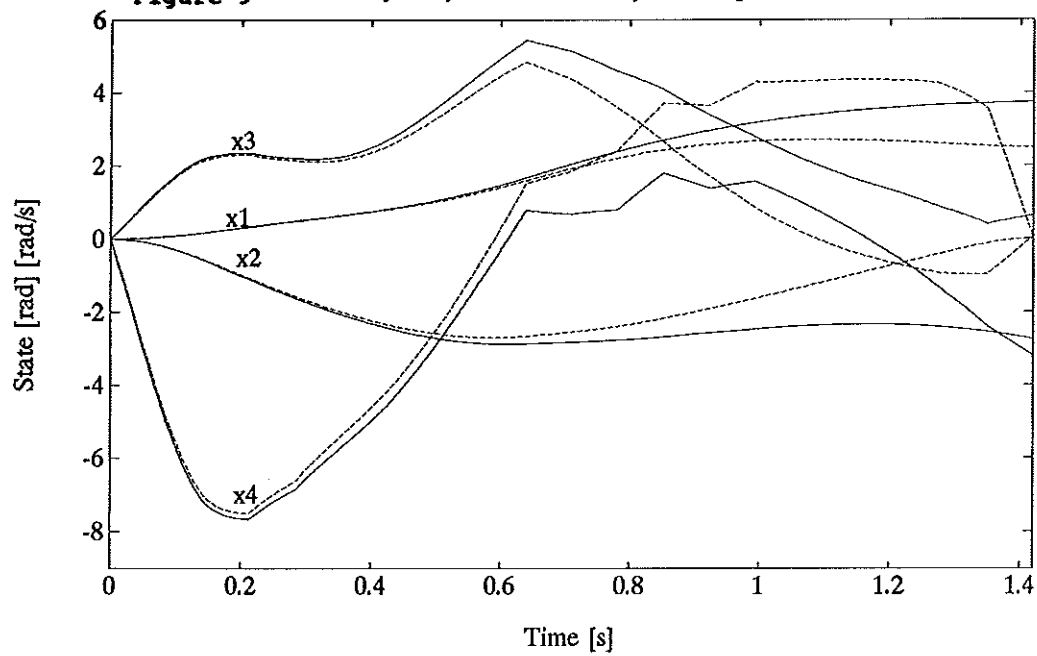


Figure 9

Trajectory and uncertain system response



Conclusions

In this thesis we have demonstrated, through the digital control of an industrial two link cartesian manipulator, that solving digital control problems without making any approximations, i.e. explicitly considering the inter-sample behavior, relaxes the demand for a "small" sampling time. In case of manipulator motion control this is very important since the computational burden on the computer is generally high.

Except for rigid cartesian manipulators, rigid manipulators constitute highly nonlinear systems, which are linear in the control. In this thesis we derived a new numerical test to verify whether bang-bang solutions to nonlinear non-singular time-optimal control problems, linear in the control, satisfy Pontryagin's Minimum Principle. This test revealed the new important fact that the probability for a bang-bang solution with more than $n-1$ switches to satisfy Pontryagin's Minimum Principle is almost zero, where n is the dimension of the system. In practical situations the search may therefore be restricted to solutions with no more than $n-1$ switches. The method has been applied to non-singular time-optimal control problems for rigid manipulators. The results were used to demonstrate that a method based on control parameterization, which uses the piecewise constant nature of digital controls, generates near time-optimal solutions for non-singular time-optimal manipulator control problems. We expect it to generate near time-optimal solutions for singular problems as well. Furthermore this method allows for the introduction of velocity bounds for the individual links of the manipulator. In practice these bounds have to be considered as well.

We extended the solution to the problem where a rigid manipulator has to travel a path in minimum time, given bounds on the control variables, to include velocity bounds for the individual links as well.

CONCLUSIONS

We further developed a type of linear quadratic regulator and tracker, called the digital regulator and tracker. Based on this development for the first time we presented a numerical method to compute both the digital regulator and tracker for linear time-varying stochastic systems.

The digital tracker directly resulted in the design computation and implementation of digital controllers for an industrial two link cartesian manipulator. The digital controllers need a very small number of computations to be performed on-line and explicitly take into account the inter-sample behavior and the piecewise constant nature of the control.

The digital regulator for time-varying linear stochastic systems, allowed the design and computation of digital compensators for nonlinear systems disturbed by additive white system and measurement noise. These digital compensators are used to control small deviations from a trajectory to zero and explicitly consider the inter-sample behavior. The trajectory represents a desired admissible behavior of the deterministic part of the system. It often is the outcome of a nonlinear optimal control problem. We demonstrated that taking into account the piecewise constant nature of the control may simplify the solution of these nonlinear optimal control problems.

For manipulator motion control we proposed the use of a digital compensator, based on the digital regulator for time-varying linear stochastic systems, to control deviations from a trajectory to zero. The optimal control problem which determines the trajectory should take into account the piecewise constant nature of the control. The result constitutes a digital feedback controller, which needs only a very small number of computations to be performed on-line. Furthermore it explicitly considers the piecewise constant nature of the control and the inter-sample behavior.

Since the proposed manipulator motion controllers need a very small number of computations to be performed on-line and explicitly take into account the piecewise constant nature of the control and the inter-sample behavior, the demand for "small" sampling times may be relaxed. Therefore even for rigid manipulators with a large number of degrees of freedom, they are suited for implementation in relatively simple, slow computers.

For nonlinear systems we introduced the concept of first order controllability and reconstructibility. We demonstrated that rigid manipulators are both first order controllable and reconstructible systems. These properties were shown to be important to guarantee the successful use of a continuous-time compensator to control nonlinear systems disturbed by additive white system and measurement noise. In case of digital compensators these properties have to be reconsidered. This presents an area of possible future research.

The identification of the dynamic parameters of manipulators has not been considered in this thesis. The success of the optimal control approach depends on the accuracy of the manipulator dynamic model. Although we expect it must be possible to identify manipulator parameters accurately, since manipulators are well defined mechanical systems, it is often mentioned in the literature that the inertia parameters are difficult to obtain. Obviously this is another area which needs further investigation.

Only if the nonlinear manipulator dynamics cannot be obtained accurately, or if the load the manipulator has to carry is really unknown, this calls for robust or adaptive control approaches. It is the authors opinion that those approaches should not be used just to avoid the use of nonlinear dynamic models.

CURRICULUM VITAE

Louis Gerard van Willigenburg werd geboren op 21 juli 1958 in Leiden. In 1976 behaalde hij het diploma Atheneum B van de Visser 't Hooft scholengemeenschap te Leiden, in 1983 het diploma elektrotechnisch ingenieur van de Technische Universiteit Delft. Van 1986 tm. augustus 1990 was hij werkzaam als wetenschappelijk assistent bij de afdeling Technische Natuurkunde van de Technische Universiteit Delft. Vanaf september 1990 is hij werkzaam als Universitair Docent bij de vakgroep Agro-techniek en Fysica, sectie meet, regel en systeem techniek van de Landbouw Universiteit Wageningen. Zijn onderzoeks interesse omvat de digitale regeling van mechanische systemen, industriële processen en binnenklimaat.

